ASD-TDR-62-1014

ANALYSIS OF MULTILOOP VEHICULAR CONTROL SYSTEMS

TECHNICAL DOCUMENTARY REPORT No. ASD-TDR-62-1014

MARCH 1964

AF FLIGHT DYNAMICS LABORATORY
RESEARCH AND TECHNOLOGY DIVISION
AIR FORCE SYSTEMS COMMAND
WRIGHT-PATTERSON AIR FORCE BASE, OHIO

Project No. 8219, Task No. 821905

(Prepared under Contract No. AF 33(616)-8024 by
Systems Technology, Inc., Inglewood, California
Authors: D. T. McRuer, I. L. Ashkenas, and H. R. Pass)

NOTICES

When Government drawings, specifications, or other data are used for any purpose other than in connection with a definitely related Government procurement operation, the United States Government thereby incurs no responsibility nor any obligation whatsoever; and the fact that the Government may have formulated, furnished, or in any way supplied the said drawings, specifications, or other data, is not to be regarded by implication or otherwise as in any manner licensing the holder or any other person or corporation, or conveying any rights or permission to manufacture, use, or sell any patented invention that may in any way be related thereto.

Qualified requesters may obtain copies of this report from the Defense Documentation Center (DDC), (formerly ASTIA), Cameron Station, Bldg. 5, 5010 Duke Street, Alexandria, Virginia, 22314.

This report has been released to the Office of Technical Services, U.S. Department of Commerce, Washington 25, D. C., in stock quantities for sale to the general public.

Copies of this report should not be returned to the Research and Technology Division, Wright-Patterson Air Force Base, Ohio, unless return is required by security considerations, contractual obligations, or notice on a specific document.

1100 - April 1964 - 162-33-650

FOREWORD

This report represents one phase of an effort aimed at extending the techniques of airframe–human pilot systems analysis used for the derivation of fundamental vehicle handling qualities. Previous investigations have studied lateral and longitudinal piloting situations applying single-loop feedback analysis methods and employing a mathematical model of the human controller as a servo element. The multiloop systems analysis technique developed herein, although intended for manual control applications, is equally suitable for automatic control system investigations.

The research reported was sponsored by the Flight Control Laboratory of the Aeronautical Systems Division (now part of the AF Flight Dynamics Laboratory, Research and Technology Division) under Project No. 8219, Task No. 821905. It was conducted at Systems Technology, Inc., under Contract No. AF 33(616)-8024, with Mr. I. L. Ashkenas and Mr. D. T. McRuer serving as principal investigators. The Air Force project engineer was Mr. R. J. Wasicko.

The authors gratefully acknowledge technical and editorial contributions made by Messrs. R. L. Stapleford and R. J. Wasicko and the careful work of the STI production staff.

ABSTRACT

The multiloop vehicular control system analysis technique developed is designed to maximize the transfer to the multiloop problem of knowledge and insights obtained from elementary single-loop vehicular control system analyses. The matrices representing the closed-loop multiloop system are expanded in a special fashion to forms in which the elementary single-loop systems explicitly appear. In the course of the development, the concept of the vehicle coupling numerator is introduced as an additional property of vehicle response behavior. The over-all closed-loop system analysis consists of successive closures of single, elementary system loops and loops involving vehicle transfer function numerators and coupling numerators.

The method is developed initially using a general multiloop system. Two simple, practical multiloop systems in aircraft control are then used as examples of the analysis technique; one illustrates a multiloop situation utilizing a single vehicle control input and the other involves multiloop control using two vehicle control inputs.

This technical documentary report has been reviewed and is approved.

Charles B. Westbrook

CHARLES B. WESTBROOK
Chief, Control Criteria Branch
Flight Control Division
AF Flight Dynamics Laboratory

CONTENTS

FIGURES

FIGURES (CONT'D)

TABLES

SYMBOLS

$[a]$	Matrix of a_{ij}'s (see Eq 9)
a_{ij}	Typical coefficient element in Laplace-transformed equations of motion describing vehicle characteristics (see Eq 1)
a_y	Lateral acceleration; generally measured at a dirtance l_x from the c.g., $a_y \equiv a_{y_{c.g.}} + l_x\dot{r} \cos \alpha_o + l_x\dot{p} \sin \alpha_o$
A	Gain of transfer function particularized by subscript
b	Wing span
B	Polynomial coefficient
c	Mean aerodynamic chord
C	Polynomial coefficient
C_D	Total drag coefficient, Drag/$(1/2)\rho U_o^2 S$
C_{D_α}	Drag coefficient variation with angle of attack, $\partial C_D/\partial\alpha$
C_{D_δ}	Drag coefficient variation with control deflection, $\partial C_D/\partial\delta$
C_{D_u}	Nondimensional variation of C_D with speed, $U_o\partial C_D/2\partial u$
C_l	Rolling moment coefficient, (Roll moment)/$(1/2)\rho U_o^2 Sb$
C_{l_β}	Dihedral parameter, $\partial C_l/\partial\beta$
C_{l_δ}	Roll control effectiveness, $\partial C_l/\partial\delta$
C_{l_p}	Roll damping coefficient, $\partial C_l/\partial(pb/2U_o)$
C_{l_r}	Roll coefficient due to yawing velocity, $\partial C_l/\partial(rb/2U_o)$
C_L	Lift coefficient, $nW/(1/2)\rho U_o^2 S$
C_{L_α}	Lift curve slope, $\partial C_L/\partial\alpha$
C_{L_δ}	Control surface lift effectiveness, $\partial C_L/\partial\delta$
C_{L_u}	Nondimensional variation of C_L with speed, $U_o\partial C_L/2\partial u$
C_M	Pitching moment coefficient, (Pitching moment)/$(1/2)\rho U_o^2 Sc$
C_{M_α}	Pitching moment coefficient variation with angle of attack, $\partial C_M/\partial\alpha$

$C_{M_{\dot{\alpha}}}$	$\partial C_M/\partial(\dot{\alpha}c/2U_o)$
C_{M_δ}	Control-surface pitch effectiveness, $\partial C_M/\partial\delta$
C_{M_q}	Pitch damping coefficient, $\partial C_M/\partial(qc/2U_o)$
C_{M_u}	Nondimensional variation of C_M with speed, $U_o\partial C_M/2\partial u$
C_n	Yawing moment coefficient, (Yawing moment)/$(1/2)\rho U_o^2 Sb$
C_{n_β}	Static directional stability, $\partial C_n/\partial\beta$
C_{n_δ}	Yaw control effectiveness, $\partial C_n/\partial\delta$
C_{n_p}	$\partial C_n/\partial(pb/2U_o)$
C_y	Lateral force coefficient, (Lateral force)/$(1/2)\rho U_o^2 S$
C_{y_β}	Variation of C_y with sideslip angle, $\partial C_y/\partial\beta$
C_{y_δ}	Lateral force effectiveness, $\partial C_y/\partial\delta$
db	Decibel $\equiv 20 \log_{10} \lvert\ \rvert = \lvert\ \rvert_{db}$
D	Denominator polynomial of G(s)
[E]	Matrix of coefficients E_{ij} (see Eq 7 and 13)
[F]	Matrix of coefficients F_{ij} (see Eq 7 and 11)
g	Acceleration due to gravity
G(s)	Open-loop transfer function; also, specific transfer function as particularized by subscript(s)
h	Altitude
H_δ	Vehicle transfer function = N_{h_δ}/Δ (see Eq 66)
I_x, I_y, I_z	Moments of inertia about the X, Y, and Z axis, respectively
I_{xz}	Product of inertia in XZ plane
$j\omega$	The imaginary portion of the complex variable, $s = \sigma \pm j\omega$
K_{h_δ}	The zero frequency value of the transfer function $H'_\delta(s)$
K_{θ_δ}	The zero frequency value of the transfer function $\Theta_\delta(s)$
K	Open-loop gain; the frequency-invariant portion of a transfer function as $s \rightarrow 0$, particularized by subscript(s)
l_x	Distance along the fuselage longitudinal reference axis from the c.g., positive forward

L_β	$\rho S U_o^2 b C_{l_\beta}/2I_x$
L_δ	$\rho S U_o^2 b C_{l_\delta}/2I_x$
L_i'	$[L_i + (I_{xz}/I_x)N_i]/[1 - (I_{xz}^2/I_x I_z)]$, i = p, r, β, etc.
L_p	$\rho S U_o b^2 C_{l_p}/4I_x$
L_r	$\rho S U_o b^2 C_{l_r}/4I_x$
m	Mass
M_α	$U_o M_w$
$M_{\dot{\alpha}}$	$U_o M_{\dot{w}}$
M_δ	$\rho S U_o^2 c C_{M_q}/2I_y$
M_q	$\rho S U_o c^2 C_{M_q}/4I_y$
M_u	$\rho S U_o c C_{M_u}/I_y$
M_w	$\rho S U_o c C_{M_\alpha}/2I_y$
$M_{\dot{w}}$	$\rho S c^2 C_{M_{\dot{\alpha}}}/4I_y$
n	Vertical load factor
N	Numerator polynomial of G(s)
N_β	$\rho S U_o^2 b C_{n_\beta}/2I_z$
N_δ	$\rho S U_o^2 b C_{n_\delta}/2I_z$
$N_{\delta_1 \delta_2}^{q_i q_k}$	Coupling numerator particularized by superscripts and subscripts (see Eq 27)
N_{h_δ}	Numerator of transfer function relating altitude to control deflection particularized by subscript
N_i'	$[N_i + (I_{xz}/I_z)L_i]/[1 - (I_{xz}^2/I_x I_z)]$, i = p, r, β, etc.
N_p	$\rho S U_o b^2 C_{n_p}/4I_z$
$N_{q_i \delta_j}$	Numerator of vehicle transfer function relating generalized output, q_i, to a generalized control deflection, δ_j
N_r	$\rho S U_o b^2 C_{n_r}/4I_z$
N_{r_δ}	Numerator of transfer function relating yaw rate to control deflection particularized by subscript
p	Roll rate, angular velocity about the X axis, positive right wing going down

q	Generalized output of the system; or pitch rate, angular velocity about the Y axis, positive nose going up
$Q_{i_{\delta_j}}$	Vehicle generalized transfer function
r	Yaw rate, angular velocity about the Z axis, positive nose going right
$R_\delta(s)$	Vehicle transfer function relating yaw rate to control surface deflection, $r(s)/\delta(s)$
s	Laplace operator, $\sigma \pm j\omega$
S	Wing area
$1/T$	Inverse time constant, particularized by subscript
u	Output motion quantity (linear perturbed velocity along the X axis)
U_δ	Vehicle transfer function
U_o	Linear steady state velocity along the X axis
v	Linear perturbed velocity along the Y axis
w	Output motion quantity (linear perturbed velocity along the Z axis)
W	Weight
W_δ	Vehicle transfer function
X_α	$U_o X_w$; $\rho S U_o^2 (C_L - C_{D_\alpha})/2m$
X_δ	$\rho S U_o^2 (-C_{D_\delta})/2m$
X_u	$\rho S U_o (-C_D - C_{D_u})/m$
X_w	$\rho S U_o (C_L - C_{D_\alpha})/2m$
Y_δ	$U_o Y_\delta^*$
Y_δ^*	$\rho S U_o C_{y_\delta}/2m$
Y_v	$\rho S U_o C_{y_\beta}/2m$
Z_α	$U_o Z_w$
Z_δ	$\rho S U_o^2 (-C_{L_\delta})/2m$
Z_u	$\rho S U_o (-C_L - C_{L_u})/m$
Z_w	$\rho S U_o (-C_{L_\alpha} - C_D)/2m$

α	w/U_o, perturbed angle of attack under no-wind condition
α_o	Angle between fuselage longitudinal reference axis and X axis
β	v/U_o, sideslip angle under no-wind condition
δ	Control deflections, particularized by subscript
$\Delta(s)$	Denominator of airframe transfer functions; characteristic equation when set equal to zero
Δ_{ij}	Cofactor of characteristic determinant (see Eq 32 and 33)
ζ	Damping ratio of linear second-order transfer function quantity, particularized by subscript
η	External disturbances on the vehicle, particularized by subscript
θ	Pitch angle
Θ_δ	Transfer function relating pitch angle to control surface deflection, $\theta(s)/\delta(s)$
ξ	The negative of the damping ratio for a special value of s; $\xi = \frac{\sigma}{\sqrt{\sigma^2 + \omega^2}}$
ρ	Mass density of air
σ	The real portion of the complex variable $s = \sigma \pm j\omega$
φ	Roll angle
$\Phi_\delta(s)$	Transfer function relating roll angle to control surface deflection, $\varphi(s)/\delta(s)$
ω	Frequency; $j\omega$ is the imaginary portion of the complex variable $s = \sigma \pm j\omega$
ω	Undamped natural frequency of a second-order mode, particularized by subscript

Subscripts

a	Aileron, aileron axis transfer functions
a	Altimeter
c	Command; crossover; controlled element
d	Dutch roll
e	Elevator; system error
eff	Effective
E	Lead equalization

lat	Lateral
long	Longitudinal
p	Phugoid
r	Rudder; yaw axis transfer functions
R	Roll subsidence
sp	Short period
T	Throttle
δ	Servo characteristics, e.g., ω_δ
ϵ	Error
θ	Pitch transfer functions
ρ	Washout
φ	Roll transfer functions

Notational Rules for Closed-Loop Quantities

1. The number of primes present indicates the number of loops closed previously which affect the quantity considered.

2. The notation for the closed-loop factor is the same as that for the open-loop factor (plus a prime) when the closed-loop and open-loop transfer function factors have the same form. In this case the origin of the closed-loop factor is always at hand (e.g., $\omega_d \rightarrow \omega_d'$, $\omega_p \rightarrow \omega_p'$, $\omega_\varphi \rightarrow \omega_\varphi'$, $T_R \rightarrow T_R'$, $T_{\varphi_1} \rightarrow T_{\varphi_1}'$, $T_{d_1} \rightarrow T_{d_1}'$, etc.).

3. When the closed-loop factors differ in form from their open-loop origins several possibilities exist:

   a. For closed-loop factors which have the same form as, and are approaching, open-loop zeros, the closed-loop factor notation is that of the open-loop zeros (plus a prime). For example, open-loop quantities $(s + 1/T_s)$ and $(s + 1/T_{d_2})$, which couple to form a quadratic approaching the open-loop zeros of $(s^2 + 2\zeta_r\omega_r s + \omega_r^2)$, would give rise to a closed-loop factor ordinarily denoted as $(s^2 + 2\zeta_r'\omega_r' s + \omega_r'^2)$.

   b. For closed-loop factors which differ in form from both the open-loop pole factors from which they depart and the open-loop zero factors which they ultimately approach, a special notation is coined which ordinarily reflects the origin of the factor. For example, closed-loop poles which start from $s = 0$ and $s = -1/T_R$, then couple to form a quadratic factor, and subsequently decouple to end finally at two real zeros, would be denoted as $s^2 + 2\zeta_R'\omega_R' s + \omega_R'^2$ in the quadratic region.

c. Closed-loop factors which have no readily identified origin or end point, such as one starting at $s = 0$ and approaching $s = \infty$ as gain increases, are given a specially coined notation, e.g., $1/T_c'$.

4. When the application of these rules by rote would result in confusion in the local context, a new form is substituted for the closed-loop factor involved. Primes, however, are always retained.

SECTION I

INTRODUCTION

The intelligent treatment of linear multiloop systems requires an analysis technique which is comparable, in providing insight for synthesis activities, to the graphic and physically meaningful techniques available for single-loop analysis. Such provision of synthesis-oriented insights and physical appreciation is central to the intelligent, interpretative analysis necessary to achieve near-optimum synthesis of complex systems. Perhaps the most important class of such complex multiloop systems involves control of vehicles having many degrees of freedom. In these systems the vehicle is usually the most complex and troublesome dynamic element in the system; so much so as to ordinarily be the object of separate study and technology. Many of the loops required in the control system are primarily intended to correct the vehicle's dynamic deficiencies. Consequently, the adequacy of any multiloop analysis method evolved will strongly depend on how easily and creatively the available knowledge of vehicle dynamics can be utilized in the evolution of the multiloop control. Most of the existing multiloop analysis techniques (see Ref 1 for a partial summary) essentially ignore this critical feature, and thereby fail to take full advantage of vehicle stability and control technology and the insights it can bring to vehicular control problems.

The most common technique for the pencil-and-paper analysis of multiloop vehicular control systems is the method of equivalent stability derivatives (Refs 2–6). Equivalent stability derivatives are especially useful when combined with literal expressions for the approximate factors of the vehicle transfer functions (Refs 2 and 3). However, the method is restricted practically to ideal (no lag) or nearly ideal controllers, and it is most easily applied (although not limited) to control feedbacks which augment existing, rather than create new, derivatives. Within these limits it is an extremely useful analysis and synthesis tool.

Original manuscript submitted December 1962; revised manuscript released by authors January 1964 for publication as an ASD Technical Documentary Report.

By far the most common means for multiloop system study and synthesis is repetitive analysis using the analog computer. With the aid of this tool and a background comprising knowledge of the vehicle equations of motion, an appreciation of the gross single-loop effects of probable feedbacks, approximate factors for the vehicle, past computer solutions, etc., the analyst can relatively rapidly arrive at a set of loop closures which define a "good" system. A "good" system in this respect will exhibit fast, well-damped, accurate responses to all representative commands and will act similarly in suppressing disturbances (i.e., responses to commands and disturbances will be akin to those of a well-damped, low-order system). The "good" system will also be relatively insensitive to changes from nominal values in the vehicle or controller characteristics, will tend to be unaffected by the introduction of small parasitic nonlinearities, etc. With the computer there is no essential difficulty in treating controller lags or, for that matter, nonlinearities.

Exclusive reliance on the analog computer does have some deficiencies. For instance, some insight into the over-all system is irretrievably lost because of the dominance of only particular modes in the time-histories. Also, modes which may be of great importance when the conditions are changed slightly are suppressed, sensitivities are difficult to evaluate, gross trends and grand simplifications are harder to come by than with some analytical schemes, etc. Finally, elements described only in frequency response terms, such as experimentally measured subsystem describing functions and human pilot descriptions, cannot be used directly in computer operations. Thus insight is constricted and initiative stifled, as always happens when only a single approach to a problem is utilized.

The properties desired of a multiloop analysis technique, in the light of the above remarks, should include:

1. Analytical formulations which show, as separate entities, vehicle-alone and controller-alone characteristics expressed in conventional and well-understood terms—thereby providing a close tie to the individual elements and the physical problem.
2. Analytical operations which can be performed using the more efficient of the classical graphical techniques of servoanalysis—thereby enhancing transfer of skill and intuition.

3. Analysis sequences and procedures which are highly responsive to physical insights and intuition; and which lead, when used by a skilled practitioner, to "good" systems with a minimum of iteration.

4. Problem solution presentations, and results, which are supplementary as well as equivalent to the results obtained using the analog computer.

This report develops and explains a multiloop analysis technique which is intended to satisfy most of the wants discussed above.

Like almost all "new" methods the technique advanced here has some precedents which were significant in its evolution. Various steps in the technique to be explained were evolved over a fairly long period of time, starting about 1957 at Systems Technology, Inc. An analysis technique used in Ref 7 played an important role in suggesting some aspects of the development. Also, an analysis procedure having some features similar to that presented here was used by Mataga in Ref 8.

In many respects the unified servoanalysis procedure, as reported in Ref 9, and the sensitivity and modal response analysis techniques reported in Ref 10, are the analytical companions to the multiloop analysis techniques reported here. This trio of reports is intended to cover, with a unified eclectic point of view regarding methods, most of the significant analysis problems of linear servo theory.

The body of the report is presented in three sections. The major analytical effort appears in Section II for a sequence of generalized systems. Generalized equations of motion are used as a starting point, then formulated as matrix equations to simplify much of the analytical development. Certain key observations on the desired types of matrix expansions are then made, after which the analytical development is largely straightforward algebra. At the end of this section some practical problems of application deriving from physical considerations are listed and discussed in general. The last two sections of the report are intended to elucidate by example some of the aspects of the method which derive predominantly from these physical considerations. These sections start with the generalized treatment, and specialize it for two concrete examples. The discussion of Section III treats a longitudinal example for an altitude control system. This particular system is the simplest possible multiloop system insofar as its basic loop structure is concerned. The lateral example, covered

in Section IV, is considerably more complex and serves as a simplified prototype for most multiloop vehicular control problems.

SECTION II

ANALYSIS OF GENERALIZED MULTILOOP SYSTEMS

In this section the essential features of a multiloop analysis technique will be developed. A generalized notation for vehicle and controller variables is introduced early and used throughout the developments. Matrix formulations are appropriate for multiloop problems, and could be used from the outset; but, to make the developments easier to follow for the reader unfamiliar with matrices, exemplary equations of motion are intermixed with matrix generalizations. In most of the developments an inductive approach is used wherein systems of limited complexity are used to formulate equations which are then expressed in matrix form. The matrix equations so obtained are both a shorthand for the limited complexity system equations and, viewed more broadly, the appropriate equations for far more complex systems. Thus an attempt is made to satisfy the often conflicting desires for concreteness and generality.

Several types of systems appear in the course of the development. These differ primarily in their level of complexity, which has been selected to be just sufficient to illustrate the local points being made. The first system considered (in articles A – C) is the most complex; it is used to illustrate the generalized notation, matrix formulation, and closed-loop system characteristic equation development. When closed-loop transfer function numerator terms become the subject of detailed examination, a somewhat simpler system is introduced for purposes of clarity. Finally, in article D, a still simpler system is used to explain the steps involved in the final phases of the analysis process. The two simpler systems are special cases of the more complex one, which is introduced below.

A. GENERALIZED SYSTEM

The generalized vehicular control system to be analyzed is shown in the block diagram of Fig. 1. Despite its foreboding appearance, the system is relatively simple, being just complex enough to represent most flight control situations and to allow easy inductive generalizations. The system consists of

a vehicle plus control equipment comprising sensing, equalizing, and actuating elements. The vehicle has three independent degrees of freedom, and is subject to control forces and moments applied by two control deflections and two external disturbances. The control deflections are functions of command inputs, feedbacks from the three degrees of freedom, and a possible fourth feedback from an auxiliary variable which is a function of the independent degrees of freedom. Additional auxiliary feedbacks may also be present, but the single one shown will illustrate the analytical process relating to such quantities. Generalization by induction to include added auxiliary feedbacks will later be seen to be straightforward.

The Fig. 1 block diagram can be simplified to one having only unity feedback loops by reinterpreting the command, $\overline{J}_j$, and forward loop, $\overline{G}_{ij}$, transfer blocks. This could be done in the q_2 loop, for example, by replacing $\overline{J}_2(s)$ with $J_2(s) = \overline{J}_2(s)/H_2(s)$, and replacing $\overline{G}_{12}(s)$ and $\overline{G}_{22}(s)$ by $G_{12}(s) = \overline{G}_{12}(s)H_2(s)$ and $G_{22}(s) = \overline{G}_{22}(s)H_2(s)$, respectively. The unity feedback loops block diagram of Fig. 2 results when similar steps are taken throughout. This block diagram is still somewhat overcomplicated in that command inputs are shown for all feedback loops. Actual commands ordinarily exist for only one loop, or possibly two.

The analytical operations involved in the above reduction to unity feedbacks, and many other operations to follow, are based on the assumption that system elements can be described by linear, constant-coefficient, differential equations. Accordingly, all motion and transfer quantities in Figs. 1 and 2 are shown as functions of s, the Laplace transform complex variable. The assumption of linearity also facilitates the manipulation of system equations and allows the principle of superposition to be used. Superposition provides a great convenience because the generalized closed-loop transfer functions need be developed for only one command input. Closed-loop transfer functions for other commands can then be found by proper juggling of subscripts and suitable interchange of elements within particular matrices.

To go along with the economy of notation provided by the use of matrix methods, the functional dependence of most quantities on s is not indicated hereafter. For example, the vehicle equations of motion for the three independent degrees of freedom are written as

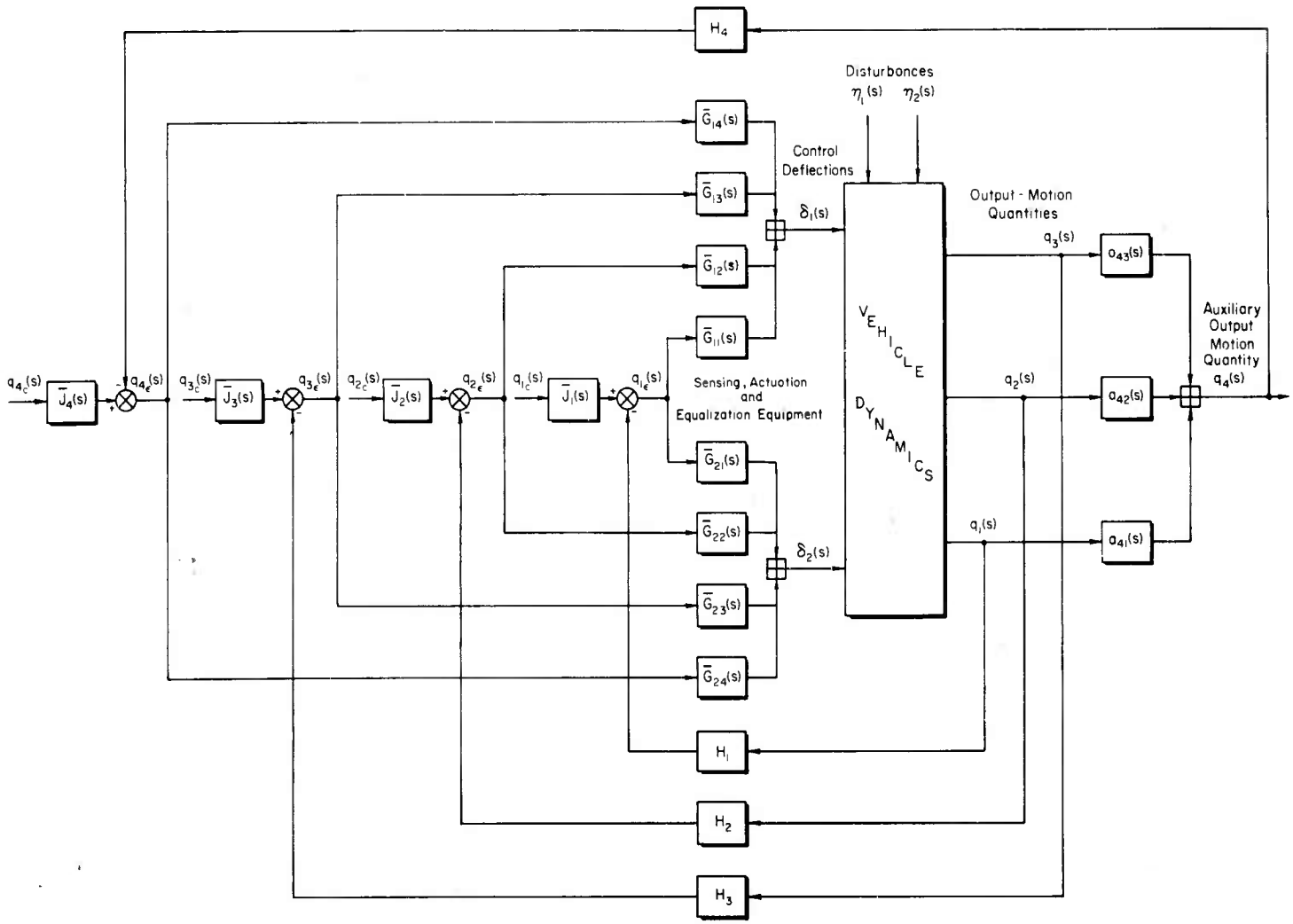

Figure 1. General Control System for a Vehicle with Three Degrees of Freedom and Two Control Inputs

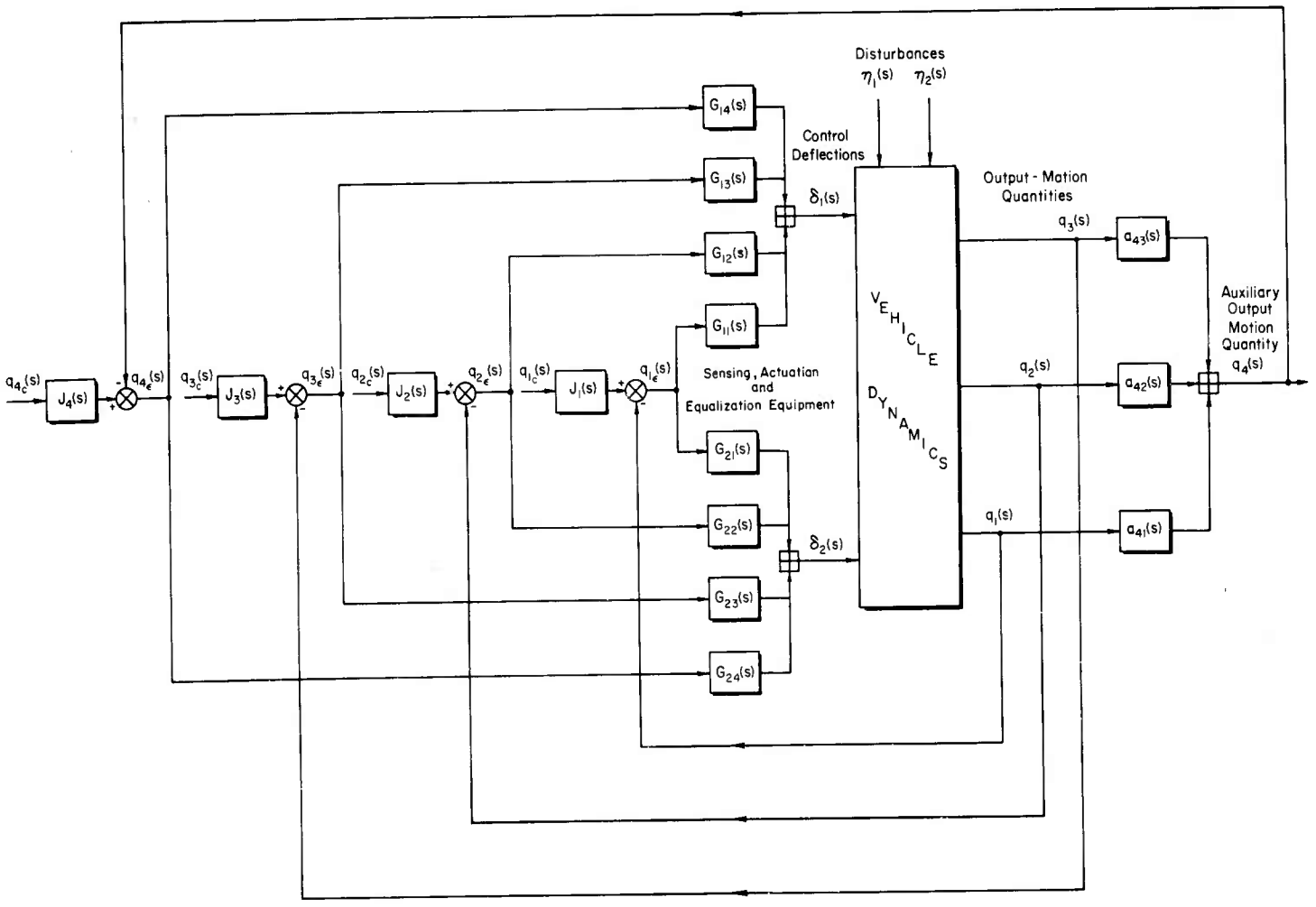

Figure 2. Equivalent Unity-Feedback Block Diagram of General Control System for a Vehicle

$$
\begin{aligned}
a_{11}q_1 + a_{12}q_2 + a_{13}q_3 &= F_{11}\delta_1 + F_{12}\delta_2 + E_{11}\eta_1 + E_{12}\eta_2 \\
a_{21}q_1 + a_{22}q_2 + a_{23}q_3 &= F_{21}\delta_1 + F_{22}\delta_2 + E_{21}\eta_1 + E_{22}\eta_2 \\
a_{31}q_1 + a_{32}q_2 + a_{33}q_3 &= F_{31}\delta_1 + F_{32}\delta_2 + E_{31}\eta_1 + E_{32}\eta_2
\end{aligned} \tag{1}
$$

where the a_{ij}'s are functions of s and vehicle characteristics such as stability derivatives (Ref 11). Then, the vehicle transfer functions for the responses of the independent outputs to control deflections are

$$
\begin{aligned}
\frac{q_1}{\delta_1} &= Q_{1\delta_1} = \frac{N_{q_1\delta_1}}{\Delta} \\
\frac{q_1}{\delta_2} &= Q_{1\delta_2} = \frac{N_{q_1\delta_2}}{\Delta} \\
\frac{q_2}{\delta_1} &= Q_{2\delta_1} = \frac{N_{q_2\delta_2}}{\Delta} \\
&\vdots \qquad\quad \vdots \qquad\quad \vdots \\
\frac{q_i}{\delta_j} &= Q_{i\delta_j} = \frac{N_{q_i\delta_j}}{\Delta}
\end{aligned} \tag{2}
$$

where Δ is the characteristic determinant of the vehicle equations,

$$
\Delta = \begin{vmatrix} a_{11} & a_{12} & a_{13} \\ a_{21} & a_{22} & a_{23} \\ a_{31} & a_{32} & a_{33} \end{vmatrix} \tag{3}
$$

and the numerator, $N_{q_i\delta_j}$, is obtained by replacing the column of q_i coefficients in Δ by the column of δ_j coefficients given on the right side of Eq 1.

Additional shorthand defining the system and the closed-loop transfer functions is also needed. The information required to specify a particular multiloop system is

The command or input to the system

The vehicle output to be controlled

The control deflections to be used

The error signals (or feedbacks) that activate the controllers

This information, using a particular system as an example, will be designated as follows:

$$q_{1_c},\ q_4 \longrightarrow \delta_2\ ;\ q_2,\ q_4 \longrightarrow \delta_1 \tag{4}$$

Here the feedback signals to δ_2 are q_1 and q_4, and to δ_1 are q_2 and q_4. The system input is a command, q_{1_c}, which also implies the directly controlled output. Note that the $q_1 \longrightarrow \delta_2$ feedback is implied by the q_{1_c}, so a separate call-out is redundant. The closed-loop transfer function for this system is designated by

$$\left[\frac{q_1}{q_{1_c}}\right]_{\substack{q_2,\ q_4 \longrightarrow \delta_1 \\ q_1,\ q_4 \longrightarrow \delta_2}} \tag{5}$$

and the appropriate controller equations are

$$\begin{aligned} \delta_1 &= G_{12}(-q_2) + G_{14}(-q_4) \\ \delta_2 &= G_{21}(-q_1) + G_{24}(-q_4) + J_1 G_{21} q_{1_c} \end{aligned} \tag{6}$$

A disturbance, such as η_1, can also appear as a system input.

Other simplifying notation pertinent to specific steps involved in the development of closed-loop system transfer functions will be presented later as required.

B. FORMULATION OF THE SYSTEM EQUATIONS

The complete equations of motion for the vehicle including the auxiliary output motion quantity, q_4, can be considered in two ways. The first uses the three degrees of freedom set, Eq 1, as the vehicle equations and then obtains

auxiliary outputs as linear combinations of the three independent outputs. For example, for q_4 the linear combination would be $q_4 = a_{41}q_1 + a_{42}q_2 + a_{43}q_3$. After substituting this relationship into the control deflection equations, the terms $-G_{14}a_{41}q_1$, $-G_{14}a_{42}q_2$, and $-G_{14}a_{43}q_3$ will appear in the equation for δ_1 and the terms $-G_{24}a_{41}q_1$, $-G_{24}a_{42}q_2$, and $-G_{24}a_{43}q_3$ will appear in the equation for δ_2. When combined with the terms representing controller action on the independent outputs, equivalent controller transfer functions are formed. For example, $G_{14}a_{41} + G_{11}$, $G_{14}a_{42} + G_{12}$, and $G_{14}a_{43} + G_{13}$ replace G_{11}, G_{12}, and G_{13} as the forward loop transfer functions relating q_{1_ϵ}, q_{2_ϵ}, and q_{3_ϵ}, respectively, to δ_1. The q_{4_c} command function can be assigned similarly to the commands for the independent vehicle outputs. Thus, when this approach is used the auxiliary output motion quantity, q_4, effectively disappears into the controller portion of the system.

The second method of including an auxiliary output motion quantity is to treat it in the same way as the independent vehicle outputs. With this scheme the auxiliary output is viewed in association with the vehicle portion of the system. Confining attention to the exemplary case, the three degrees of freedom set, Eq 1, is combined with the equation for q_4. The latter is, of course, redundant as a system equation. Thus,

$$\begin{aligned}
a_{11}q_1 + a_{12}q_2 + a_{13}q_3 &= F_{11}\delta_1 + F_{12}\delta_2 + E_{11}\eta_1 + E_{12}\eta_2 \\
a_{21}q_1 + a_{22}q_2 + a_{23}q_3 &= F_{21}\delta_1 + F_{22}\delta_2 + E_{21}\eta_1 + E_{22}\eta_2 \\
a_{31}q_1 + a_{32}q_2 + a_{33}q_3 &= F_{31}\delta_1 + F_{32}\delta_2 + E_{31}\eta_1 + E_{32}\eta_2 \\
-a_{41}q_1 - a_{42}q_2 - a_{43}q_3 + q_4 &= 0
\end{aligned} \tag{7}$$

or in matrix notation (Ref 12),

$$[a][q] = [F][\delta] + [E][\eta] \tag{8}$$

where

$$[a] = \begin{bmatrix} a_{11} & a_{12} & a_{13} & 0 \\ a_{21} & a_{22} & a_{23} & 0 \\ a_{31} & a_{32} & a_{33} & 0 \\ -a_{41} & -a_{42} & -a_{43} & 1 \end{bmatrix} \tag{9}$$

$$[q] = \begin{bmatrix} q_1 \\ q_2 \\ q_3 \\ q_4 \end{bmatrix} \tag{10}$$

$$[F] = \begin{bmatrix} F_{11} & F_{12} \\ F_{21} & F_{22} \\ F_{31} & F_{32} \\ 0 & 0 \end{bmatrix} \tag{11}$$

$$[\delta] = \begin{bmatrix} \delta_1 \\ \delta_2 \end{bmatrix} \tag{12}$$

$$[E] = \begin{bmatrix} E_{11} & E_{12} \\ E_{21} & E_{22} \\ E_{31} & E_{32} \\ 0 & 0 \end{bmatrix} \tag{13}$$

$$[\eta] = \begin{bmatrix} \eta_1 \\ \eta_2 \end{bmatrix} \tag{14}$$

With four simultaneous commands to each controller, the transformed equations of motion of the controllers for the system of Fig. 2 are

$$\begin{aligned} \delta_1 &= G_{11}(J_1 q_{1_c} - q_1) + G_{12}(J_2 q_{2_c} - q_2) + G_{13}(J_3 q_{3_c} - q_3) + G_{14}(J_4 q_{4_c} - q_4) \\ \delta_2 &= G_{21}(J_1 q_{1_c} - q_1) + G_{22}(J_2 q_{2_c} - q_2) + G_{23}(J_3 q_{3_c} - q_3) + G_{24}(J_4 q_{4_c} - q_4) \end{aligned} \tag{15}$$

or in matrix notation,

$$\begin{aligned}[\delta] &= [G][q_\epsilon] \\ &= [G][J][q_c] - [G][q] \\ &= [G_c][q_c] - [G][q] \end{aligned} \tag{16}$$

where

$$[G] = \begin{bmatrix} G_{11} & G_{12} & G_{13} & G_{14} \\ G_{21} & G_{22} & G_{23} & G_{24} \end{bmatrix} \tag{17}$$

$$[J] = \begin{bmatrix} J_1 & J_2 & J_3 & J_4 \end{bmatrix} \tag{18}$$

$$[G_c] = \begin{bmatrix} G_{11}J_1 & G_{12}J_2 & G_{13}J_3 & G_{14}J_4 \\ G_{21}J_1 & G_{22}J_2 & G_{23}J_3 & G_{24}J_4 \end{bmatrix} \tag{19}$$

$$[q_c] = \begin{bmatrix} q_{1_c} \\ q_{2_c} \\ q_{3_c} \\ q_{4_c} \end{bmatrix} \tag{20}$$

With the formulation of the matrix equations, the system block diagram of Fig. 2 can be replaced by the matrix block diagram shown in Fig. 3. This is as deceptive in its simplicity as Fig. 1 is for apparent complexity. The system equations of motion can be found from either Fig. 3 or Eq 8 and 16. Thus, substituting Eq 16 into Eq 8, transposing and collecting like terms, leads to

$$\Big[[a] + [F][G]\Big][q] = [F][G_c][q_c] + [E][\eta] \tag{21}$$

and after premultiplying by the inverse of $\Big[[a] + [F][G]\Big]$, the explicit expression for $[q]$ becomes

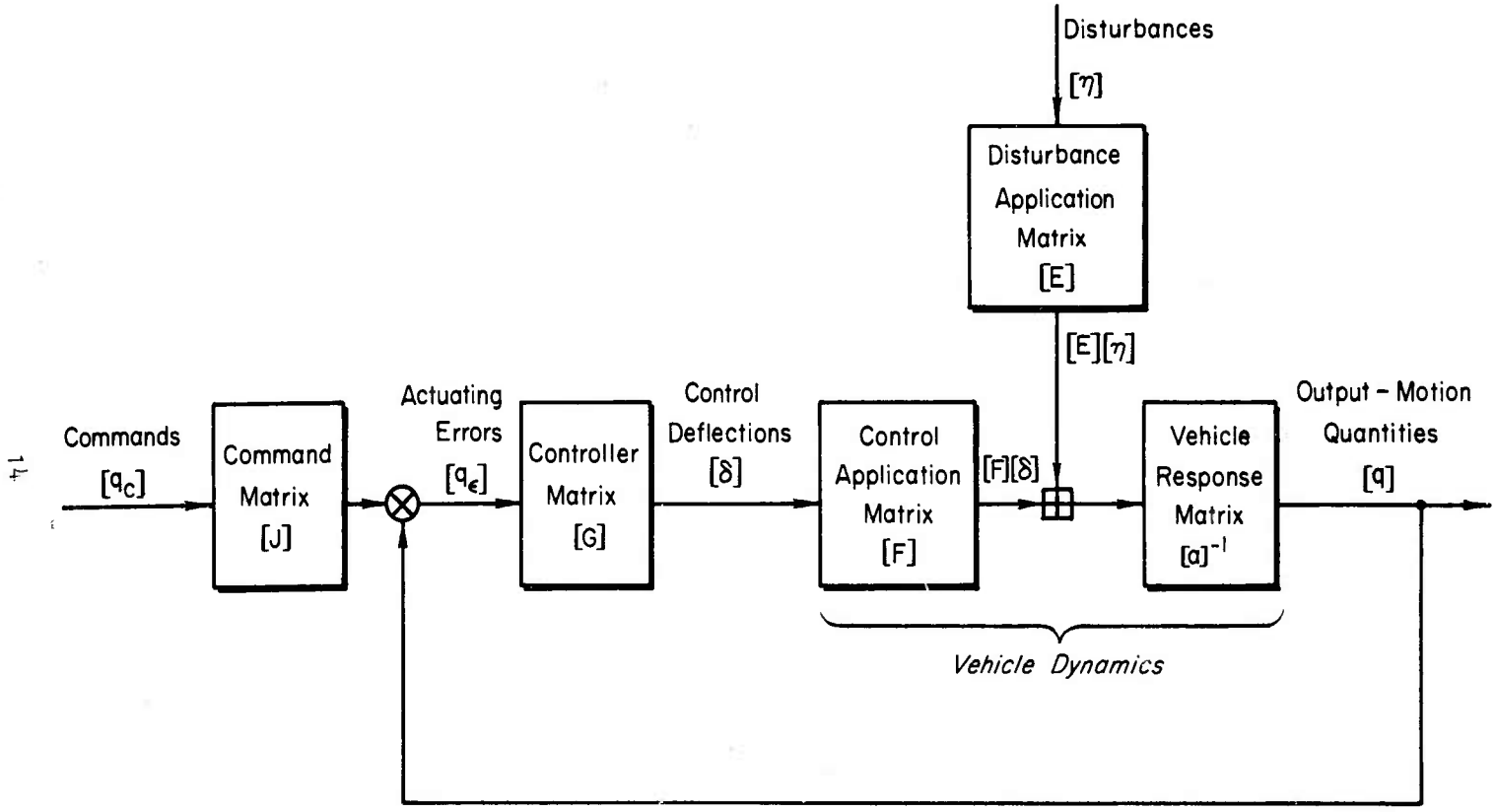

Figure 3. Matrix Block Diagram for General Control System

$$[q] = \left[[a] + [F][G]\right]^{-1}\left\{[F][G_c][q_c] + [E][\eta]\right\} \tag{22}$$

This is the formal solution for the closed-loop system. However, much remains to be done before it has any concrete value in analysis or synthesis procedures using servo methods.

C. REDUCTION OF THE MATRIX EQUATIONS

From Eq 9, 11, and 17, after performing the indicated matrix multiplication and addition,

$$[a] + [F][G] = \begin{bmatrix} a_{11} + F_{11}G_{11} + F_{12}G_{21} & a_{12} + F_{11}G_{12} + F_{12}G_{22} & a_{13} + F_{11}G_{13} + F_{12}G_{23} & F_{11}G_{14} + F_{12}G_{24} \\ a_{21} + F_{21}G_{11} + F_{22}G_{21} & a_{22} + F_{21}G_{12} + F_{22}G_{22} & a_{23} + F_{21}G_{13} + F_{22}G_{23} & F_{21}G_{14} + F_{22}G_{24} \\ a_{31} + F_{31}G_{11} + F_{32}G_{21} & a_{32} + F_{31}G_{12} + F_{32}G_{22} & a_{33} + F_{31}G_{13} + F_{32}G_{23} & F_{31}G_{14} + F_{32}G_{24} \\ -a_{41} & -a_{42} & -a_{43} & 1 \end{bmatrix} \tag{23}$$

When set equal to zero, the determinant of Eq 23 is the closed-loop system characteristic equation; for reasonable controller dynamics (e.g., G_{ij} a second- or third-order system), and a normal vehicle (e.g., a_{ij} first- or second-order in s), it can be a fearsome thing indeed. The routine application of digital computing methods can be used to factor the characteristic equation when all elements are specified numerically. However, in a synthesis procedure, the G's are unknown within a wide range of possible variation. Computing routines which cover such

ranges in increments have been used, but the mass of data to be digested can be immense. Physical appreciation and the transfer to the multiloop problem of understanding gained with simpler systems is almost nil. The net result, more often than not, is to forget direct analysis except possibly as a check on the final results obtained after using an analog computer to narrowly delimit the ranges of suitable controller functions. In any event, pencil-and-paper methods of conventional servoanalysis are not well suited to the problem presented by Eq 21 through 23 as they stand.

Four considerations which relate to a change in the detailed form of the problem to one better suited for servoanalysis procedures are:

1. The vehicle is ordinarily the most complex element in the system and its dynamics tend to be dominant.
2. The study of vehicle-alone dynamics often has separate status as an engineering field (e.g., aeronautical stability and control). Consequently, the vehicle dynamics are fairly well understood.
3. Many of the feedback loops involved in multiloop systems exist primarily to correct vehicle dynamic deficiencies (i.e., parallel equalization) or to suppress particular types of disturbances. The type and general form of most such feedbacks can be derived readily from a knowledge of the vehicle-alone dynamics.
4. Conventional servoanalysis methods are ideally suited to close single loops, e.g., to find $G(s)/[1+G(s)]$ given $G(s)$.

A fruitful approach to the multiloop problem will use these factors to advantage. The scheme developed here does so by (1) expanding the determinant of Eq 23 in such a way that the vehicle characteristic determinant, Δ, and the vehicle transfer function numerators, $N_{q_{i\delta_j}}$, appear explicitly in the closed-loop system characteristic equation, and (2) treating the resulting expressions as a series of "equivalent" single-loop servo systems. The first step provides vehicle-alone dynamics as recognizable separate entities in the system equations instead of as elements in a hodgepodge of vehicle and control terms. This allows direct application of vehicle-alone knowledge and understanding to multiloop control problems. The second step permits many of the fruitful insights and techniques of single-loop servoanalysis to be applied to multiloop situations.

Expansion of the determinant of Eq 23 in such a way as to retain vehicle-alone transfer function elements as separate entities is accomplished in Appendix A.

The result is:

$$\Delta_{sys} = \begin{vmatrix} a_{11} + F_{11}G_{11} + F_{12}G_{21} & a_{12} + F_{11}G_{12} + F_{12}G_{22} & a_{13} + F_{11}G_{13} + F_{12}G_{23} & F_{11}G_{14} + F_{12}G_{24} \\ a_{21} + F_{21}G_{11} + F_{22}G_{21} & a_{22} + F_{21}G_{12} + F_{22}G_{22} & a_{23} + F_{21}G_{13} + F_{22}G_{23} & F_{21}G_{14} + F_{22}G_{24} \\ a_{31} + F_{31}G_{11} + F_{32}G_{21} & a_{32} + F_{31}G_{12} + F_{32}G_{22} & a_{33} + F_{31}G_{13} + F_{32}G_{23} & F_{31}G_{14} + F_{32}G_{24} \\ -a_{41} & -a_{42} & -a_{43} & 1 \end{vmatrix}$$

$$= \Delta + \sum_{i=1}^{4} \sum_{j=1}^{2} G_{ji} N_{q_i \delta_j} + \sum_{\substack{i=1 \\ i \neq k}}^{4} \sum_{k=1}^{4} G_{1i} G_{2k} N_{\delta_1 \delta_2}^{q_i q_k} \qquad (24)$$

Δ and $N_{q_i \delta_j}$ are the characteristic function of the vehicle and the numerator of the $Q_{i\delta_j}$ transfer function, respectively. They are tabulated in terms of airframe parameters for the usual degrees of freedom and control deflections involved in aircraft control in Refs 2, 3, and 11. In the notation presented so far in this report,

$$\Delta = \begin{vmatrix} a_{11} & a_{12} & a_{13} & 0 \\ a_{21} & a_{22} & a_{23} & 0 \\ a_{31} & a_{32} & a_{33} & 0 \\ -a_{41} & -a_{42} & -a_{43} & 1 \end{vmatrix}$$

$$\Delta = \begin{vmatrix} a_{11} & a_{12} & a_{13} \\ a_{21} & a_{22} & a_{23} \\ a_{31} & a_{32} & a_{33} \end{vmatrix} \tag{25}$$

and, as a particular example using the auxiliary output motion quantity,

$$N_{q_4\delta_j} = \begin{vmatrix} a_{11} & a_{12} & a_{13} & F_{1j} \\ a_{21} & a_{22} & a_{23} & F_{2j} \\ a_{31} & a_{32} & a_{33} & F_{3j} \\ -a_{41} & -a_{42} & -a_{43} & 0 \end{vmatrix} \tag{26}$$

$N_{q_i\delta_j}$'s for the independent outputs (i = 1,2,3) will simplify to 3 x 3 determinants.

Terms of the form $N_{\delta_1\delta_2}^{q_iq_k}$ in Eq 24 are called coupling numerators. They are found by replacing the ith and kth columns of Eq 9 by the first and second columns, respectively, of Eq 11. As a particular example using independent outputs,

$$N_{\delta_1\delta_2}^{q_3q_2} = \begin{vmatrix} a_{11} & F_{12} & F_{11} & 0 \\ a_{21} & F_{22} & F_{21} & 0 \\ a_{31} & F_{32} & F_{31} & 0 \\ -a_{41} & 0 & 0 & 1 \end{vmatrix}$$

$$= \begin{vmatrix} a_{11} & F_{12} & F_{11} \\ a_{21} & F_{22} & F_{21} \\ a_{31} & F_{32} & F_{31} \end{vmatrix} \tag{27}$$

This determinant is recognized as the characteristic determinant with the q_3 and q_2 column terms replaced by δ_1 and δ_2 control effectiveness terms, respectively. The awkward but highly descriptive symbol $N_{\delta_1\delta_2}^{q_3q_2}$ is intended to suggest

this replacement. It is apparent that $N_{\delta_1\delta_2}^{q_i q_k}$ has no meaning when i = k. By arbitrarily defining this to be equal to zero, the "i ≠ k" note on Eq 24 can be removed. The coupling numerators have other properties of interest such as

$$N_{\delta_1\delta_1}^{q_i q_k} = N_{\delta_2\delta_2}^{q_i q_k} = 0 \tag{28}$$

$$N_{\delta_1\delta_2}^{q_i q_k} = -N_{\delta_2\delta_1}^{q_i q_k} = N_{\delta_2\delta_1}^{q_k q_i} \tag{29}$$

$$N_{\delta_1\delta_2}^{q_i q_k} = \frac{1}{\Delta}\left(N_{q_i\delta_1} N_{q_k\delta_2} - N_{q_i\delta_2} N_{q_k\delta_1}\right) \tag{30}$$

Common coupling numerators for aircraft control are presented in Appendix B.

While the system characteristic equation, Δ_{sys}, is the denominator for all closed-loop transfer functions, regardless of command inputs, the numerators depend on the particular command input. The outputs due to command inputs can be obtained from Eq 22. With disturbances zero,

$$[q] = \left[[a] + [F][G]\right]^{-1}[F][G_c][q_c] \tag{31}$$

where $[q]$, $[F]$, and $[q_c]$ are given in Eq 10, 11, and 20, respectively. The matrix $\left[[a] + [F][G]\right]^{-1}$ is, after inversion, expressible as

$$\left[[a] + [F][G]\right]^{-1} = \frac{\begin{bmatrix} \Delta_{11} & \Delta_{21} & \Delta_{31} & \Delta_{41} \\ \Delta_{12} & \Delta_{22} & \Delta_{32} & \Delta_{42} \\ \Delta_{13} & \Delta_{23} & \Delta_{33} & \Delta_{43} \\ \Delta_{14} & \Delta_{24} & \Delta_{34} & \Delta_{44} \end{bmatrix}}{\Delta_{sys}} \tag{32}$$

where the numerator is the transpose of the matrix made up of the cofactors of Eq 24. Thus,

$$\Delta_{11} = \begin{vmatrix} a_{22} + F_{21}G_{12} + F_{22}G_{22} & a_{23} + F_{21}G_{13} + F_{22}G_{23} & F_{21}G_{14} + F_{22}G_{24} \\ a_{32} + F_{31}G_{12} + F_{32}G_{22} & a_{33} + F_{31}G_{13} + F_{32}G_{23} & F_{31}G_{14} + F_{32}G_{24} \\ -a_{42} & -a_{43} & 1 \end{vmatrix} \quad (33)$$

is the cofactor of $(a_{11} + F_{11}G_{11} + F_{12}G_{21})$ in the determinant of Eq 24. Similarly, Δ_{12} is the cofactor of $(a_{12} + F_{11}G_{12} + F_{12}G_{22})$ in the same determinant. The other matrix involved in Eq 31 is $[F][G_c][q_c]$. For the typical case where $[G_c] = [G]$, the matrix multiplication of $[F][G][q_c]$ results in

$$[F][G][q_c] = \begin{bmatrix} (F_{11}G_{11} + F_{12}G_{21})q_{1_c} & (F_{11}G_{12} + F_{12}G_{22})q_{2_c} & (F_{11}G_{13} + F_{12}G_{23})q_{3_c} & (F_{11}G_{14} + F_{12}G_{24})q_{4_c} \\ (F_{21}G_{11} + F_{22}G_{21})q_{1_c} & (F_{21}G_{12} + F_{22}G_{22})q_{2_c} & (F_{21}G_{13} + F_{22}G_{23})q_{3_c} & (F_{21}G_{14} + F_{22}G_{24})q_{4_c} \\ (F_{31}G_{11} + F_{32}G_{21})q_{1_c} & (F_{31}G_{12} + F_{32}G_{22})q_{2_c} & (F_{31}G_{13} + F_{32}G_{23})q_{3_c} & (F_{31}G_{14} + F_{32}G_{24})q_{4_c} \\ 0 & 0 & 0 & 0 \end{bmatrix} \quad (34)$$

Using only q_{1_c} as an example (i.e., $q_{2_c} = q_{3_c} = q_{4_c} = 0$), the closed-loop system transfer function is

$$\frac{q_1}{q_{1_c}} = \frac{\Delta_{11}(F_{11}G_{11} + F_{12}G_{21}) + \Delta_{21}(F_{21}G_{11} + F_{22}G_{21}) + \Delta_{31}(F_{31}G_{11} + F_{32}G_{21})}{\Delta_{sys}} \quad (35)$$

Closed-loop transfer functions for q_2/q_{1_c}, etc., or transfer functions for disturbance inputs, such as q_1/η_1, are obtained in a similar way.

Although the development can be continued along the above lines, the details are so tedious that the main stream of the argument is obscured. Therefore, a considerably simpler system, shown in Fig. 4, will be used. (The matrix block diagram of Fig. 3 still applies.) Even this system is more complex than most flight control systems, so still further simplifications will later be made.

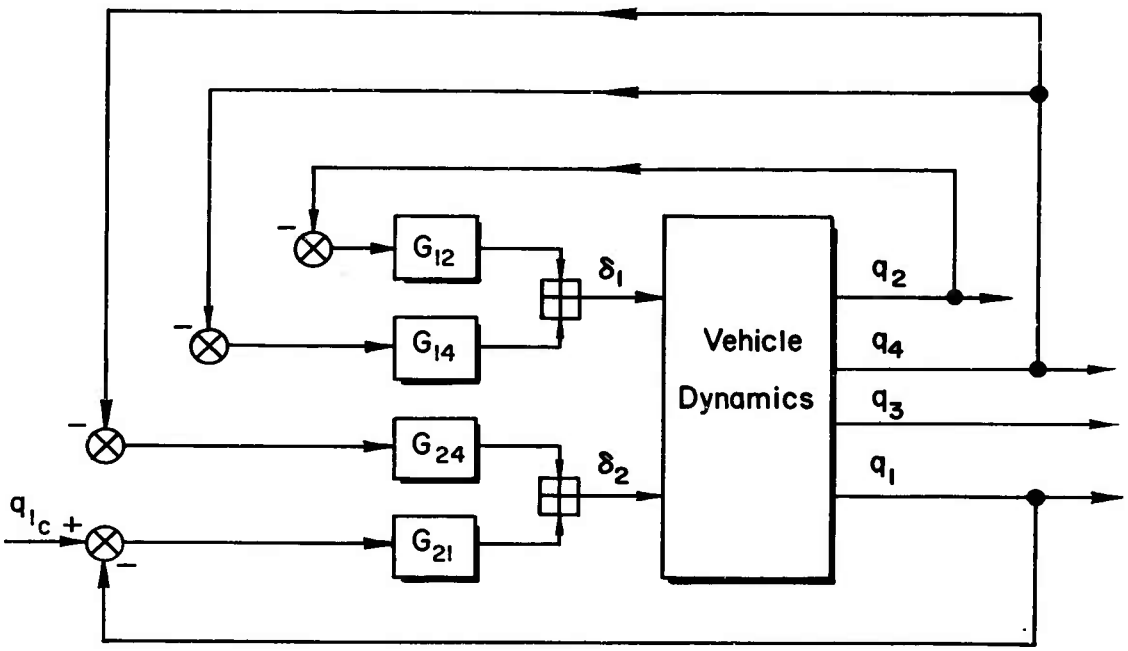

Figure 4. Block Diagram of Multiloop System

q_{1_c}, $q_4 \rightarrow \delta_2$; q_2, $q_4 \rightarrow \delta_1$

In Fig. 4, all of the command and disturbance inputs are zero except q_{1_c}, and there is only one feedback to the controlled variable. The remaining feedbacks are intended only to modify the basic vehicle characteristics. The closed-loop transfer function of the primary controlled variable, q_1, is, from Eq 35,

$$\left.\frac{q_1}{q_{1_c}}\right]_{\substack{q_2, q_4 \rightarrow \delta_1 \\ q_1, q_4 \rightarrow \delta_2}} = G_{21} \frac{F_{12}\Delta_{11} + F_{22}\Delta_{21} + F_{32}\Delta_{31}}{\Delta_{sys}} \qquad (36)$$

or, written as determinants,

$$\left.\frac{q_1}{q_{1_c}}\right]_{\substack{q_2,\ q_4\to\delta_1 \\ q_1,\ q_4\to\delta_2}} = \frac{\begin{vmatrix} F_{12}G_{21} & a_{12}+F_{11}G_{12} & a_{13} & F_{11}G_{14}+F_{12}G_{24} \\ F_{22}G_{21} & a_{22}+F_{21}G_{12} & a_{23} & F_{21}G_{14}+F_{22}G_{24} \\ F_{32}G_{21} & a_{32}+F_{31}G_{12} & a_{33} & F_{31}G_{14}+F_{32}G_{24} \\ 0 & -a_{42} & -a_{43} & 1 \end{vmatrix}}{\begin{vmatrix} a_{11}+F_{12}G_{21} & a_{12}+F_{11}G_{12} & a_{13} & F_{11}G_{14}+F_{12}G_{24} \\ a_{21}+F_{22}G_{21} & a_{22}+F_{21}G_{12} & a_{23} & F_{21}G_{14}+F_{22}G_{24} \\ a_{31}+F_{32}G_{21} & a_{32}+F_{31}G_{12} & a_{33} & F_{31}G_{14}+F_{32}G_{24} \\ -a_{41} & -a_{42} & -a_{43} & 1 \end{vmatrix}} \qquad (37)$$

The denominator can be most readily obtained by specializing Eq 24; that is,

$$\Delta_{sys} = \Delta + G_{12}N_{q_{2\delta_1}} + G_{14}N_{q_{4\delta_1}} + G_{21}N_{q_{1\delta_2}} + G_{24}N_{q_{4\delta_2}} + G_{12}G_{21}N_{\delta_1\delta_2}^{q_2q_1} + G_{12}G_{24}N_{\delta_1\delta_2}^{q_2q_4} + G_{14}G_{21}N_{\delta_1\delta_2}^{q_4q_1} \qquad (38)$$

In the numerator and denominator of Eq 37, the cofactors of terms containing G_{21} are identical. Thus, q_1/q_{1_c} can be obtained directly from the system characteristic as given in Eq 24 or 38. The closed-loop transfer function q_1/q_{1_c} is then

$$\left.\frac{q_1}{q_{1_c}}\right]_{\substack{q_2,\ q_4\to\delta_1 \\ q_1,\ q_4\to\delta_2}} = \frac{G_{21}\left(N_{q_{1\delta_2}} + G_{12}N_{\delta_1\delta_2}^{q_2q_1} + G_{14}N_{\delta_1\delta_2}^{q_4q_1}\right)}{\Delta + G_{12}N_{q_{2\delta_1}} + G_{14}N_{q_{4\delta_1}} + G_{24}\left(N_{q_{4\delta_2}} + G_{12}N_{\delta_1\delta_2}^{q_2q_4}\right) + \left[G_{21}\left(N_{q_{1\delta_2}} + G_{12}N_{\delta_1\delta_2}^{q_2q_1} + G_{14}N_{\delta_1\delta_2}^{q_4q_1}\right)\right]} \qquad (39)$$

Equation 39 contains vehicle transfer function numerators and denominators as

separate entities. By dividing the numerator and denominator of Eq 39 by Δ, q_1/q_{1_c} can be expressed in terms including vehicle transfer functions themselves; that is,

$$\left.\frac{q_1}{q_{1_c}}\right]_{\substack{q_2,\ q_4\to\delta_1 \\ q_1,\ q_4\to\delta_2}} = \frac{G_{21}Q_{1\delta_2}\left(1 + G_{12}\dfrac{N_{\delta_1\delta_2}^{q_2q_1}}{N_{q_1\delta_2}} + G_{14}\dfrac{N_{\delta_1\delta_2}^{q_4q_1}}{N_{q_1\delta_2}}\right)}{1 + G_{12}Q_{2\delta_1} + G_{14}Q_{4\delta_1} + G_{24}Q_{4\delta_2}\left(1 + G_{12}\dfrac{N_{\delta_1\delta_2}^{q_2q_4}}{N_{q_4\delta_2}}\right) + \left[G_{21}Q_{1\delta_2}\left(1 + G_{12}\dfrac{N_{\delta_1\delta_2}^{q_2q_1}}{N_{q_1\delta_2}} + G_{14}\dfrac{N_{\delta_1\delta_2}^{q_4q_1}}{N_{q_1\delta_2}}\right)\right]} \tag{40}$$

where $Q_{2\delta_1}$, $Q_{4\delta_1}$, $Q_{1\delta_2}$, and $Q_{4\delta_2}$ are vehicle transfer functions.

The bracketed term in the denominator of either Eq 39 or 40 is seen to be identical to the numerator terms. This makes it easy to recognize that the open-loop transfer function q_1/q_{1_ϵ} is just

$$\left.\frac{q_1}{q_{1_\epsilon}}\right]_{\substack{q_2,\ q_4\to\delta_1 \\ q_4\to\delta_2}} = \frac{G_{21}\left(N_{q_1\delta_2} + G_{12}N_{\delta_1\delta_2}^{q_2q_1} + G_{14}N_{\delta_1\delta_2}^{q_4q_1}\right)}{\Delta + G_{12}N_{q_2\delta_1} + G_{14}N_{q_4\delta_1} + G_{24}\left(N_{q_4\delta_2} + G_{12}N_{\delta_1\delta_2}^{q_2q_4}\right)} \tag{41}$$

or, dividing both numerator and denominator by Δ,

$$\left.\frac{q_1}{q_{1_\epsilon}}\right]_{\substack{q_2,\ q_4\to\delta_1 \\ q_4\to\delta_2}} = \frac{G_{21}Q_{1\delta_2}\left(1 + G_{12}\dfrac{N_{\delta_1\delta_2}^{q_2q_1}}{N_{q_1\delta_2}} + G_{14}\dfrac{N_{\delta_1\delta_2}^{q_4q_1}}{N_{q_1\delta_2}}\right)}{1 + G_{12}Q_{2\delta_1} + G_{14}Q_{4\delta_1} + G_{24}Q_{4\delta_2}\left(1 + G_{12}\dfrac{N_{\delta_1\delta_2}^{q_2q_4}}{N_{q_4\delta_2}}\right)} \tag{42}$$

Although not directly apparent because of their complexity, Eq 39 through 42 are of a form to permit knowledge of vehicle-alone characteristics to be used with maximum benefit in system synthesis procedures based on conventional servoanalysis methods. All of the terms contain vehicle-alone transfer functions or ratios of coupling and conventional numerators; and only controller transfer functions (the G's) multiply such terms. Also, the total transfer function forms of Eq 39 through 42 can be generated readily by successive loop closures (a mere seven in the case of Eq 39 and 40!) using these elemental vehicle and controller characteristics. Remarkably, it is possible, as will be illustrated by subsequent examples, to rapidly and effectively perform these operations in a fashion leading to a good closed-loop system while retaining physical appreciation and developing insights throughout the process.

Indirectly controlled output transfer functions, q_n/q_{i_c} $(n \neq i)$, are also required for some purposes. Such transfer functions as

$$\left.\frac{q_n}{q_{1_c}}\right]_{\substack{q_2,\ q_4 \to \delta_1 \\ q_1,\ q_4 \to \delta_2}} = \frac{N_n}{\Delta_{sys}} \tag{43}$$

can be determined from an expansion of Eq 22. The characteristic function, Δ_{sys}, has already been given in symbolic terms for the general system in Eq 24 and for the simplified system of Fig. 4 in Eq 38, so expressions for N_n alone are required. These are easily obtained from N_i by replacing q_i subscripts and superscripts by q_n's in the transfer function numerator. For example, using q_1/q_{1_c} as given by Eq 39, the closed-loop transfer function q_3/q_{1_c} becomes

$$\left.\frac{q_3}{q_{1_c}}\right]_{\substack{q_2,\ q_4 \to \delta_1 \\ q_1,\ q_4 \to \delta_2}} = \frac{G_{21}\left(N_{q_{3_{\delta_2}}} + G_{12}N^{q_2q_3}_{\delta_1\delta_2} + G_{14}N^{q_4q_3}_{\delta_1\delta_2}\right)}{\Delta + G_{12}N_{q_{2_{\delta_1}}} + G_{14}N_{q_{4_{\delta_1}}} + G_{24}\left(N_{q_{4_{\delta_2}}} + G_{12}N^{q_2q_4}_{\delta_1\delta_2}\right) + G_{21}\left(N_{q_{1_{\delta_2}}} + G_{12}N^{q_2q_1}_{\delta_1\delta_2} + G_{14}N^{q_4q_1}_{\delta_1\delta_2}\right)} \tag{44}$$

This indirectly controlled output transfer function can also be obtained by multiplying and dividing Eq 44 by $G_{21}\left(N_{q_1\delta_2} + G_{12}N_{\delta_1\delta_2}^{q_2q_1} + G_{14}N_{\delta_1\delta_2}^{q_4q_1}\right)$ and using Eq 39. The result of these operations is

$$\left.\frac{q_3}{q_{1_c}}\right]_{\substack{q_2,\ q_4\to\delta_1 \\ q_1,\ q_4\to\delta_2}} = \left(\frac{N_3}{N_1}\right)\left.\frac{q_1}{q_{1_c}}\right]_{\substack{q_2,\ q_4\to\delta_1 \\ q_1,\ q_4\to\delta_2}} \tag{45}$$

where

$$\frac{N_3}{N_1} = \frac{N_{q_3\delta_2} + G_{12}N_{\delta_1\delta_2}^{q_2q_3} + G_{14}N_{\delta_1\delta_2}^{q_4q_3}}{N_{q_1\delta_2} + G_{12}N_{\delta_1\delta_2}^{q_2q_1} + G_{14}N_{\delta_1\delta_2}^{q_4q_1}} \tag{46}$$

An alternate procedure for formulating the system closed-loop transfer function numerator and denominator expansions is presented in Appendix C.

D. GENERAL ANALYSIS PROCEDURE

The developments above provide general formulations of the multiloop problem in matrix form, and illustrate a special expansion for the matrix equations. The results of the special expansion are various closed-loop transfer functions expressed in terms of elemental vehicle and controller characteristics. The final step is the application of conventional servoanalysis techniques to the transfer functions as formulated above. This phase will be discussed here in general terms, and the specifics will be illustrated in succeeding sections using particular systems.

To make the discussion as simple and concrete as possible while retaining the generalized notation, consider the system given by the block diagram of Fig. 5. This is the simplest possible multiloop system using multiple control deflections. It is just complex enough to exhibit, on a rudimentary scale, the major features of far more complicated systems. Further simplification, to a system with one active control deflection but retaining two output motion feedbacks, results in a multiloop system which is too limited to illustrate all the features of interest.

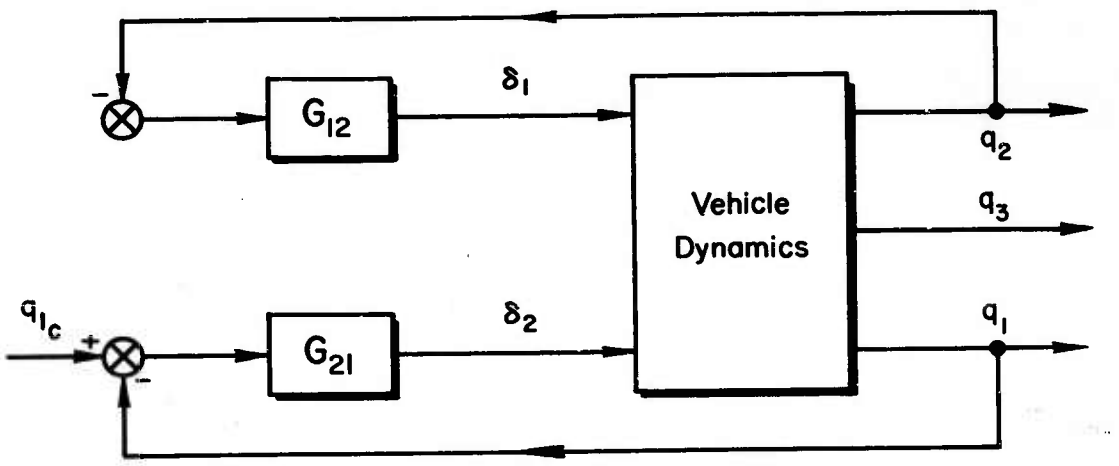

Figure 5. Block Diagram of Multiloop System

$q_{1_c} \rightarrow \delta_2$; $q_2 \rightarrow \delta_1$

Specialization of Eq 39 and 40 to the system of Fig. 5 ($G_{14} = G_{24} = 0$) results in the closed-loop transfer function forms given below.

$$\left.\frac{q_1}{q_{1_c}}\right]_{\substack{q_2 \rightarrow \delta_1 \\ q_1 \rightarrow \delta_2}} = \frac{G_{21}\left(N_{q_{1\delta_2}} + G_{12}N^{q_2q_1}_{\delta_1\delta_2}\right)}{\Delta + G_{12}N_{q_{2\delta_1}} + G_{21}\left(N_{q_{1\delta_2}} + G_{12}N^{q_2q_1}_{\delta_1\delta_2}\right)} \tag{47}$$

$$\left.\frac{q_1}{q_{1_c}}\right]_{\substack{q_2 \rightarrow \delta_1 \\ q_1 \rightarrow \delta_2}} = \frac{G_{21}Q_{1\delta_2}\left(1 + G_{12}\dfrac{N^{q_2q_1}_{\delta_1\delta_2}}{N_{q_{1\delta_2}}}\right)}{1 + G_{12}Q_{2\delta_1} + G_{21}Q_{1\delta_2}\left(1 + G_{12}\dfrac{N^{q_2q_1}_{\delta_1\delta_2}}{N_{q_{1\delta_2}}}\right)} \tag{48}$$

The open-loop transfer function for the command loop, with the other (q_2) loop closed, is a special case of Eq 41 and 42; that is,

$$\left.\frac{q_1}{q_{1_\epsilon}}\right]_{q_2 \to \delta_1} = \frac{G_{21}\left(N_{q_1\delta_2} + G_{12}N_{\delta_1\delta_2}^{q_2q_1}\right)}{\Delta + G_{12}N_{q_2\delta_1}} \tag{49}$$

$$= G_{21}Q_{1\delta_2}\left[\frac{1 + G_{12}\dfrac{N_{\delta_1\delta_2}^{q_2q_1}}{N_{q_1\delta_2}}}{1 + G_{12}Q_{2\delta_1}}\right] \tag{50}$$

The vehicle characteristics for this system are given by:

$$\Delta = \begin{vmatrix} a_{11} & a_{12} & a_{13} \\ a_{21} & a_{22} & a_{23} \\ a_{31} & a_{32} & a_{33} \end{vmatrix} \tag{51}$$

$$Q_{1\delta_2} = \frac{N_{q_1\delta_2}}{\Delta} = \frac{\begin{vmatrix} F_{12} & a_{12} & a_{13} \\ F_{22} & a_{22} & a_{23} \\ F_{32} & a_{32} & a_{33} \end{vmatrix}}{\Delta} \tag{52}$$

$$Q_{2\delta_1} = \frac{N_{q_2\delta_1}}{\Delta} = \frac{\begin{vmatrix} a_{11} & F_{11} & a_{13} \\ a_{21} & F_{21} & a_{23} \\ a_{31} & F_{31} & a_{33} \end{vmatrix}}{\Delta} \tag{53}$$

$$N_{\delta_1\delta_2}^{q_2q_1} = \begin{vmatrix} F_{12} & F_{11} & a_{13} \\ F_{22} & F_{21} & a_{23} \\ F_{32} & F_{31} & a_{33} \end{vmatrix} \tag{54}$$

An "equivalent block diagram" for Eq 47 through 50 is given in Fig. 6. This block diagram is "equivalent" in the sense that its reduction via loop closures and block diagram algebra results in Eq 49 or 50 for the open command (q_1) loop, and in Eq 47 or 48 for the complete closed-loop system. In one limiting case, when $G_{12} = 0$ (the q_2 loop opened), the resulting single-loop system is just the command loop closed around the vehicle-alone transfer function, $Q_{1_{\delta_2}}$. For the other limiting case, $G_{21} = 0$, the q_2 loop is the only one closed, and the modified vehicle dynamics are those resulting from the closure of a single unity-feedback loop about the transfer function $G_{12}Q_{2_{\delta_1}}$.

A very instructive way to consider the effect of the closed q_2 loop is to lump all of its consequences into "effective" vehicle changes. In this view, closure of the q_2 loop changes the command loop effective-vehicle transfer function from $Q_{1_{\delta_2}}$ to $Q'_{1_{\delta_2}}$ (see Fig. 6). Referring to Eq 49 and 50, the effective-vehicle characteristics, $Q'_{1_{\delta_2}}$, will be the open-loop transfer function of the command loop with the controller transfer function G_{21} removed.

$$Q'_{1_{\delta_2}} = \frac{N_{q_{1_{\delta_2}}} + G_{12}N_{\delta_1\delta_2}^{q_2q_1}}{\Delta + G_{12}N_{q_{2_{\delta_1}}}} \tag{55}$$

$$= Q_{1_{\delta_2}}\left[\frac{1 + G_{12}\dfrac{N_{\delta_1\delta_2}^{q_2q_1}}{N_{q_{1_{\delta_2}}}}}{1 + G_{12}Q_{2_{\delta_1}}}\right] \tag{56}$$

In general, s appears in higher orders in the denominators of $G_{12}Q_{2_{\delta_1}}$ and $G_{12}N_{\delta_1\delta_2}^{q_2q_1}/N_{q_{1_{\delta_2}}}$ than in the numerators, so

$$G_{12}Q_{2_{\delta_1}}\Big]_{s\to\infty} \longrightarrow 0$$

$$G_{12}\left.\frac{N_{\delta_1\delta_2}^{q_2q_1}}{N_{q_{1_{\delta_2}}}}\right]_{s\to\infty} \longrightarrow 0$$

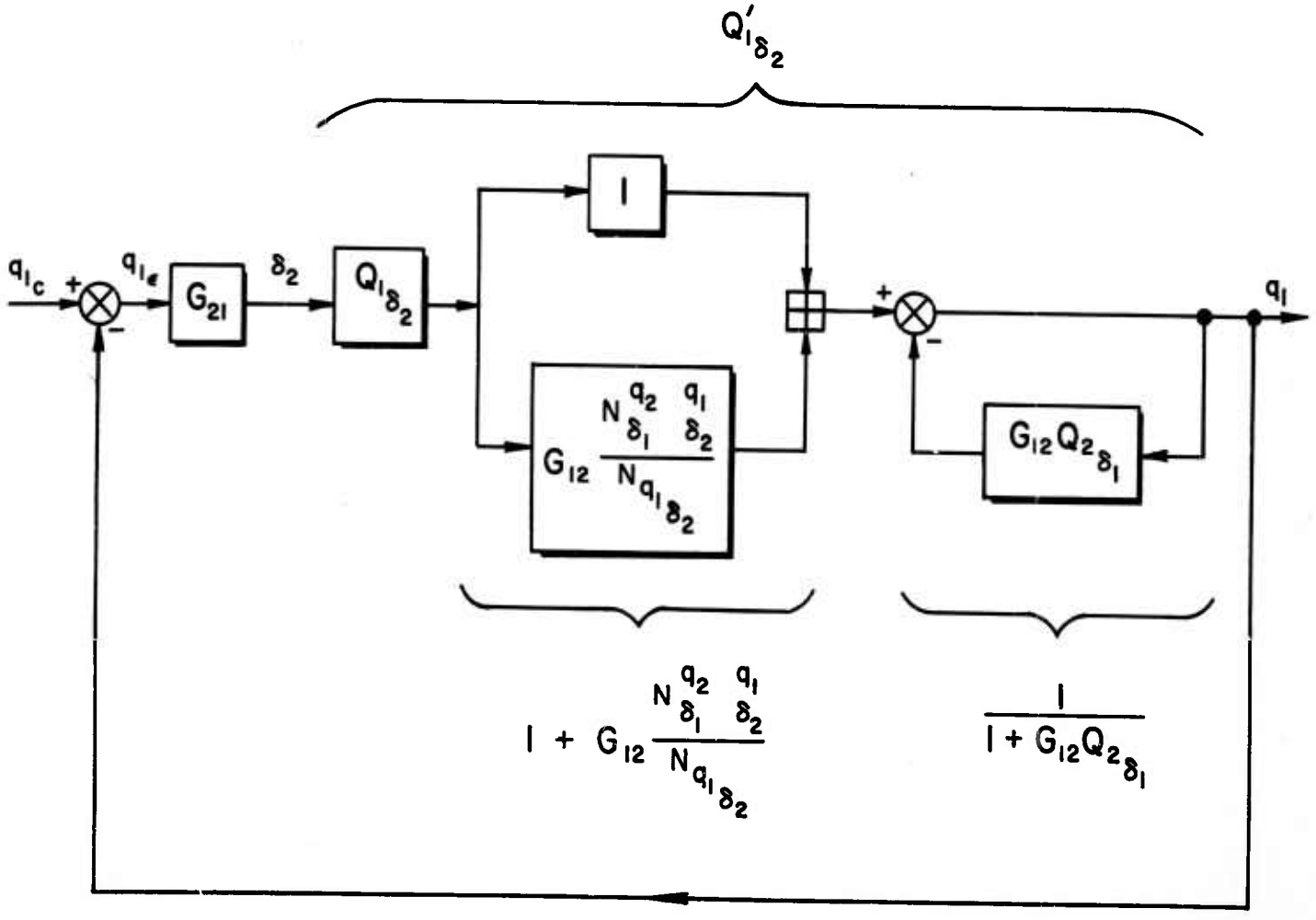

Figure 6. Equivalent Block Diagram for the System
$q_{1c} \rightarrow \delta_2$; $q_2 \rightarrow \delta_1$

Therefore the so-called root locus, or high frequency, gain of $Q'_{1\delta_2}$ is identical to that for $Q_{1\delta_2}$.

The primed notation on $Q'_{1\delta_2}$ is used to indicate merely that one loop has been closed, and is not intended to specify the particular loop closure involved. If, for example, a loop closure of $q_3 \rightarrow \delta_1$ replaced the $q_2 \rightarrow \delta_1$ closure in Fig. 5, the transfer function $Q'_{1\delta_2}$ would still indicate the resulting command loop effective-vehicle transfer function. The precise meaning of the primed notation consequently depends on the local context. (Later, the primed notation is used in a similar fashion on individual transfer function terms to indicate the number of prior loop closures.)

Finding the complete form of $Q'_{1\delta_2}$ involves operations converting

$$G_{12}Q_{2\delta_1} \quad \text{to} \quad \frac{1}{1 + G_{12}Q_{2\delta_1}},$$

and

$$G_{12}\frac{N_{\delta_1\delta_2}^{q_2q_1}}{N_{q_1\delta_2}} \quad \text{to} \quad 1 + G_{12}\frac{N_{\delta_1\delta_2}^{q_2q_1}}{N_{q_1\delta_2}},$$

Such operations are easily accomplished by closing the single loops shown in Fig. 7 using any of a variety of conventional servoanalysis techniques. Letting $G_{12} = N_{12}/D_{12}$, where both N_{12} and D_{12} are polynomials in s, with the leading coefficient of D_{12} equal to unity and the leading coefficient of N_{12} being the root locus gain of G_{12}, the results desired from the loop closures are:

$$\frac{1}{1 + G_{12}Q_{2\delta_1}} = \frac{D_{12}\Delta}{D_{12}\Delta + N_{12}N_{q_2\delta_1}}$$

$$= \frac{D_{12}\Delta}{(\text{Closed-loop pole factors of } \textcircled{1})} \qquad (57)$$

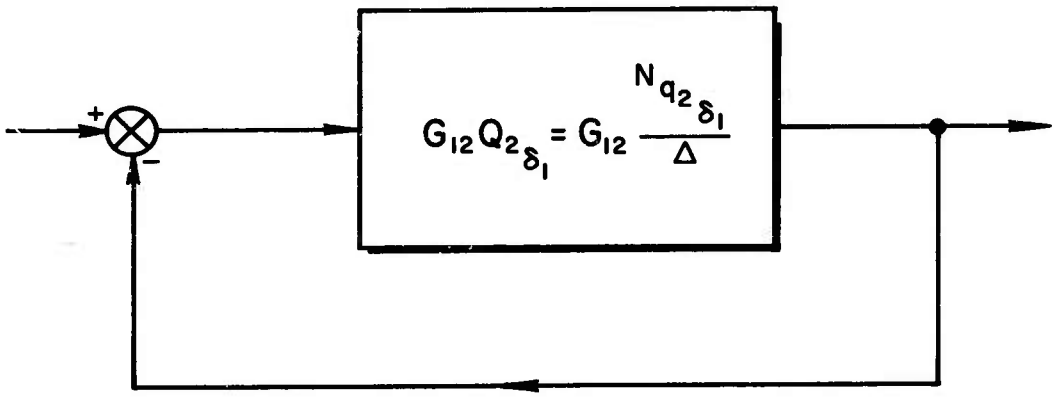

a) Closure ①

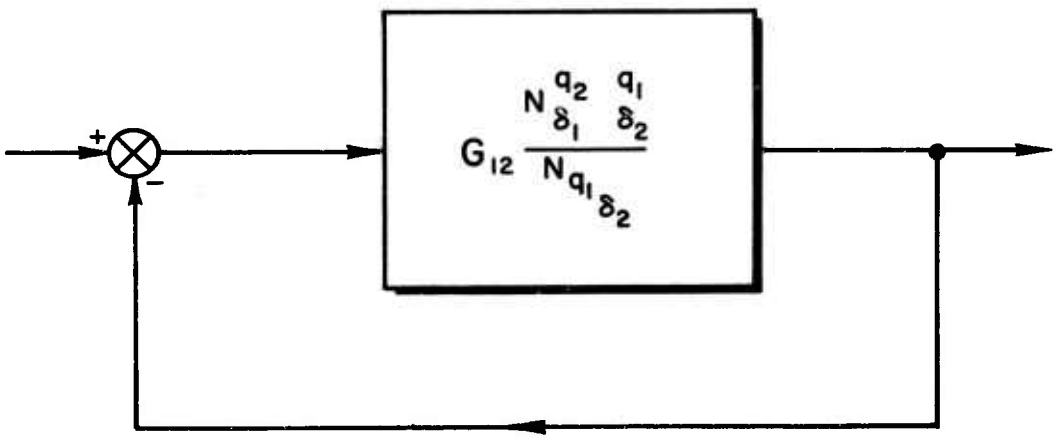

b) Closure ②, "Coupling Loop"

Figure 7. q_2 Loop Closures Involved in the System $q_{1_c} \rightarrow \delta_2$; $q_2 \rightarrow \delta_1$

$$1 + G_{12}\frac{N^{q_2q_1}_{\delta_1\delta_2}}{N_{q_1\delta_2}} = \frac{D_{12}N_{q_1\delta_2} + N_{12}N^{q_2q_1}_{\delta_1\delta_2}}{D_{12}N_{q_1\delta_2}}$$

$$= \frac{(\text{Closed-loop pole factors of } \textcircled{2})}{D_{12}N_{q_1\delta_2}} \qquad (58)$$

where ① and ② refer to the single-loop systems shown in Fig. 7. For fixed vehicle characteristics, G_{12} is the only variable quantity in both relationships. Thus, choosing G_{12} appropriate to either ① or ② automatically determines the other closure (② or ①). The closures of ① and ② are, therefore, "simultaneous." Loop ① is a primary closure directly affecting the vehicle's poles, whereas loop ② (as will be seen below) affects the vehicle zeros pertinent to a particular input control deflection—in this case, δ_2. Accordingly, loop ②, or its reflection in Fig. 6, is often called a "coupling loop."

The two loops are further related in that the high frequency open- and closed-loop asymptotes of systems ① and ② are usually nearly identical, i.e., the "root-locus gains" are almost the same. This is easiest to see for typical aircraft characteristics in which the highest order s terms in Δ stem from the main diagonal ($a_{11}a_{22}a_{33}$), and the control effectiveness terms (F_{ij}) all have the same form in s (usually constants). Then, at frequencies much greater than all the poles and zeros in Δ, denoted as "|s| large", pertinent quantities become

$$\left[N^{q_2q_1}_{\delta_1\delta_2}\right]_{|s|\text{ large}} \rightarrow \left[(F_{12}F_{21} - F_{11}F_{22})a_{33}\right]_{|s|\text{ large}}$$

$$\left[N_{q_1\delta_2}\right]_{|s|\text{ large}} \rightarrow \left[F_{12}a_{22}a_{33}\right]_{|s|\text{ large}}$$

so

$$\left[\frac{N^{q_2q_1}_{\delta_1\delta_2}}{N_{q_1\delta_2}}\right]_{|s|\text{ large}} \rightarrow \left[\frac{F_{21}}{a_{22}} - \frac{F_{11}F_{22}}{a_{22}F_{12}}\right]_{|s|\text{ large}} \qquad (59)$$

and, similarly,

$$Q_{2\delta_1}\Big]_{|s| \text{ large}} \longrightarrow \frac{a_{11}a_{33}F_{21}}{a_{11}a_{22}a_{33}}\Big]_{|s| \text{ large}} = \frac{F_{21}}{a_{22}}\Big]_{|s| \text{ large}} \tag{60}$$

When $F_{21} \gg F_{11}F_{22}/F_{12}$, a relatively common occurrence in aircraft, Eq 59 and 60 are very nearly the same. This correspondence should be kept in mind when actually performing the simultaneous closures of ① and ②.

When the results of the simultaneous closures are combined and multiplied by the vehicle transfer function $Q_{1\delta_2}$, then $Q'_{1\delta_2}$, the effective q_1/δ_2 transfer function of the vehicle with the q_2 loop closed, is

$$Q'_{1\delta_2} = Q_{1\delta_2}\left[\frac{1 + G_{12}\dfrac{q_2q_1}{N_{\delta_1\delta_2}}}{1 + G_{12}Q_{2\delta_1}}\right]$$

$$= \frac{N_{q_{1\delta_2}}}{\Delta}\frac{(\text{Closed-loop pole factors of } ②)}{D_{12}N_{q_{1\delta_2}}}\frac{D_{12}\Delta}{(\text{Closed-loop pole factors of } ①)}$$

$$= \frac{(\text{Closed-loop pole factors of } ②)}{(\text{Closed-loop pole factors of } ①)} \tag{61}$$

As already noted in connection with Eq 55 and 56, the net "root-locus gain" for $Q'_{1\delta_2}$, after the closures of ① and ②, will be the same as that for $Q_{1\delta_2}$. This high-frequency gain is implicitly contained in the $Q'_{1\delta_2}$ numerator term resulting from closure of loop ② (it arises from the $D_{12}N_{q_{1\delta_2}}$ numerator term in Eq 58).

After $Q'_{1\delta_2}$ is found, the final q_1/q_{1_c} closed-loop system characteristics are determined by another loop closure using the system of Fig. 8.

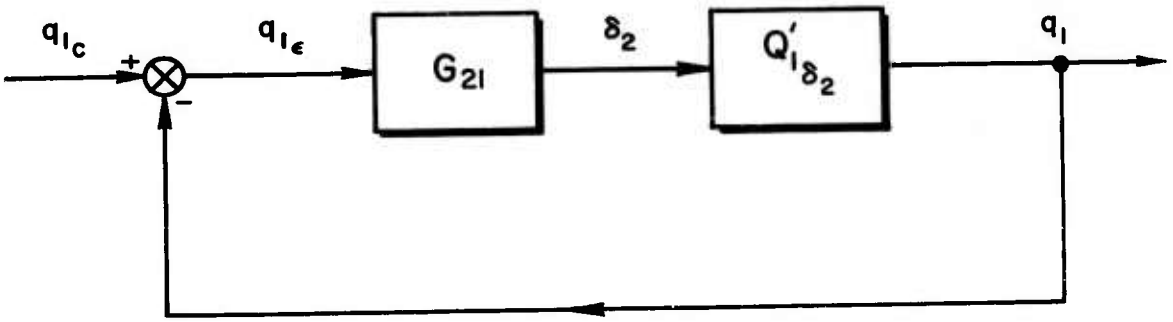

Figure 8. Command Loop Closure for the System $q_{1_c} \rightarrow \delta_2$; $q_2 \rightarrow \delta_1$

In summary, the steps involved in the analysis of the system in Fig. 5 are:

1. The control channels are divided into two categories, "inner" and "outer" loops, reflecting the closure sequence. The q_2 (or δ_1) loop was closed first, and thus was the "inner" loop; whereas the q_1 (or δ_2) loop, being closed second, was the "outer" loop.

2. The "inner loop," $G_{12}Q_{2\delta_1}$ (①, Fig. 7) is closed with tentatively selected equalization and gains, and the closed inner-loop roots are found. These roots become the vehicle's poles for the outer-loop closure.

3. Using the same gain and equalization selected above, i.e., the same G_{12}, the coupling loop (②, Fig. 7) is closed. The closed-loop roots resulting from this closure become the vehicle's zeros for the outer-loop closure.

4. The outer loop is closed in a conventional manner around the modified outer-loop vehicle transfer function.

5. Possible repetitions of steps 2 through 4 with different equalizations and gains if the result of step 4 is not satisfactory.

The generalization of these steps to handle more complex systems, such as that of Fig. 4, is a straightforward extension.

E. APPLICATION TO SYSTEM SYNTHESIS

Fundamentally, the five analysis steps summarized above can represent one cut in a cut-and-try synthesis procedure. In such procedures a trial system is analyzed to determine its dynamic characteristics, which are then compared with dynamic performance objectives. Deficiencies revealed by the comparison are, hopefully, eliminated or reduced by modifications resulting in a new system for trial. This system, in turn, is analyzed and assessed, etc. The iterations continue until the trial system characteristics are consonant with the dynamic performance objectives.

The number of iterations required to achieve the penultimate system depends on the designer's intuition, on his ability to transfer insights into analytical procedure, and on his capacity to draw new knowledge and understanding from the analysis results. An analysis procedure cannot substitute for background and experience—but the procedure can be matched with a presumed background so as to achieve a balanced analyst–analysis procedure "system." The background presumed as a match for the multiloop analysis method advanced here is: an intimate knowledge of single-loop servoanalysis techniques; a detailed understanding of vehicle dynamics; and a thorough appreciation of the changes in effective-vehicle dynamics caused by idealized (i.e., no sensor or servo lags) single-loop controllers. Assuming this core technology, the multiloop analysis procedure has been designed to maximize the insightful generating aspects and clarity of each analysis step.

When full advantage is taken of the insights provided by the presumed background level, the multiloop analysis procedure can form the basis for almost direct synthesis (i.e., the number of analysis iteration cycles required to achieve the final system approaches one). The trick, of course, is to start off with a good trial system, which amounts to almost knowing the answer. To illustrate the possible impact of background information on the evolution of the initial trial system a few items are listed below, using the two-loop system of Fig. 5 as a particular example.

1. Hints about desirable inner-loop (q_2 loop) characteristics can be revealed by studies of the outer-loop system using several possible alternatives for the vehicle-alone transfer function, $Q_{1_{\delta_2}}$, as representative of $Q'_{1_{\delta_2}}$. In such

studies, the approximate effects of possible inner-loop feedbacks on $Q_1'_{\delta_2}$ can be determined readily using the literal approximate factors of $Q_{1\delta_2}$ (see Refs 2 and 3) and the equivalent stability derivatives corresponding to idealized controllers (Refs 2–5).

2. An appreciation for the approximate forms <u>obtainable</u> for the closed inner loops and, consequently, for the outer-loop effective-vehicle transfer function $Q_1'_{\delta_2}$, can be advanced from studies of the inner-loop closure involving $Q_{2\delta_1}$. Again approximate factors and equivalent stability derivatives as well as single-loop servoanalysis are used.

3. Preliminary indications of tradeoffs between parallel (the q_2 loop closure) and series (G_{21}) equalization are implicit in the above single-loop-closure studies. Thus, single-loop closures about the various $Q_{1\delta_2}$ forms considered indicate the corresponding types of equalization needed in G_{21}; and the approximate forms <u>possible</u> (with particular inner-loop feedback quantities) and <u>desirable</u> (with particular forms of G_{21}) for $Q_1'_{\delta_2}$ can be inferred.

Studies of the above types either involve vehicle characteristics as variable or emphasize controller equalization as variable. Both types of studies use well-known analytical operations and, for aircraft, a large body of quite general results exist (see, for example, Refs 2, 3, 13, and 14). Using the approximate, but highly indicative, information gathered from such past results as a guide, and adding the additional analytical complication required to account for the dynamics of such elements as sensors and servos, an excellent first-cut trial system is easily obtained. The exact analysis routine summarized previously can then be used in the final steps of a practical synthesis procedure. For systems as simple as that shown in Fig. 5, repetitious operations can often be avoided completely by this bringing of previous single-loop system knowledge to bear upon the multiloop problem.

In spite of the above remarks on synthesis, it is well to remember that the process outlined does not involve unique operations in compliance with a straightforward routine. One of the more tricky aspects has been casually bypassed until now. This is the selection of a particular block diagram, or sequence of closures, from the several possible. The block diagram itself has little significance—it is the loop closure sequence represented graphically by the block diagram which is important in eliminating or reducing iterations when

the analysis technique is used as a synthesis tool. From the point of view of pure analysis the closure sequence is immaterial. But in synthesis the closure sequence can be all-important. For instance, certain loops are necessarily closed before others for which they provide parallel equalization; and the necessary use of incomplete loop closure criteria causes some loop closure sequences to result in extreme variations in loop adjustments as a function of iteration, whereas for other sequences there is practically no change from one iteration to the next, etc. Because of considerations like these there are at least some preferred loop closure sequences and sometimes even a uniquely desired one. Desirable sequences are not always simple to determine. Fortunately, for vehicular control systems a set of factors can be promulgated which, when properly considered, will ordinarily provide the insight needed to construct a unique block diagram (or closure sequence) which, in the practical sense of minimizing interloop interactions, will also minimize iterations. These are summarized in Table I.

As should be apparent from Table I, many of the detailed insights involved can stem from analysis of single-loop systems and from simplified multiloop analyses. Thus, the equivalent stability derivative approach, vehicle approximate transfer functions, and single-sensor-loop studies already mentioned play yet another dominant role in multiloop vehicular systems synthesis.

After thorough consideration of the factors in Table I, a quasi-unique block diagram, or sequence of closures, can usually be established. The next problem is that of closure criteria for the several loops. Again only engineering judgment factors, which must ultimately be translated into concrete performance measures, can be delineated. The factors to be considered in establishing the actual closure criteria for each loop include:

1. The use of an inner loop as equalization for a subsequent outer loop.

2. Stability and response of loops which may be outer loops in one mode of operation and inner loops in another operational mode.

3. The "sensitivity factors" (pole, zero, and gain sensitivities, Ref 10) of the various loops and their influence on the outer loops. Ordinarily, inner-loop

TABLE I

FACTORS INVOLVED IN SELECTING A UNIQUE CLOSURE SEQUENCE

Factor	Remarks
"Command" Loop	For a given system analysis the command loop is ordinarily made the last, or outer, loop.
Relative Bandwidth	The bandwidth of a given loop closure is measured roughly by the crossover frequency ω_c. (If more than one crossover frequency exists, the largest is taken as ω_c.) The general sequence of loop closures in a multiloop system should then be in order of decreasing ω_c, e.g., $\omega_{c_{\text{inner loop}}} > \omega_{c_{\text{outer loop}}}$.
Closure Characteristics of a Loop as a Single Feedback System	Those loops which would require extensive equalization as individual single loops will ordinarily be made outer loops so that inner loops can relieve the equalization requirements.
Subsidiary Feedbacks	Feedbacks intended to provide equalization for subsequent loops, or to suppress subsidiary degrees of freedom which have undesirable effects on subsequent loops, are invariably "inner" loops.
Interdependent Loops	Some loops contain common elements in their open-loop transfer functions which make independent closures impossible or undesirable. These loops are closed either simultaneously, or in close sequence.
Multimode Character	Flight control "systems" are ordinarily a composite of several systems, one for each mode of operation. A common result is a variety of "command" loops in which "outer" loops in one "system" (corresponding to one mode of operation) may be "inner" loops of another. It is desirable to have the closures for a given loop the same, or closely connected, for each of the several "systems" (modes).
Equalization Economy	Practical considerations (e.g., equipment complexity; maximum-signal/minimum-increment-of-control or "dynamic range"; minimization of internal disturbance effects; etc.) ordinarily restrict equalization of signals obtained from any one sensor to no more than approximate integration, proportional, and rate. When more equalization is required, a subsidiary loop is ordinarily needed.

closures selected should be such that the effects of inner-loop parameter variations on the outer loops are as small as possible.

These considerations, taken in context with over-all system performance specifications, can ordinarily serve as guidelines for the selection of specific closure criteria.

SECTION III

LONGITUDINAL EXAMPLE - ALTITUDE CONTROL SYSTEM

To illustrate the previous general treatment two concrete examples will be presented, one for aircraft longitudinal control (in this section) and the other for lateral control (in Section IV). Loop closure sequence and criteria constitute a large part of the practical synthesis problem, so their selection will receive detailed attention in the ensuing treatment. In particular, the general factors involved in the selection of loop closure sequence (Table I) will be specialized for each of the examples; and some of the background considerations pertinent to closure criteria will be discussed prior to the selection of representative quantities and values. Once the sequence and criteria are fixed the analysis itself is routine, and the detailed examples are then presented as straightforward numerical exercises.

The longitudinal system is an altitude control system wherein the airframe is controlled by the elevator which, in turn, is activated by feedbacks involving the pitch angle, θ, and the altitude, h. This system is illustrated in the block diagram of Fig. 9. Here the usual "e" subscript on the elevator deflection symbol, δ_e, is eliminated to simplify the notation.

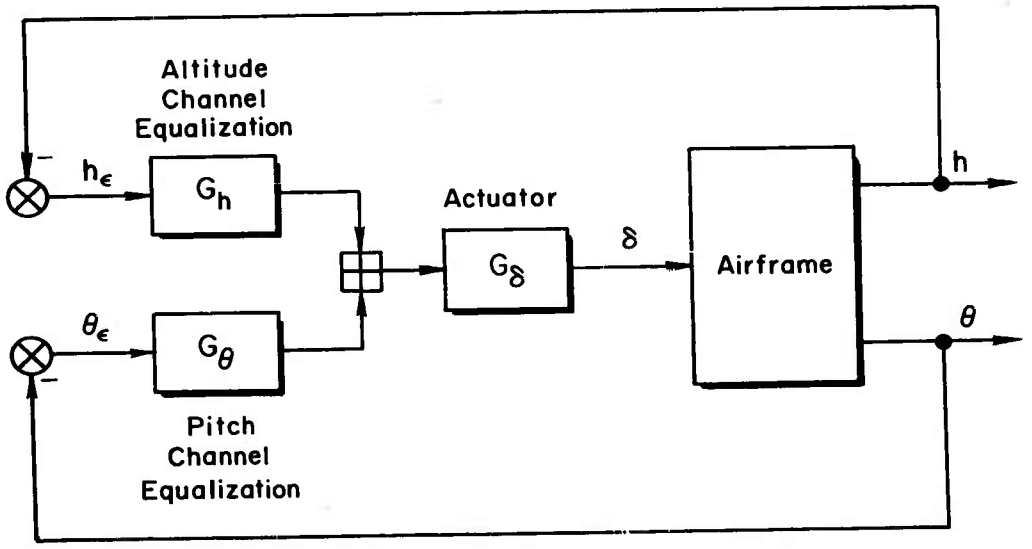

Figure 9. Longitudinal Control System

This system has a very simple multiloop form because only one control deflection, δ, is used. The surface actuator is, therefore, common to both feedback channels—a feature emphasized in the block diagram by indicating an actuator transfer function block, G_δ, separate from the altitude and pitch channel equalizations.

A. LOOP CLOSURE SEQUENCE AND GENERAL CLOSURE CONSIDERATIONS

For this system a unique sequence of closures is easy to justify using Table II, as a special case of Table I, to illustrate the reasoning. Some of the less obvious remarks in Table II may become more apparent after the discussion below. All of the factors considered in Table II indicate, or are compatible with, a closure sequence with h as the outer loop. The block diagram of Fig. 9 can now be shown with an h_c command, as in Fig. 10, and the system can be designated as

$$h_c,\ \theta \longrightarrow \delta \tag{62}$$

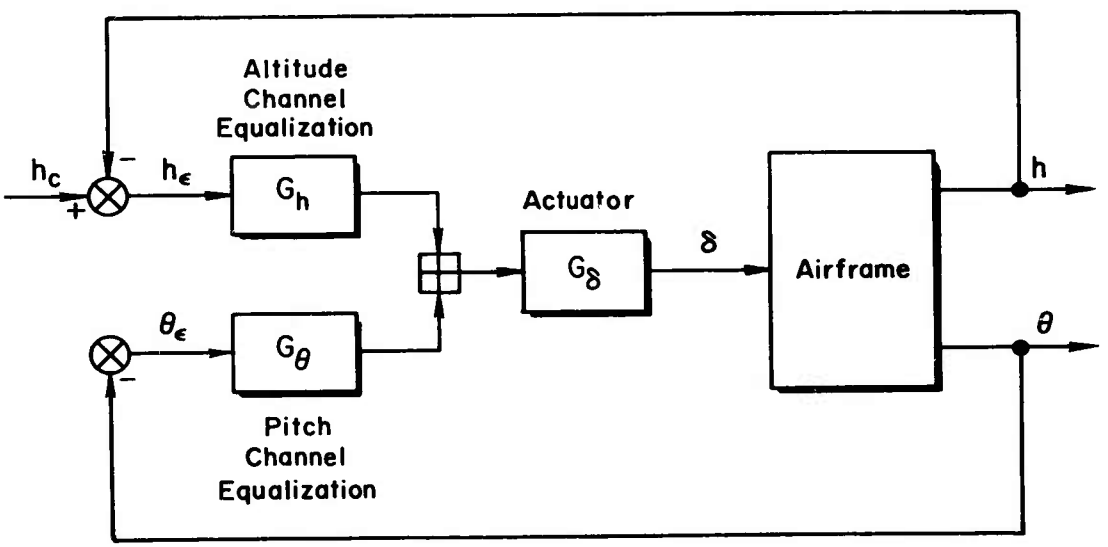

Figure 10. Altitude Control System
$h_c,\ \theta \rightarrow \delta$

TABLE II

FACTORS INVOLVED IN SELECTING LOOP CLOSURE SEQUENCE FOR LONGITUDINAL CONTROL SYSTEM

Factor	Remarks	Consequences	
		Inner Loop	Outer Loop
Command Loop	Either h_c or θ_c is a possibility		
Relative Bandwidth	One reason for θ feedbacks is for (short period) attitude stiffness and stabilization in the presence of external disturbances. Intent of h feedback is to control the (phugoid) height oscillations of the vehicle as a point mass. Therefore since in general $\omega_{sp} > \omega_p$, $\omega_{c_{\theta_{loop}}} > \omega_{c_{h_{loop}}}$.	θ	h
Closure Characteristics as a Single Loop and Equalization Economy	h loop requires lead equalization to obtain other than very low frequency ω_c. Such lead equalization, while possible, is seldom competitive with other ways of achieving the same end. (Exception can occur if h is terrain clearance rather than altitude.) θ loops are easily closed with moderate equalization, and provide the equivalent to lead equalization for the h loop.	θ	h
Subsidiary Feedbacks	θ, being roughly proportional to $\dot{h}$ at frequencies near h loop crossover, can relieve equalization requirements on h.	θ	h
Multimode Character	Attitude command system is a common mode without altitude control.	θ	

B. SPECIALIZATION OF SYSTEM EQUATIONS

The controller equation for the system is

$$\delta = G_{\delta h}(h_c - h) - G_{\delta\theta}\theta \tag{63}$$

where $G_{\delta h} = G_h G_\delta$ and $G_{\delta\theta} = G_\theta G_\delta$. As a special case of the general equations in the last section the quantities involved here are as given below.

Control Deflections: $\delta_1 = 0$

$\delta_2 = \delta$

Output - Motion Quantities: $q_1 = u$, $q_3 = \theta$

$q_2 = w$, $q_4 = h = \frac{1}{s}(U_0\theta - w)$

Vehicle Transfer Functions: $Q_{1\delta_2} = U_\delta$, $Q_{3\delta_2} = \Theta_\delta$

$Q_{2\delta_2} = W_\delta$, $Q_{4\delta_2} = H_\delta$

Controller Transfer Functions: $G_{21} = G_{22} = 0$

$G_{23} = G_{\delta\theta}$, $G_{24} = G_{\delta h}$

The closed-loop transfer function h/h_c can be determined directly from Eq 39 and 40 if Fig. 10 is considered a special case of Fig. 4 and the terms and symbols adjusted accordingly.

$$\left.\frac{h}{h_c}\right]_{h,\theta \to \delta} = \frac{G_{\delta h}N_{h_\delta}}{\Delta + G_{\delta\theta}N_{\theta_\delta} + G_{\delta h}N_{h_\delta}} = \frac{G_{\delta_h}H_\delta}{1 + G_{\delta\theta}\Theta_\delta + G_{\delta h}H_\delta} \tag{64}$$

For the purposes of this report all literal airframe transfer functions are written as in Refs 2, 3, or 11, all of which are compatible. Numerical transfer functions, when required for plotting or other purposes, are based on the typical case given in Ref 11. However, although derived using these numerical values, many plots are presented in generic form with the poles and zeros identified by their literal values to enhance the clarity of presentation. In

terms of such literal values the generic airframe-alone transfer functions, expressed in the root-locus form, are:

$$\Theta_\delta = \frac{N_{\theta\delta}}{\Delta} = \frac{A_\theta(s + 1/T_{\theta_1})(s + 1/T_{\theta_2})}{(s^2 + 2\zeta_p\omega_p s + \omega_p^2)(s^2 + 2\zeta_{sp}\omega_{sp}s + \omega_{sp}^2)} \tag{65}$$

$$H_\delta = \frac{N_{h\delta}}{\Delta} = \frac{A_h(s + 1/T_{h_1})(s + 1/T_{h_2})(s + 1/T_{h_3})}{s(s^2 + 2\zeta_p\omega_p s + \omega_p^2)(s^2 + 2\zeta_{sp}\omega_{sp}s + \omega_{sp}^2)} \tag{66}$$

As already noted, approximate factors relating the poles and zeros in Eqs 65 and 66 with the aerodynamic and inertial parameters of the airframe are given in Refs 2 and 3.

The appropriate equivalent block diagram for Fig. 10 is shown in Fig. 11. H'_δ, the equivalent vehicle transfer function with the θ loop closed, is also shown in this figure.

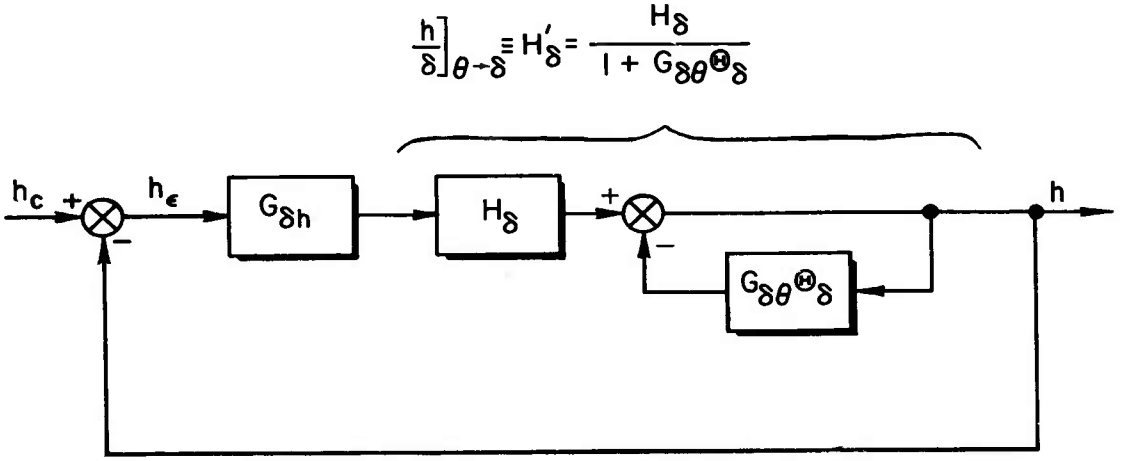

Figure 11. Equivalent Block Diagram for Altitude Control System h_c, $\theta \rightarrow \delta$

C. INNER LOOP CONSIDERATIONS

1. Inner Loop Alone

Establishing the closure criteria for the two loops is somewhat more involved than the closure sequence selection. Considering the fundamental vehicle dynamics and possible disturbances, and recognizing that the attitude loop will probably be the outer loop (i.e. attitude commands) in some operational mode of the flight control system, the θ loop alone should be capable of:

(1) Providing good attitude regulation of the vehicle in the presence of external disturbances (e.g. gusts), and both short and long term vehicle asymmetries such as sudden changes in: c.g. with stores release, thrust moment with power changes, external configuration with actuation of auxiliary surfaces such as flaps or brakes, etc.; and slow changes in: c.g. with fuel consumption, flight operating conditions, etc.

(2) Accomplishing commanded changes in attitude with good response.

For nominal airframe characteristics these aims can be accomplished using a controller with lead equalization, and a crossover frequency, ω_c, somewhat greater than the short period undamped natural frequency. Typical characteristics for such a system are illustrated in the sketches of Fig. 12. The conventions established in Fig. 12, for identifying the meaning of the various line-values used on the Bode plots, are followed in all remaining plots. Neglecting the controller lag dynamics, the open loop transfer function in Bode form will be

$$G(s) = \frac{\theta}{\theta_c} = \frac{K_\theta K_{\theta_\delta}(T_{\theta_1}s + 1)(T_{\theta_2}s + 1)(T_E s + 1)}{\left[\left(\frac{s}{\omega_p}\right)^2 + \frac{2\zeta_p s}{\omega_p} + 1\right]\left[\left(\frac{s}{\omega_{sp}}\right)^2 + \frac{2\zeta_{sp}s}{\omega_{sp}} + 1\right]} \qquad (67)$$

where T_E is the lead equalization time constant. (This equalization can be developed directly from a θ sensor using passive elements, or from a rate sensor plus a θ sensor.) The actual values for the closed-loop transfer function factors are readily found by the decomposition technique using the $G(j\omega)$ and $G(-\sigma)$ Bode plots of Fig. 12, or from a root locus. These techniques,

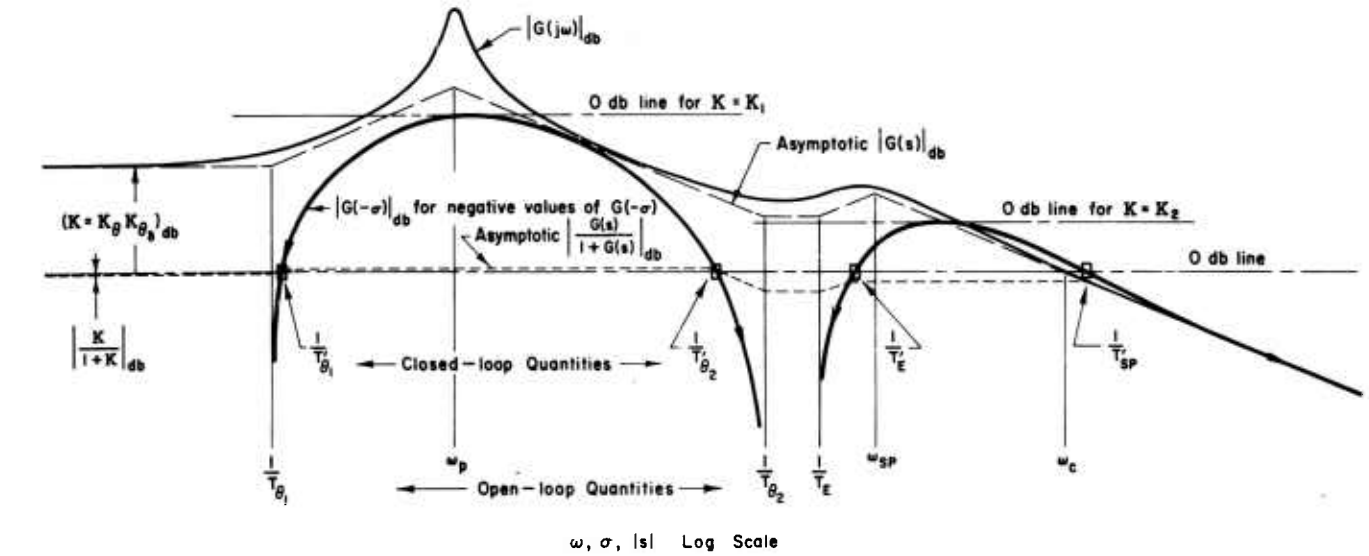

(b) Open and Closed Loop Bode Diagrams

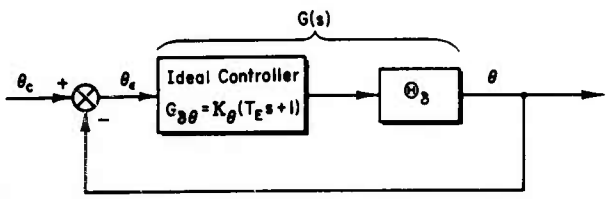

(a) Block Diagram

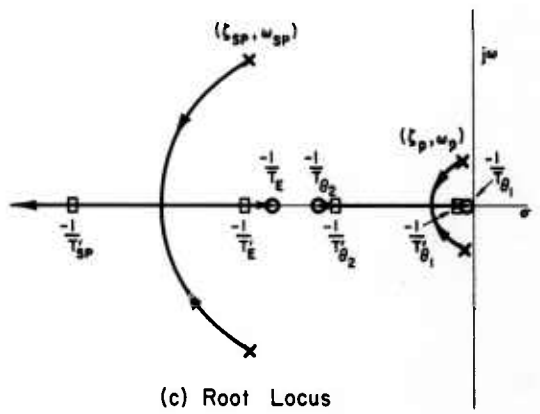

(c) Root Locus

Figure 12. Open- and Closed-Loop Characteristics of Attitude Control System with Ideal Controller and Nominal Airframe

and others involved in unified servoanalysis procedures, are covered elsewhere (Ref 9).

When closed with values of open-loop dc gain, K, as shown in Fig. 12, the resulting closed-loop transfer function is

$$\frac{G(s)}{1 + G(s)} = \frac{\theta}{\theta_c} = \left(\frac{K}{1 + K}\right)\frac{(T_{\theta_1}s + 1)(T_{\theta_2}s + 1)(T_E s + 1)}{(T'_{\theta_1}s + 1)(T'_{\theta_2}s + 1)(T'_E s + 1)(T'_{sp}s + 1)} \tag{68}$$

Eq 68 uses several aspects of the notational scheme adopted in this report for multiloop analysis results, so a short aside is pertinent to discuss notation using this concrete example. All of the closed-loop poles have one prime, indicating that they result from one loop closure. Also the actual notation selected for the closed-loop poles reflects their approximate values. Thus $1/T_{\theta_1}'$, $1/T_{\theta_2}'$ and $1/T_E'$, are all near the open-loop numerator terms $1/T_{\theta_1}$, $1/T_{\theta_2}$, and $1/T_E$, respectively. If a much lower value of K had been used, such that the closed-loop factors remained quadratics (i.e. $K < K_1$), then the closed-loop denominator would have had the form

$$\left[\left(\frac{s}{\omega'_p}\right)^2 + \frac{2\zeta'_p s}{\omega'_p} + 1\right]\left[\left(\frac{s}{\omega'_{sp}}\right)^2 + \frac{2\zeta'_{sp}s}{\omega'_{sp}} + 1\right]$$

In this case the notation used for the closed-loop quantities reflects their origin in open-loop quantities. If intermediate values of gain had been used, such that the closed-loop phugoid were more than critically damped but the closed-loop short period were still quadratic (i.e. $K_1 < K < K_2$), then the closed-loop denominator would have the form

$$(T_{\theta_1}'s + 1)(T_{\theta_2}'s + 1)\left[\left(\frac{s}{\omega'_{sp}}\right)^2 + \frac{2\zeta'_{sp}s}{\omega'_{sp}} + 1\right]$$

So, as gain is increased, the notation for the closed-loop phugoid and short period modes has the following transitions:

Phugoid:

Open-loop (K = 0)	$\left[\left(\frac{s}{\omega_p}\right)^2 + \frac{2\zeta_p s}{\omega_p} + 1\right]$
Closed-loop, quadratic ($K < K_1$)	$\left[\left(\frac{s}{\omega'_p}\right)^2 + \frac{2\zeta'_p s}{\omega'_p} + 1\right]$
Closed-loop, overdamped ($K_1 < K$)	$(T'_{\theta_1}s + 1)(T'_{\theta_2}s + 1)$

Short Period:

Open-loop (K = 0)	$\left[\left(\frac{s}{\omega_{sp}}\right)^2 + \frac{2\zeta_{sp} s}{\omega_{sp}} + 1\right]$
Closed-loop, quadratic ($K < K_2$)	$\left[\left(\frac{s}{\omega'_{sp}}\right)^2 + \frac{2\zeta'_{sp} s}{\omega'_{sp}} + 1\right]$
Closed-loop, overdamped ($K_2 < K$)	$(T'_E s + 1)(T'_{sp}s + 1)$

The rules for this notational sequence can be summarized as:

1. The number of primes present indicates the number of loop closures.
2. When the closed-loop form is the same as the open-loop form, the notation for the closed-loop factor is the same as the open-loop factor, plus a prime. In this case the origin of the closed-loop factor is always at hand.
3. The notation for closed-loop factors which differ in form from their open-loop origins reflects the open-loop zeros which the factors approach as $K \longrightarrow \infty$. When no open-loop zero exists in this situation, a special form is coined which reflects the origin of the fact (e.g. $1/T'_{sp}$).

These rules are special cases of those summarized in the nomenclature section at the front of this report.

For the attitude system closed with high gain, as in Fig. 12, the closed-loop dc gain, $K/(1 + K)$, is approximately one, and the dipole pairs $(T_{\theta_1}s + 1)/(T'_{\theta_1}s + 1)$, $(T_{\theta_2}s + 1)/(T'_{\theta_2}s + 1)$, and $(T_E s + 1)/(T'_E s + 1)$ in θ/θ_c all nearly cancel. Thus Eq 68 becomes approximately

$$\frac{\theta}{\theta_c} \doteq \frac{1}{T'_{sp}s + 1} \tag{69}$$

As an attitude command system, this is very good indeed; also attitude regulation properties are adequate. So from the standpoint of attitude control, the system shown is satisfactory. However, two caveats are worth mentioning. First, for some flight conditions the low-frequency region centered about ω_p may not exhibit such large amplitude ratio relative to that near short period, thereby making it difficult to attain values of K much greater than one. Such conditions can be corrected by low frequency lag-lead equalization (e.g. adding an integral of θ_ϵ to the controller). Second, the controller assumed is ideal, with servo and/or sensor lags ignored, and the loop gain can, theoretically, be increased indefinitely without any stability difficulties. Controller lags will be taken into account later in the detailed analysis. Their presence limits the allowable gain for stability, and is one reason lead equalization (i.e. the $T_E s + 1$ factor) is needed in the attitude loop.

2. The Inner Loop as Equalization for the Outer Loop

When considered in company with the h outer loop the attitude loop closure should be of such form as to relieve outer loop equalization requirements. With the ideal controller considered above, the effective airframe altitude transfer function H'_δ becomes

$$\left.\frac{h}{\delta}\right]_{\theta \to \delta} \equiv H'_\delta = H_\delta \frac{1}{1 + G_{\delta\theta}\Theta_\delta}$$

$$= \left\{ \frac{K_{h\delta}(T_{h_1}s + 1)(T_{h_2}s + 1)(T_{h_3}s + 1)}{s\left[\left(\frac{s}{\omega_p}\right)^2 + \frac{2\zeta_p s}{\omega_p} + 1\right]\left[\left(\frac{s}{\omega_{sp}}\right)^2 + \frac{2\zeta_{sp}s}{\omega_{sp}} + 1\right]} \right\} \left\{ \frac{\left[\left(\frac{s}{\omega_p}\right)^2 + \frac{2\zeta_p s}{\omega_p} + 1\right]\left[\left(\frac{s}{\omega_{sp}}\right)^2 + \frac{2\zeta_{sp}s}{\omega_{sp}} + 1\right]}{(1+K_\theta K_{\theta\delta})(T'_{\theta_1}s+1)(T'_{\theta_2}s+1)(T'_E s+1)(T'_{sp}s+1)} \right\}$$

$$= \frac{K_{h\delta}}{(1 + K_\theta K_{\theta\delta})} \left\{ \frac{(T_{h_1}s + 1)(T_{h_2}s + 1)(T_{h_3}s + 1)}{s(T'_{\theta_1}s + 1)(T'_{\theta_2}s + 1)(T'_E s + 1)(T'_{sp}s + 1)} \right\} \qquad (70)$$

The forms of H_δ and H'_δ are illustrated in the sketches of Fig. 13. To emphasize the basic differences in the dynamic rather than static forms, a common gain factor is used. Actually H'_δ would appear $(1 + K_\theta K_{\theta\delta})_{db} \doteq (K_\theta K_{\theta\delta})_{db}$ below the plot for $(1 + K_\theta K_{\theta\delta})H'_\delta$. Comparison of these forms (which are minimum phase

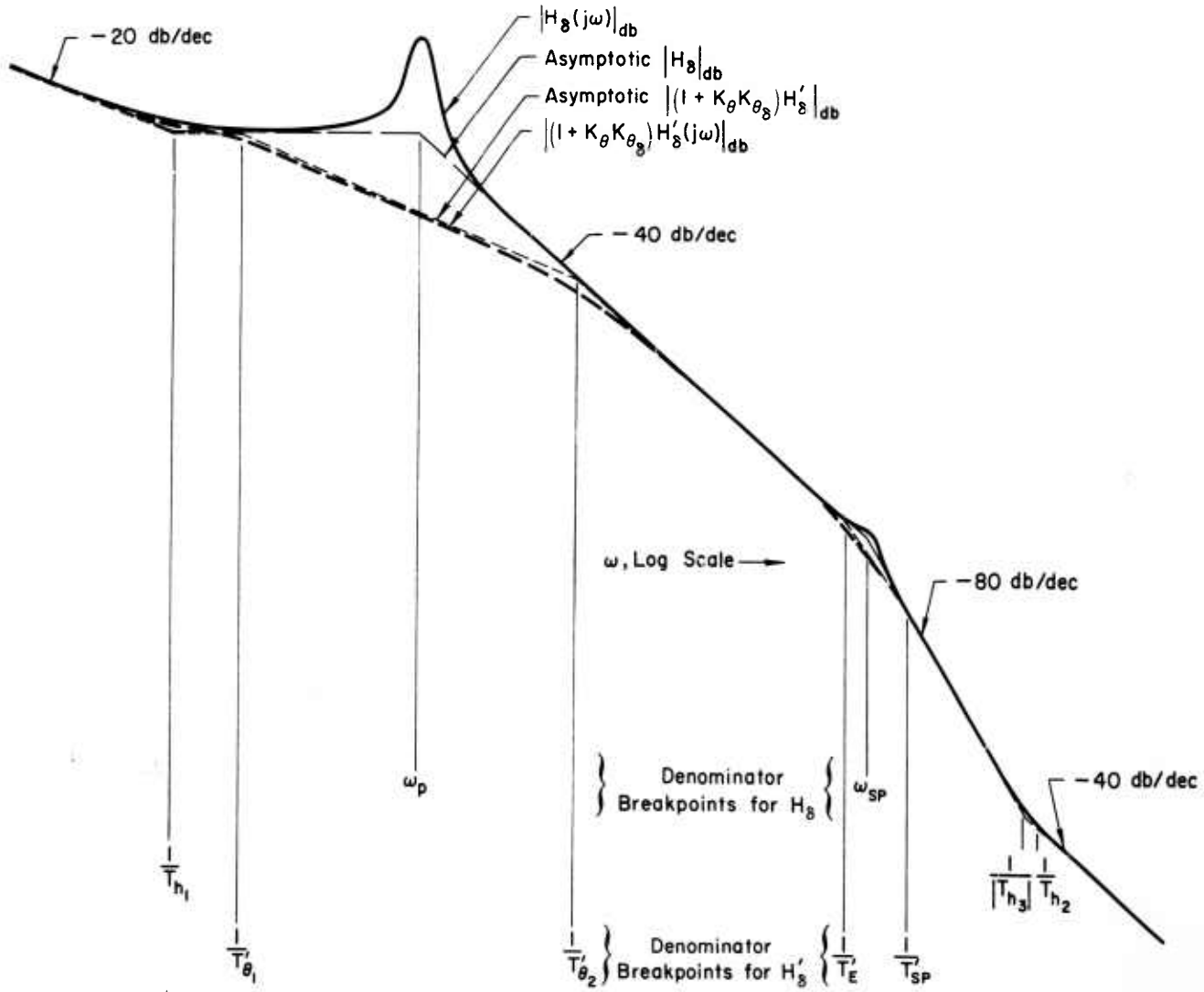

Figure 13. Comparison of H_δ and $(1 + K_\theta K_{\theta\delta})H'_\delta$

except for the breakpoint at $1/T_{h_3}$) readily indicates the superiority of H_δ' over H_δ. For a pure gain altitude controller operating on H_δ, the crossover frequency must be well below $1/T_{h_1}$, (to avoid the lightly damped phugoid) and the resulting closed-loop system response will exhibit a very lightly damped or even slightly unstable oscillation of the phugoid variety. When the vehicle-alone phugoid is unstable, as it may be for flight conditions involving pitching moment changes with speed, a stable pure gain closure is impossible. On the other hand, a pure gain h controller is completely suitable for the H_δ' system, and stable crossovers in the neighborhood of $1/T_{\theta_2}'$ are readily obtained. The dominant closed-loop mode is then a quadratic having an undamped natural frequency near ω_c, and the gain can be selected to yield well-damped responses. For these statements to be true, the inner loop gains must be high enough to overdamp the phugoid, and preferably high enough to force the $1/T_{\theta_2}'$ pole to the neighborhood of $1/T_{\theta_2}$, thereby effectively maximizing available bandwidth. High gain θ inner loops are, therefore, a fundamental requirement for pure gain altitude controllers.

An obvious alternate to the above system is to use lead equalization in the h loop. This is sometimes necessary anyway (e.g. in terrain following), but it always introduces additional difficulties. For example, the system (with no inner attitude loop) will produce drastic pitch angle changes when the airframe hits a vertical gust. Considerations of this nature are important when comparing competing systems for the altitude control task.

A final point worth mentioning is the possibility of $1/T_{h_1}$ becoming negative. As discussed in Ref 2 this depends primarily upon the drag and thrust characteristics of the vehicle. In practice negative values of $1/T_{h_1}$ cannot be avoided near the absolute ceiling or in landing-approach when flying at speeds below that for minimum drag. When this occurs an altitude system using only elevator control will exhibit a divergence (with a time constant which approaches T_{h_1}) and will therefore be unacceptable.

D. NUMERICAL EXAMPLE

The preceding discussion covers most of the general aspects of an altitude control system with an inner attitude loop. The present article provides a numerical example.

To make the example more realistic, a high frequency second-order lag is used to approximate the servo characteristics, and a first-order lag to simulate altitude sensor dynamics. Thus, the servo transfer function is

$$G_\delta = \frac{1}{(\frac{s}{\omega_\delta})^2 + \frac{2\zeta_\delta s}{\omega_\delta} + 1} \tag{71}$$

The inner-loop controller transfer function is,

$$G_{\delta\theta} = \frac{K_\theta(T_E s + 1)}{\left[(\frac{s}{\omega_\delta})^2 + \frac{2\zeta_\delta s}{\omega_\delta} + 1\right]} \tag{72}$$

and the outer-loop controller transfer function becomes

$$G_{\delta h} = \frac{K_h}{(T_a s + 1)\left[(\frac{s}{\omega_\delta})^2 + \frac{2\zeta_\delta s}{\omega_\delta} + 1\right]} \tag{73}$$

where T_a is the time constant of the altimeter installation.

Numerical values for the altitude sensor and servo will be taken as

$$\zeta_\delta = 0.7,\ \omega_\delta = 50,$$
$$1/T_a = 15 \tag{74}$$

The vehicle characteristics are similar to the nominal case previously used as an example throughout Ref 11. These are:

$$\Theta_\delta = \frac{(4.85)(\frac{s}{.0098} + 1)(\frac{s}{1.371} + 1)}{\left[(\frac{s}{.063})^2 + \frac{2(.0714)s}{(.063)} + 1\right]\left[(\frac{s}{4.27})^2 + \frac{2(.493)s}{(4.27)} + 1\right]} \tag{75}$$

$$H_\delta = \frac{(2275)(\frac{s}{.0064} + 1)(\frac{s}{19.2} + 1)(-\frac{s}{19.2} + 1)}{s\left[(\frac{s}{.063})^2 + \frac{2(.0714)s}{(.063)} + 1\right]\left[(\frac{s}{4.27})^2 + \frac{2(.493)s}{(4.27)} + 1\right]} \tag{76}$$

The attitude channel equalization time constant would ordinarily be found by an attitude subsystem optimization procedure which considered the vehicle dynamics over the entire flight regime. This is beyond the present scope, so a value of $1/T_E = 2.4$, which is reasonably representative, will be arbitrarily selected for the example.

With all required numerical values fixed the analyses can proceed in a straightforward fashion to determine the two gains K_θ and K_h. The first objective is to find the poles and zeros of $1/(1 + G_{\delta\theta}\Theta_\delta)$. Siggy and $j\omega$ Bode plots of the open-loop transfer function $G_{\delta\theta}\Theta_\delta$ are presented in Fig. 14, and a root locus sketch (not to scale) is shown in Fig. 15. The actual closure used depends in practice on several factors (e.g. whether an adaptive device is to be used, effects of parasitic nonlinearities, etc.) over and above those general considerations discussed in the second article of this section (i.e. bandwidth, response of θ loop to commands, etc.). To make matters simple, a closure criterion based on a phase margin of 40 degrees is used in Fig. 14. The resulting system is compatible with all the general considerations, i.e. it will exhibit good transient response to attitude commands, good attitude regulation, reasonable insensitivity to likely parasitic nonlinearities, etc. However, the criterion may not be appropriate for certain types of adaptive gain-changing schemes, especially those involving low amplitude limit cycles as an essential characteristic.

For a phase margin of 40 degrees the gain K_θ will be 8.3 db or 2.6 in linear units. Using the decomposition and other techniques of the unified servoanalysis method (Ref 9), the closed-loop transfer function $G_{\delta\theta}\Theta_\delta/(1 + G_{\delta\theta}\Theta_\delta)$ becomes (See Fig. 14 - dotted line)

$$\frac{G_{\delta\theta}\Theta_\delta}{1+G_{\delta\theta}\Theta_\delta} = \frac{\theta}{\theta_c} = \left(\frac{K_\theta K_{\theta\delta}}{1+K_\theta K_{\theta\delta}}\right)\frac{(T_{\theta_1}s+1)(T_{\theta_2}s+1)(T_E s+1)}{(T'_{\theta_1}s+1)(T'_{\theta_2}s+1)(T'_E s+1)(T'_{sp}s+1)\left[\left(\frac{s}{\omega'_\delta}\right)^2+\frac{2\zeta'_\delta s}{\omega'_\delta}+1\right]} \tag{77}$$

$$= (0.93)\,\frac{\left(\frac{s}{.0098}+1\right)\left(\frac{s}{1.371}+1\right)\left(\frac{s}{2.4}+1\right)}{\left(\frac{s}{.011}+1\right)\left(\frac{s}{1.05}+1\right)\left(\frac{s}{3.5}+1\right)\left(\frac{s}{47.1}+1\right)\left[\left(\frac{s}{35}\right)^2+\frac{2(.32)s}{(35)}+1\right]}$$

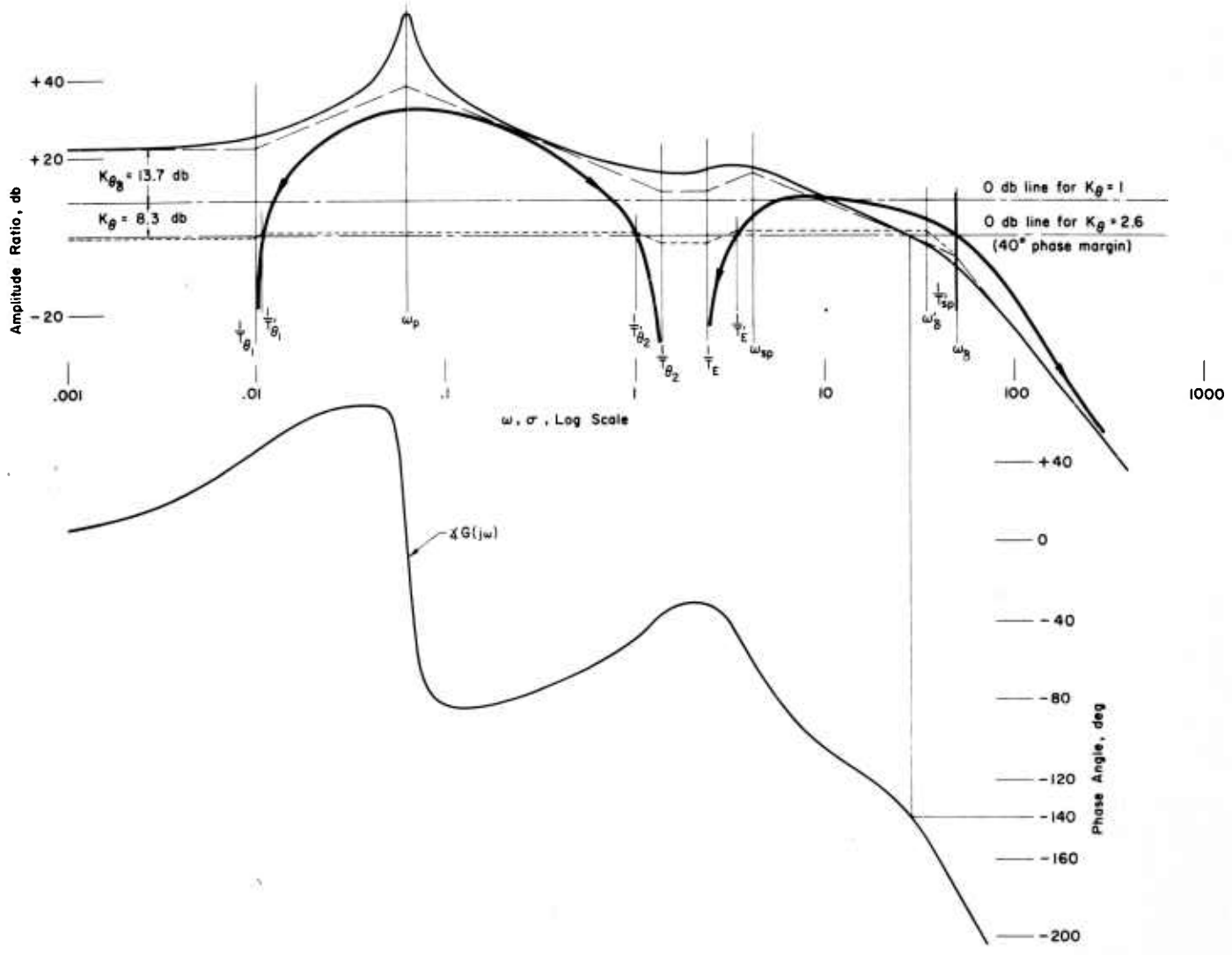

Figure 14. Open- and Closed-Loop Bodes for Example Attitude Control Subsystem, $G = G_{\delta_\theta}\Theta_\delta$

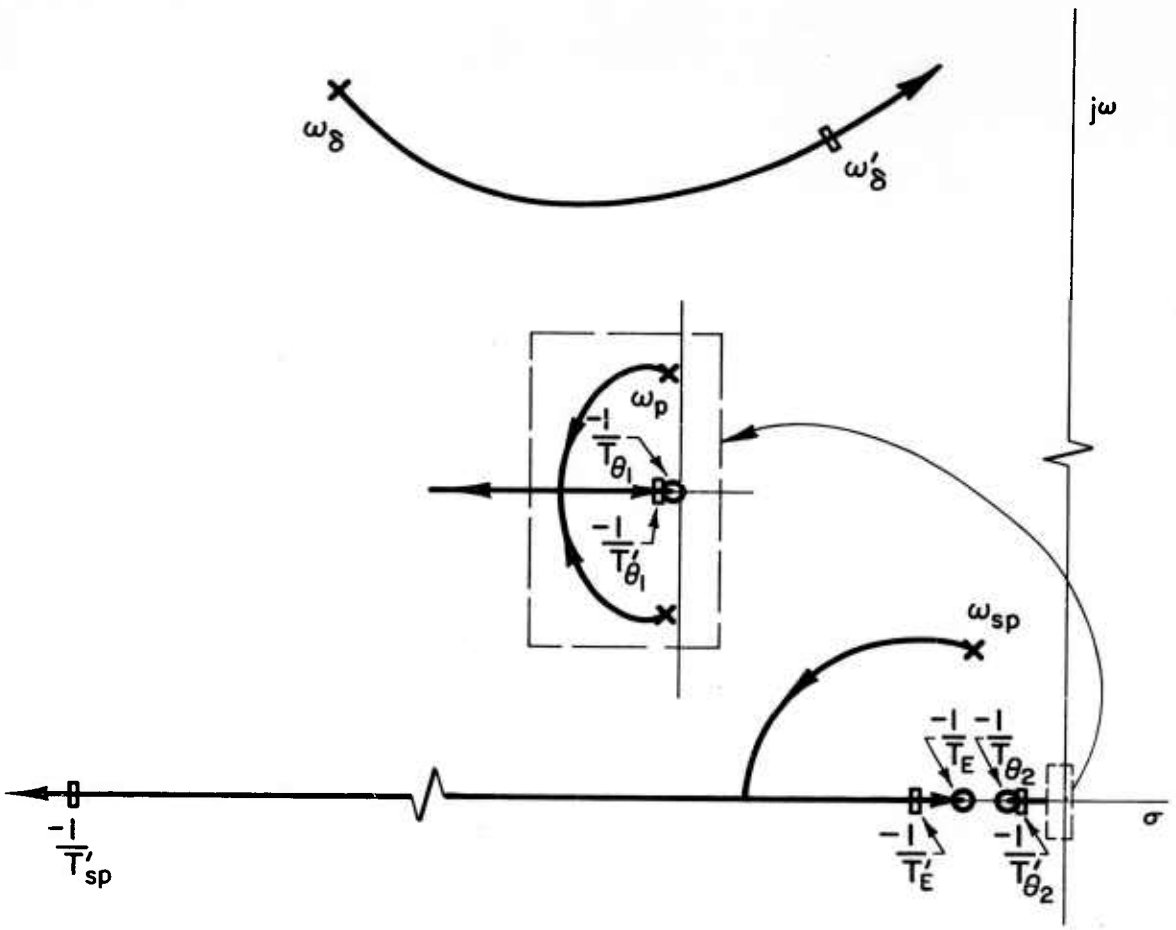

Figure 15. Root Locus Sketch for Example Attitude Control Subsystem, $G_{\delta_\theta}\Theta_\delta$

Eq 77 reveals that closing the loop has overdamped the phugoid and short period modes and reduced both damping ratio and undamped natural frequency for the quadratic mode associated with the servo. The closed-loop phugoid factors are quite close to the zeros, $1/T_{\theta_1}$ and $1/T_{\theta_2}$; and one of the closed-loop short period factors ($1/T'_E$) is near the $1/T_E$ zero. Thus, the low frequency poles and zeros are largely self-canceling and the approximate closed-loop transfer function for the attitude loop is

$$\frac{\theta}{\theta_c} \doteq \frac{1}{\left(\frac{s}{47.1}+1\right)\left[\left(\frac{s}{35}\right)^2+\frac{2(.32)s}{(35)}+1\right]} \tag{78}$$

Eq 78 is the equivalent of Eq 69, with the presence of the servo dynamics giving rise to the additional second order factor.

The closed-loop attitude system transfer function of direct interest for the subsequent altitude loop closure is

$$\frac{1}{1+G_{\delta\theta}\Theta_\delta} = \frac{1}{(1+K_\theta K_{\theta_\delta})}\left\{\frac{\left[\left(\frac{s}{\omega_p}\right)^2+\frac{2\zeta_p s}{\omega_p}+1\right]\left[\left(\frac{s}{\omega_{sp}}\right)^2+\frac{2\zeta_{sp}s}{\omega_{sp}}+1\right]\left[\left(\frac{s}{\omega_\delta}\right)^2+\frac{2\zeta_\delta s}{\omega_\delta}+1\right]}{(T_{\theta_1}'s+1)(T_{\theta_2}'s+1)(T_E's+1)(T_{sp}'s+1)\left[\left(\frac{s}{\omega_\delta'}\right)^2+\frac{2\zeta_\delta' s}{\omega_\delta'}+1\right]}\right\} \tag{79}$$

$$= \frac{1}{(13.6)}\;\frac{\left[\left(\frac{s}{.063}\right)^2+\frac{2(.0714)s}{(.063)}+1\right]\left[\left(\frac{s}{4.27}\right)^2+\frac{2(.493)s}{(4.27)}+1\right]\left[\left(\frac{s}{50}\right)^2+\frac{2(.7)s}{50}+1\right]}{\left(\frac{s}{.011}+1\right)\left(\frac{s}{1.05}+1\right)\left(\frac{s}{3.5}+1\right)\left(\frac{s}{47.1}+1\right)\left[\left(\frac{s}{35}\right)^2+\frac{2(.32)s}{(35)}+1\right]}$$

This transfer function, when combined with the airframe transfer function H_δ, gives H_δ', the effective airframe altitude transfer function with the attitude loop closed, that is,

$$H_\delta' = \frac{H_\delta}{1+G_{\delta\theta}\Theta_\delta} = \left(\frac{K_{h_\delta}}{1+K_\theta K_{\theta_\delta}}\right)\left\{\frac{(T_{h_1}s+1)(T_{h_2}s+1)(T_{h_3}s+1)\left[\left(\frac{s}{\omega_\delta}\right)^2+\frac{2\zeta_\delta s}{\omega_\delta}+1\right]}{s(T_{\theta_1}'s+1)(T_{\theta_2}'s+1)(T_E's+1)(T_{sp}'s+1)\left[\left(\frac{s}{\omega_\delta'}\right)^2+\frac{2\zeta_\delta' s}{\omega_\delta'}+1\right]}\right\} \tag{80}$$

Except for the quadratic pair due to the servo, Eq 80 is identical in form to Eq 70, which was derived for an ideal no-lag controller. When the altitude controller transfer function $G_{\delta h}$ is combined with H_δ', the numerator servo quadratic will exactly cancel the servo characteristics in the denominator of $G_{\delta h}$. The effective servo dynamics for the h loop closure therefore result from the attitude closed-loop system.

Adding controller dynamics to Eq 80 results in the open-loop altitude system transfer function,

$$G_{\delta h}H'_{\delta} = \left(\frac{K_h K_{h_\delta}}{1+K_\theta K_{\theta_\delta}}\right)\left\{\frac{(T_{h_1}s+1)(T_{h_2}s+1)(T_{h_3}s+1)}{s(T'_{\theta_1}s+1)(T'_{\theta_2}s+1)(T'_E s+1)(T'_{sp}s+1)(T_a s+1)\left[\left(\frac{s}{\omega'_\delta}\right)^2+\frac{2\zeta'_\delta s}{\omega'_\delta}+1\right]}\right\}$$

$$= K_h(167)\left\{\frac{\left(\frac{s}{.0064}+1\right)\left(\frac{s}{19.2}+1\right)\left(-\frac{s}{19.2}+1\right)}{s\left(\frac{s}{.011}+1\right)\left(\frac{s}{1.05}+1\right)\left(\frac{s}{3.5}+1\right)\left(\frac{s}{47.1}+1\right)\left(\frac{s}{15}+1\right)\left[\left(\frac{s}{35}\right)^2+\frac{2(.32)s}{(35)}+1\right]}\right\} \tag{81}$$

The jω and siggy Bode plots for this transfer function are given in Fig. 16 and a root locus sketch is shown in Fig. 17. As in the attitude loop, the open-loop characteristics in the frequency region of possible crossovers are such as to result in good closed-loop dynamic response if a phase margin of 40 to 60 degrees or so is used for the closure criterion. For a phase margin of 40 degrees, K_h will be -49.4 db or 0.0034 rad/foot.

The complete closed-loop system poles can be determined readily using unified servoanalysis techniques. However, the entire procedure is simplified considerably, with little loss in accuracy, if advantage is taken of a simplified form of $G_{\delta h}H'_{\delta}$. In Fig. 16 it will be noted that $|G_{\delta h}H'_{\delta}|$ is much less than one in the frequency region above the breakpoint at $1/T'_E$. Thus, the contributions of $G_{\delta h}H'_{\delta}$ to the system frequency response will be very small at frequencies above $\omega = 1/T'_E = 3.5$ and these contributions will be changed only very slightly if the amplitude asymptote through the break point at $\omega = 1/T'_{\theta_2} = 1.05$ is taken as the high-frequency asymptote of $G_{\delta h}H'_{\delta}$. Thus, a simplified open-loop transfer function

$$G_{\delta h}H'_{\delta} \doteq \frac{(.57)\left(\frac{s}{.0064}+1\right)}{s\left(\frac{s}{.011}+1\right)\left(\frac{s}{1.05}+1\right)} \tag{82}$$

is capable of exhibiting the major changes introduced by the h closure. The high frequency portion of this simplified plot is shown by the dashed line on Fig. 16. The higher frequency terms not contained in Eq 82 will be modified

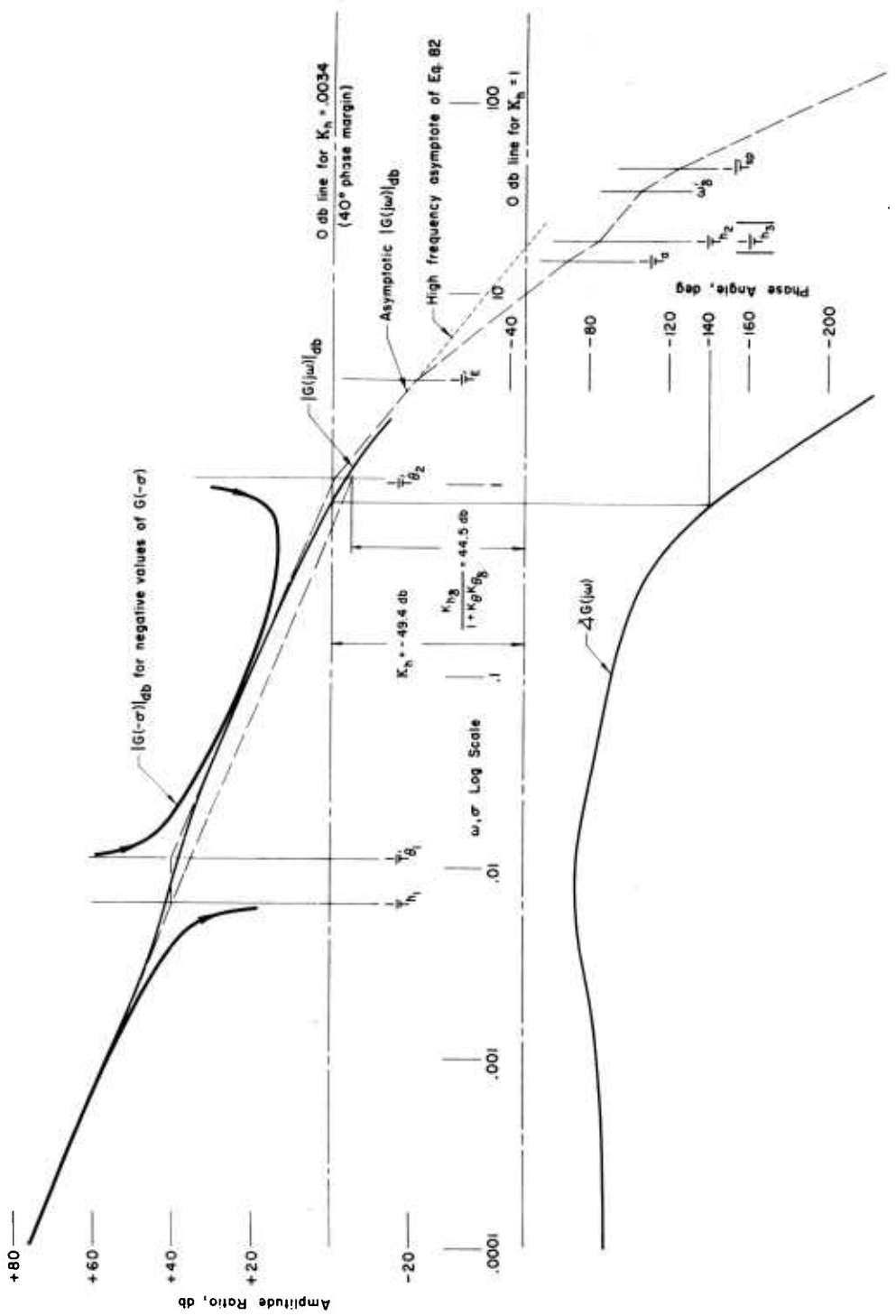

Figure 16. Open- and Closed-Loop Bodes for Example Altitude Control Outer Loop, $G = G_{6_h} H_6'$

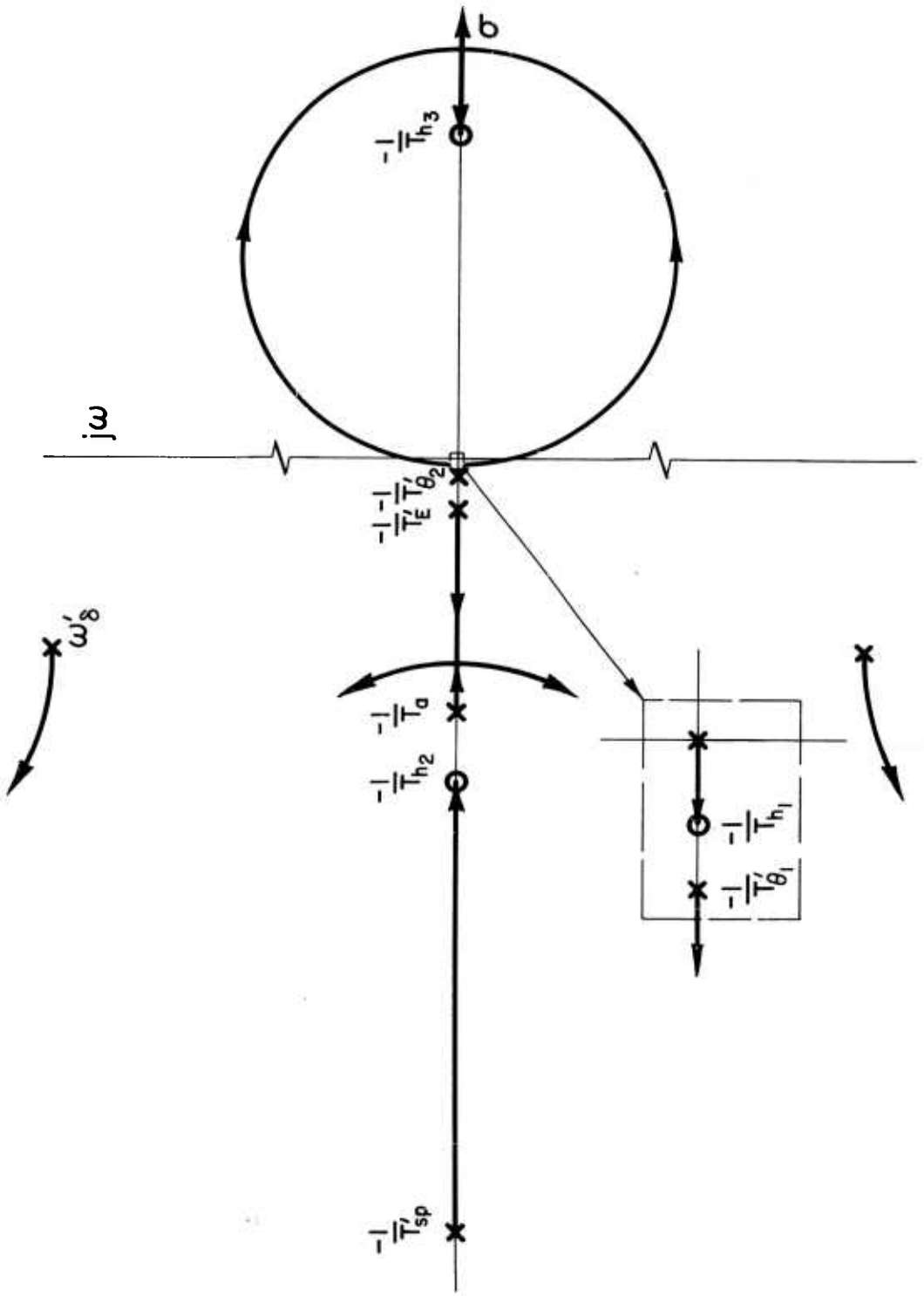

Figure 17. Root Locus Sketch for Example Altitude Control Outer Loop, $G_{\delta h} f_\delta^1$

only slightly from those given in Eq 81 by the altitude closure. Using the decomposition technique on this simplified open-loop transfer function, a simple approximation to the closed-loop transfer function is

$$\left.\frac{h}{h_c}\right]_{h,\theta \rightarrow \delta} \doteq \frac{\left(\frac{s}{.0064}+1\right)}{\left(\frac{s}{.0064}+1\right)\left[\left(\frac{s}{1.02}\right)^2+\frac{2(.52)s}{(1.02)}+1\right]}$$

$$\doteq \frac{1}{\left[\left(\frac{s}{1.02}\right)^2+\frac{2(.52)s}{(1.02)}+1\right]} \qquad (83)$$

Eq 83 gives only the dominant mode for the altitude control system. Including an approximation to the higher frequency terms from Eq 81, the total system closed-loop transfer function would be approximately

$$\left.\frac{h}{h_c}\right]_{h,\theta \rightarrow \delta} \doteq \frac{\left(\frac{s}{19.2}+1\right)\left(-\frac{s}{19.2}+1\right)}{\left[\left(\frac{s}{1.02}\right)^2+\frac{2(.52)s}{(1.02)}+1\right]\left(\frac{s}{3.5}+1\right)\left(\frac{s}{47.1}+1\right)\left(\frac{s}{15}+1\right)\left[\left(\frac{s}{35}\right)^2+\frac{2(.32)s}{(35)}+1\right]} \qquad (84)$$

E. CONCLUDING REMARKS

With the control gains set as given above the altitude control system will exhibit characteristics generally accepted as good. The transient response to an altitude command will be rapid and well damped, and the shape of the response to a step or cut-off ramp will be essentially that of a unit-numerator second-order system having a damping ratio of about 0.5 and an undamped natural frequency of 1.0 rad/sec. The steady-state altitude error will be zero; however, the airspeed will, in general, change to make this possible. (To also keep the airspeed constant would require a more sophisticated system incorporating some other control, such as a throttle loop.) The effects of vertical gusts will be largely suppressed by the attitude inner loop, which will also tend to minimize the effects of both sudden and slowly varying airframe changes (e.g. flap deflections, c.g. shifts, etc.). Further, the attitude

loop as a separate entity will also exhibit rapid, well-damped responses (to commands) which look like those of a low-order system. Only a slight dynamic droop, (due to incomplete cancellation of $1/T_E$ and $1/T_E'$, and $1/T_{\theta_2}$ and $1/T_{\theta_2}'$), and a small static droop or error (i.e. $\theta/\theta_c = 0.93$ instead of 1.0 as $s \rightarrow 0$) detract from almost ideal behavior for the attitude-alone system. Thus, the analysis procedure, as illustrated in this section, has resulted in a rapid and relatively straightforward nominal system synthesis without any repetitious analysis.

There remains some question as to the detailed selection of criteria and equalization made in the course of the analysis. Such questions can easily be answered by making a sensitivity analysis on the final closure results. For example, the sensitivities of the closed-loop poles to changes in attitude and altitude gains, attitude equalization time constant, etc. (computed using the methods of Ref 10) can be plotted as vectors on a closed-loop root diagram to illustrate the first order effects of such changes. These vectors indicate the direction and magnitude of shifts in the closed-loop poles due to specified per-unit shifts in the various open-loop quantities. Thus, the effects of small changes from the nominal values used in the present analysis would be immediately available from the sensitivity results.

A similar system synthesis could be, and normally is, accomplished using the analog computer as a tool. Somewhat more trial and error is involved, and some sensitivities are a bit more difficult to obtain. (The calculation of sensitivities is a simple additional step when the system analysis data used in this section is available.) The analysis procedure presented here was not developed to be competitive with analog results (although it is superior in many ways). Instead one of the major reasons for its development was to achieve an alternate pencil-and-paper analysis technique. The statement that similar results would be obtained in an intelligent synthesis program using the analog computer simply indicates that the desired alternate analysis method has been achieved.

As emphasized throughout the report, the loop closure sequence is extremely important if results such as those obtained above are to be readily achieved. The altitude control system provides an excellent example in this regard.

Consider, for the moment, that the h loop had been closed first, with the θ loop as the outer loop. Then the gains derived above would have been a highly unlikely result because of the involved reasoning required to establish closure criteria. For example, the h loop would have to be closed to give an unstable, or nearly unstable inner loop, which would then be stabilized by the outer attitude loop. With the closure sequence actually selected the criteria were based upon relatively simple, essentially "standard", considerations derived from an intimate knowledge of the characteristics of low order systems. Now that the system has been explored the sequence is not nearly so important, since special criteria could now be evolved to allow the synthesis of a reasonable system even with the altitude loop closed first.

SECTION IV

LATERAL EXAMPLE - BANK ANGLE CONTROL SYSTEM

As noted in the introduction to Section III, the longitudinal and lateral numerical examples are intended both to illustrate the general analytical treatment developed in Section II, and to describe further some of the considerations leading to the selection of loop closure sequence and criteria. The insight necessary for such selection can be developed by preliminary analyses which study single-loop closures for each of the several loops involved, and loop closures based on ideal controllers and approximate literal vehicle transfer function factors. In the longitudinal example single-loop closures (of H_δ and Θ_δ loops) were discussed and the results were used to guide certain aspects of the multiloop analyses. The lateral controller treated below will provide an example using the other technique mentioned, i.e. approximate factors and ideal controllers converted to equivalent stability derivatives. Otherwise, the discussion will proceed in much the same way as that adopted for the longitudinal case.

A. SPECIALIZATION OF SYSTEM EQUATIONS

The lateral system chosen as an example is basically an attitude control system intended to maintain zero yawing velocity and zero bank angle. It can alsc be used to turn the aircraft by introducing bank angle commands. In this system the rudder is activated by feedbacks involving yawing velocity, r, and the aileron is activated by the bank angle error, φ_ϵ. The block diagram is given in Fig. 18 and the system designation is

$$\begin{aligned} r &\rightarrow \delta_r \\ \varphi_c &\rightarrow \delta_a \end{aligned} \tag{85}$$

The controller equations are

$$\begin{aligned} \delta_r &= -G_{\delta_r r} r \equiv -G_r r \\ \delta_a &= G_{\delta_a \varphi}(\varphi_c - \varphi) \equiv G_\varphi(\varphi_c - \varphi) \end{aligned} \tag{86}$$

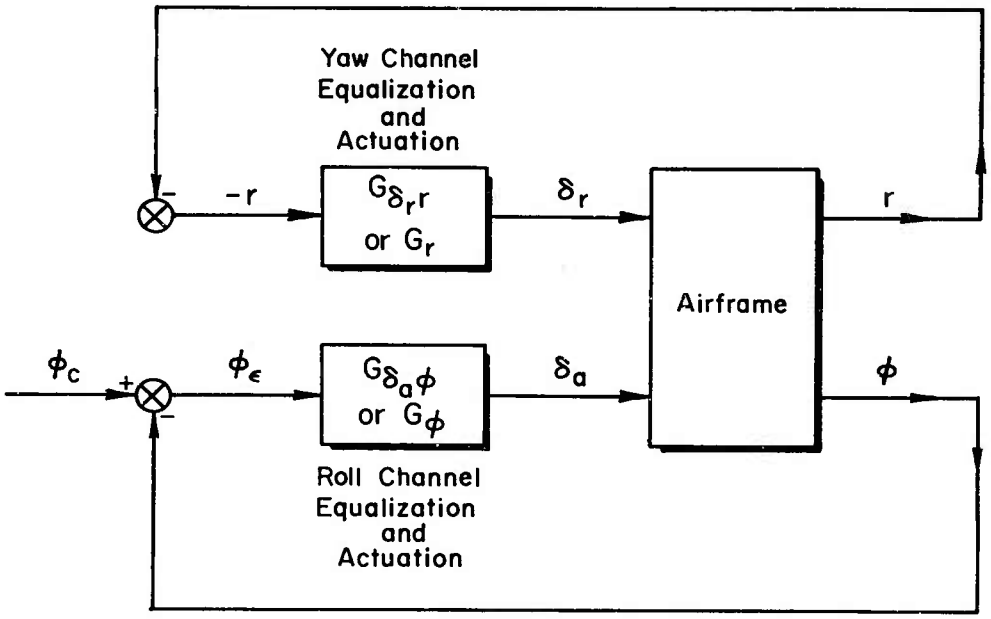

Figure 18. Bank Angle Control System

$\varphi_c \rightarrow \delta_a$, $r \rightarrow \delta_r$

where the conventional dual subscript notation for the controllers (which specifies both output and input controller quantities) can here be simplified to a single subscript without confusion. The system is basically a special case of the generalized system shown in Fig. 5. In terms of equations in Section II the quantities involved here are:

Control Deflections: $\delta_1 = \delta_r$

$\delta_2 = \delta_a$

Output Motion Quantities: $q_1 = \varphi$

$q_2 = r$

$q_3 = \beta$

Vehicle Transfer Functions: $Q_{1\delta_1} = \Phi_{\delta_r}$, $Q_{1\delta_2} = \Phi_{\delta_a}$

$Q_{2\delta_1} = R_{\delta_r}$, $Q_{2\delta_2} = R_{\delta_a}$

Controller Transfer Functions: $G_{11} = G_{13} = G_{22} = G_{23} = 0$

$$G_{12} = G_{\delta_r r} \equiv G_r$$

$$G_{21} = G_{\delta_a \varphi} \equiv G_\varphi$$

As special cases of the closed-loop transfer function forms given in Eqs 47 and 48,

$$\left.\frac{\varphi}{\varphi_c}\right]_{\substack{r \rightarrow \delta_r \\ \varphi \rightarrow \delta_a}} = \frac{G_\varphi(N_{\varphi\delta_a} + G_r N^{\varphi\ r}_{\delta_a \delta_r})}{\Delta + G_r N_{r\delta_r} + G_\varphi(N_{\varphi\delta_a} + G_r N^{\varphi\ r}_{\delta_a \delta_r})} \tag{87}$$

$$= \frac{G_\varphi \Phi_{\delta_a}(1 + G_r \dfrac{N^{\varphi\ r}_{\delta_a \delta_r}}{N_{\varphi\delta_a}})}{1 + G_r R_{\delta_r} + G_\varphi \Phi_{\delta_a}(1 + G_r \dfrac{N^{\varphi\ r}_{\delta_a \delta_r}}{N_{\varphi\delta_a}})} \tag{88}$$

The open-loop transfer function for an outer φ loop, (presuming the $r \rightarrow \delta_r$ channel is used as an inner loop and is already closed) is a special case of Eqs 49 and 50,

$$\left.\frac{\varphi}{\varphi_\epsilon}\right]_{r \rightarrow \delta_r} = \frac{G_\varphi(N_{\varphi\delta_a} + G_r N^{\varphi\ r}_{\delta_a \delta_r})}{\Delta + G_r N_{r\delta_r}} \tag{89}$$

$$= G_\varphi \Phi_{\delta_a} \frac{(1 + G_r \dfrac{N^{\varphi\ r}_{\delta_a \delta_r}}{N_{\varphi\delta_a}})}{1 + G_r R_{\delta_r}} \tag{90}$$

The airframe transfer functions in literal terms will be taken, for this example, to have the forms,

$$R_{\delta_r} = \frac{N_{r\delta_r}}{\Delta} = \frac{A_r(s + 1/T_{r_1})(s^2 + 2\zeta_r \omega_r s + \omega_r^2)}{(s + 1/T_s)(s + 1/T_R)(s^2 + 2\zeta_d \omega_d s + \omega_d^2)} \tag{91}$$

$$\Phi_{\delta_a} = \frac{N_{\varphi\delta_a}}{\Delta} = \frac{A_\varphi(s^2 + 2\zeta_\varphi \omega_\varphi s + \omega_\varphi^2)}{(s + 1/T_s)(s + 1/T_R)(s^2 + 2\zeta_d \omega_d s + \omega_d^2)} \tag{92}$$

The coefficients of these transfer functions, and literal approximate factors, in terms of aerodynamic and inertial parameters are presented in Refs 2 and 3. These stem from the three degrees of freedom equations

$$\begin{bmatrix} -\frac{g}{U_0} & 1 & (s - Y_v) \\ s(s - L'_p) & -L'_r & -L'_\beta \\ -N'_p s & (s - N'_r) & -N'_\beta \end{bmatrix} \begin{bmatrix} \varphi \\ r \\ \beta \end{bmatrix} = \begin{bmatrix} Y^*_{\delta_r} & 0 \\ L'_{\delta_r} & L'_{\delta_a} \\ N'_{\delta_r} & N'_{\delta_a} \end{bmatrix} \begin{bmatrix} \delta_r \\ \delta_a \end{bmatrix} \qquad (93)$$

which describe the lateral motions of the aircraft when only slightly perturbed from straight, wings level, and horizontal flight. By analogy with Eq 54 the "coupling numerator", $N_{\delta_a}^{\varphi\ r}{}_{\delta_r}$, is then

$$N_{\delta_a}^{\varphi\ r}{}_{\delta_r} = \begin{vmatrix} 0 & Y^*_{\delta_r} & (s - Y_v) \\ L'_{\delta_a} & L'_{\delta_r} & -L'_\beta \\ N'_{\delta_a} & N'_{\delta_r} & -N'_\beta \end{vmatrix}$$

$$= (L'_{\delta_a} N'_{\delta_r} - N'_{\delta_a} L'_{\delta_r}) \left[s - Y_v + \frac{Y^*_{\delta_r}(N'_\beta L'_{\delta_a} - L'_\beta N'_{\delta_a})}{(L'_{\delta_a} N'_{\delta_r} - N'_{\delta_a} L'_{\delta_r})} \right]$$

$$= A_{\varphi r}(s + 1/T_{\varphi r}) = K_{\varphi r}(T_{\varphi r} s + 1) \qquad (94)$$

Other coupling numerators for common multiloop systems are tabulated in Appendix B. The final line of Eq 94 also introduces the last type of special notation for multiloop analysis. Unfortunately even the double subscripts on $K_{\varphi r}$ and $T_{\varphi r}$ can be ambiguous, although not for most practical systems. If essential ambiguities ever occur, a sub and superscript combination, as in $N_{\delta_a}^{\varphi\ r}{}_{\delta_r}$, could conceivably be used (although a special, albeit inconsistent, notation would probably be clearer).

B. $\varphi \rightarrow \delta_a$ AND $r \rightarrow \delta_r$ AS SINGLE LOOPS

Because two control deflections, δ_r and δ_a, are used, analysis of the system will, as noted above, involve a "coupling numerator" closure. The system is, therefore, somewhat more complex than the altitude controller example of Section III. Another general difference is that both the $r \rightarrow \delta_r$ and $\varphi \rightarrow \delta_a$ feedbacks must play an attitude stabilization and regulation role, whereas only the θ loop had such requirements in the longitudinal system. Consequently the bandwidths of the $r \rightarrow \delta_r$ and $\varphi \rightarrow \delta_a$ loops, considered individually, should be about the same in magnitude. Also commands into either or both loops will provide a turning capability so the use of only bank angle commands, φ_c, indicated in Fig. 18 is somewhat premature. With only such rudimentary considerations, it is not obvious a priori which should be the inner loop. More insight can be gained by considering both as possible inner loops. Therefore individual loop closures of $r \rightarrow \delta_r$ and $\varphi \rightarrow \delta_a$ will be investigated below before delineating the loop closure sequence.

1. $r \rightarrow \delta_r$ as a Single Loop

The R_{δ_r} transfer function form given by Eq 91 has a numerator which is full of surprises if all manner of vehicles are considered. The cubic can factor into either a first order plus a quadratic (as indicated by Eq 91) or into three first orders. Further, the roots of the cubic can take on almost all possible variations in sign. Therefore a complete summary of the possibilities for $N_{r\delta_r}$ requires a large number of different conditions to be taken into account. Some, but not all, of these are codified in terms of approximate factors in Refs 2 and 15. For most manned aircraft, however, the number of possibilities is cut down substantially, with the factors usually being of the following nature:

$$\frac{1}{T_{r_1}} \doteq \frac{1}{T_R} > 0$$

$$\omega_r \ll \omega_d \quad , \quad \omega_r, \omega_d > 0$$

$$|\zeta_r| \ll 1 \quad , \quad \zeta_r \gtrless 0$$

The sketches of Fig. 19 illustrate typical dynamic characteristics achievable with a pure gain $r \rightarrow \delta_r$ loop closure for a typical manned aircraft. The R_{δ_r} transfer function has the features listed above, and both ζ_r and $1/T_s$ are taken to be negative. Fig. 19 indicates that the spiral can be stabilized readily ($1/T_s'$ is positive) and that considerable damping can be added to the Dutch roll mode ($\zeta_d' > \zeta_d$) without running into difficulties due to the high gain stability limitation inherent in the negative value assumed for ζ_r.

The same conclusions about Dutch roll damping augmentation and stabilization of the divergent spiral mode can be obtained using literal approximate factors and the method of equivalent stability derivatives. As given by Refs 2 and 3, the literal approximate factors for the spiral and Dutch roll damping are

$$\frac{1}{T_s} \doteq T_R \frac{g}{U_0} \left(\frac{L_\beta'}{N_\beta'} N_r' - L_r'\right) \tag{95}$$

$$2\zeta_d\omega_d \doteq -(Y_v + N_r') - \frac{L_\beta'}{N_\beta'}\left(N_p' - \frac{g}{U_0}\right) \tag{96}$$

For an ideal (no lag) controller the rudder deflection will be

$$\delta_r = -K_r r \tag{97}$$

which will create a yawing acceleration equal to $-N_{\delta_r}' K_r r$. The effective value of the stability derivative N_r' will then become

$$N_{r_{\text{effective}}}' = N_{r_{\substack{\text{vehicle}\\\text{alone}}}}' - K_r N_{\delta_r}' \tag{98}$$

The effective N_r' can be made more negative (much larger in magnitude) than the nominally negative N_r' of the vehicle-alone. Using $N_{r_{eff}}'$ to replace N_r' in Eq 96, the Dutch roll damping ($\zeta_d\omega_d$) with control is seen to be increased by the increment $K_r N_{\delta_r}'/2$. Similarly, the substitution of $N_{r_{eff}}'$ for N_r' in Eq 95 will increase $1/T_s$. For values of K_r such that the zero db line in Fig. 19 lies below the flat amplitude ratio portion running from zero to the breakpoint at $|1/T_s|$, this increment is sufficient to make

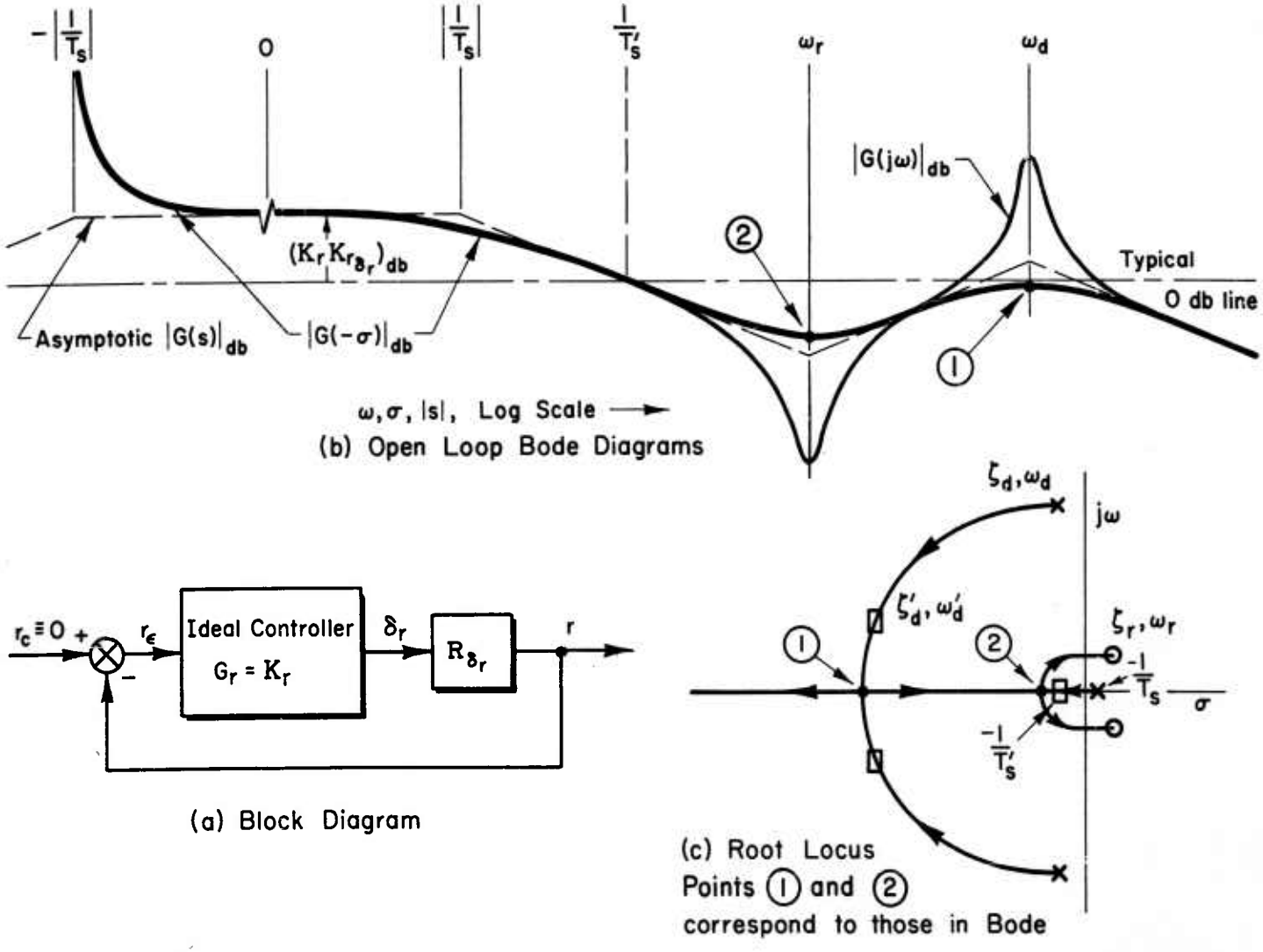

Figure 19. Sketches for Open- and Closed-Loop Characteristics of Yawing Velocity Control System with Ideal Controller and Nominal Airframe ($1/T_{r_1} \doteq 1/T_R$)

$$\left| \frac{L'_\beta}{N'_\beta} N'_{r_{eff}} \right| > \left| L'_r \right|$$

thereby reversing the original assumed inequality ($|L'_r| > |L'_\beta N'_r / N'_\beta|$) responsible for the diverging spiral mode.

Another feature of a pure gain yaw rate to rudder controller is its tendency to uncoordinate turns. This can be seen by considering the side acceleration equation for steady state, constant altitude conditions,

$$a_y = -g \sin \varphi + U_0 r = Y_v v + U_0 Y_{\delta_r}^* \delta_r \qquad (99)$$

For the turn to be coordinated a_y should be zero, so that, in the turn, $Y_v v + U_0 Y_{\delta_r}^* \delta_r$ must also be zero. When $a_y = 0$, yawing velocity and bank angle are then connected by the relationship

$$r = \frac{g}{U_0} \sin \varphi \qquad (100)$$

When $\delta_r = 0$ and Eq 100 holds, Eq 99 implies that the sideslip, v, is also zero. However, when $\delta_r = -K_r r$, the quantity $U_0 Y_{\delta_r}^* \delta_r$ will have a value other than zero, thereby requiring some sideslip if a_y is to be zero, or some lateral acceleration if v is to be zero. This deficiency of a pure gain $r \rightarrow \delta_r$ system can be eliminated either by introducing an r_c command, or by using pure lead–lag equalization ("washout") in the $r \rightarrow \delta_r$ controller. As indicated by the Bode and root locus sketches of Fig. 20 the introduction of lead–lag equalization need not strongly affect the augmented Dutch roll damping, although the spiral mode is no longer stabilized.

2. $\varphi \rightarrow \delta_a$ as a Single Loop

Single sensor control loops of the $\varphi \rightarrow \delta_a$ variety have been thoroughly documented elsewhere (e.g. Refs 2, 3, and 13). Although such systems can exhibit a wide variety of behavior depending upon the relative locations of the poles and zeros of Φ_{δ_a} and the equalization used in the controller, the most usual situations encountered are typified by the family of root loci shown in Fig. 21. Here the Dutch roll is lightly damped and, depending upon its root's location relative to the ζ_φ, ω_φ numerator, can be unstable when the loop is closed. With the exception of these "ω_φ, ω_d effects", the single axis system will exhibit

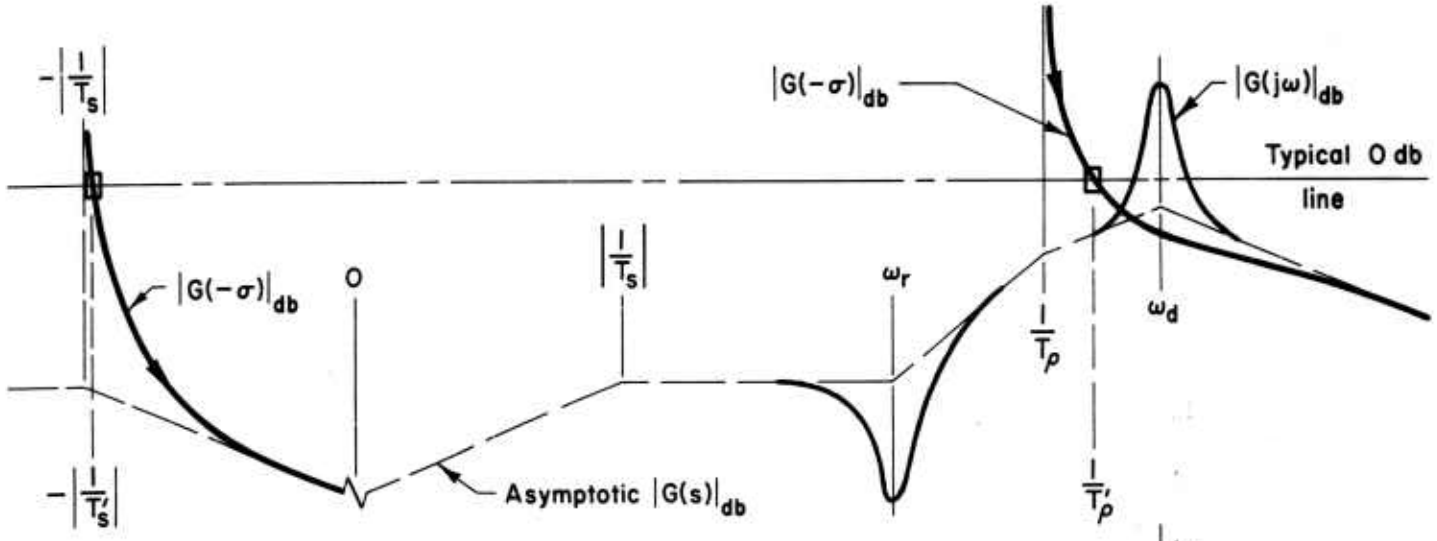

(b) Open Loop Bode Diagram

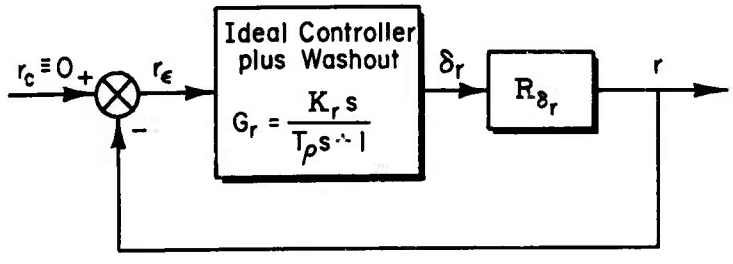

(a) Block Diagram

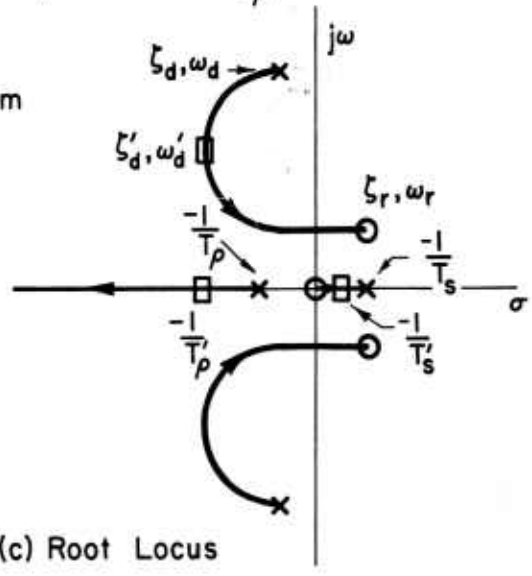

(c) Root Locus

Figure 20. Sketches for Open- and Closed-Loop Characteristics of Yawing Velocity Control System with Ideal Controller, Washout, and Nominal Airframe ($1/T_{r_1} \doteq 1/T_R$)

excellent closed-loop characteristics when simple lead equalization ($T_E s + 1$) is added to the basic airframe characteristics. This equalization can be obtained either by operating on the φ sensor signal, or by adding a roll rate gyro. In the latter case T_E is the ratio of roll rate to roll position gains.

Several means (see Ref 3) can be employed to offset deleterious ω_φ, ω_d effects such as those exhibited when the $\Phi_{\delta a}$ numerator quadratic is represented by the location marked with the "a" subscript. The method most pertinent to the present discussion is to use the yaw rate loop as a subsidiary loop to the $\varphi \rightarrow \delta_a$ loop. One helpful consequence of the yaw rate closure has already been noted in connection with Eq 96, i.e. the increase in Dutch roll damping. This will result in the Dutch roll poles being moved further into the left half plane. Another beneficial consequence of the yaw rate closure can be seen by examining the approximate factor for the $N_{\varphi_{\delta_a}}$ damping term. This is given by (Refs 2 or 3),

$$2\zeta_\varphi \omega_\varphi \doteq -(Y_v + N'_r) + \frac{N'_{\delta_a}}{L'_{\delta_a}} L'_r \qquad (101)$$

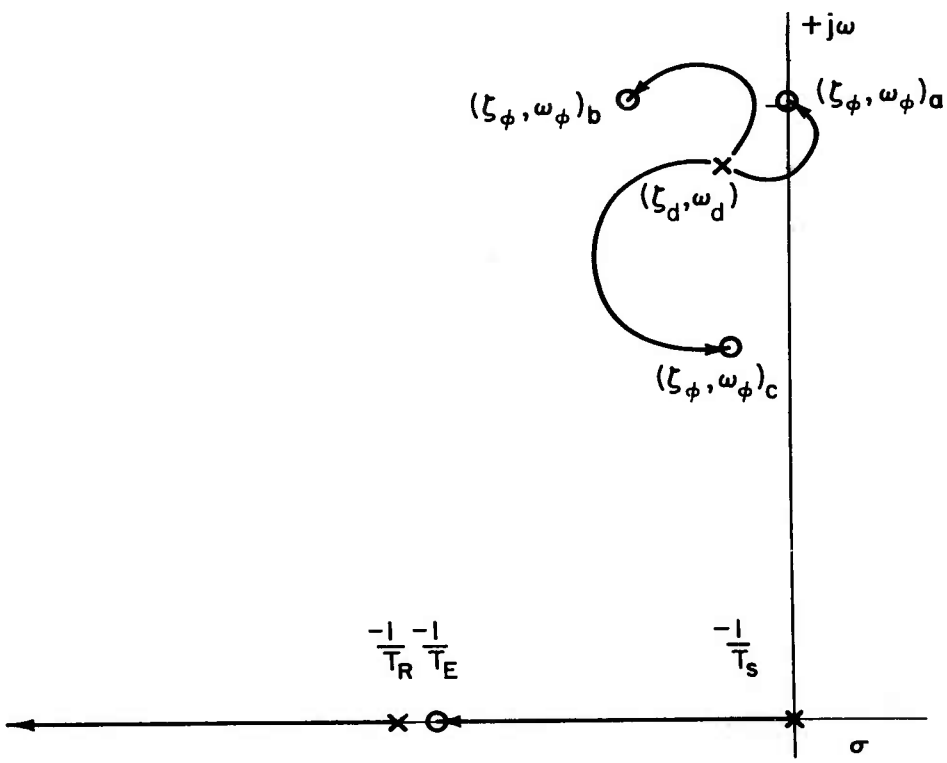

Figure 21. Root Loci for Single Axis Bank Angle Control System with Ideal Controller and Variable $N_{\varphi_{\delta_a}}$, $\delta_a = K\varphi(T_E s + 1)$

Using $N'_{r_{eff}}$ for N'_r in Eq 101 indicates that the yaw rate closure also moves the ζ_φ, ω_φ quadratic further into the left half plane. In the roll loop closure the locus will still go from ω_d to ω_φ as gain is increased, but this can no longer result in an instability if the roots corresponding to ω_φ and ω_d are sufficiently damped. Since this is accomplished by the yaw rate loop, it is seen to be an admirable inner loop for the $\varphi \rightarrow \delta_a$ system.

C. LOOP CLOSURE SEQUENCE

With the benefit of the discussions above a unique closure sequence can now be established for the $\varphi_c \rightarrow \delta_a$, $r \rightarrow \delta_r$ system. Table III specializes the general factors listed in Table I to this system. The net results of the factors summarized in Table III include the equivalent block diagram of Fig. 22, to indicate the closure sequence; the implicit requirement (which goes along with the absence of an r_c in Fig. 22) for washout (i.e. pure lead-lag) equalization in G_r; the explicit requirement for the $r \rightarrow \delta_r$ loop to appreciably augment the Dutch roll damping; and possible lead equalization in G_φ.

D. NUMERICAL EXAMPLE

The discussion above has covered the general aspects of the bank attitude control system with a washed-out yaw rate inner loop. For the numerical example of the present article a second-order lag will be used to approximate the servo characteristics, i.e.

$$G_\delta = \frac{1}{\left(\frac{s}{\omega_\delta}\right)^2 + \frac{2\zeta_\delta s}{\omega_\delta} + 1} \tag{102}$$

where $\omega_\delta = 20$ and $\zeta_\delta = 0.7$ are assumed as nominal values. The same servo characteristic will be used for the controller transfer function in both roll and yaw axes.

The airframe transfer functions are slightly modified from those of Ref 11 to provide a $\Phi_{\delta a}$ transfer function in which ω_φ is greater than ω_d. Also, for this example, a coupling numerator is needed. The airframe characteristics to be used are,

TABLE III

FACTORS INVOLVED IN BANK ATTITUDE SYSTEM LOOP CLOSURE SEQUENCE

Factor	Remarks	Consequences
Command Loop	Turn commands are introduced via φ_c. Since $r = (g/U_0) \sin \varphi$ in steady-state coordinated maneuvers, a steady-state yaw rate will exist in steady-state turns. Therefore either an r_c command must be introduced in the r channel, or $G_r(0)$ should be very small.	Washed-out $r \rightarrow \delta_r$ or a separate $r_c \rightarrow \delta_r$ is required
Relative Bandwidth	$r \rightarrow \delta_r$ is ordinarily used to increase the Dutch roll damping. $\varphi_c \rightarrow \delta_a$ must provide attitude regulation against external disturbances and command turn capability. Resulting bandwidths, $\omega_{c_{r_{loop}}}$ and $\omega_{c_{\varphi_{loop}}}$, are ordinarily about the same.	No help in determining closure sequence
Closure Characteristics as Single Loops and Equalization Economy	R_{δ_r} when ζ_r, ω_r and $1/T_r$ are positive is readily closed (see Ref 15 for other cases) with little or no equalization. Φ_{δ_a} can be difficult to close with stable results because of ω_φ, ω_d effects.	$r \rightarrow \delta_r$ inner loop; $\varphi \rightarrow \delta_a$ outer loop
Subsidiary Feedbacks	$r \rightarrow \delta_r$ suppresses ω_φ, ω_d effects, thereby relieving equalization in the φ loop and/or supplementing the action of $\varphi \rightarrow \delta_a$ as a lateral attitude controller.	$r \rightarrow \delta_r$ inner loop; $\varphi \rightarrow \delta_a$ outer loop
Interdependent Loops	The coupling numerator and R_{δ_r} closures are dependent only on G_r when vehicle characteristics are fixed.	Coupling numerator and R_{δ_r} closures are simultaneous
Multimode Character	A yawing velocity loop, without $\varphi_c \rightarrow \delta_a$, is a very common control mode to augment Dutch roll damping. On high performance manned aircraft it is almost invariably required to operate separately as well as in conjunction with other loops.	Inner loop should be $r \rightarrow \delta_r$

$$\Phi'_{\delta_a} = \Phi_{\delta_a}\left[\frac{1 + G_r \dfrac{N^{\phi\ r}_{\delta_a \delta_r}}{N_{\phi\delta_a}}}{1 + G_r R_{\delta_r}}\right]$$

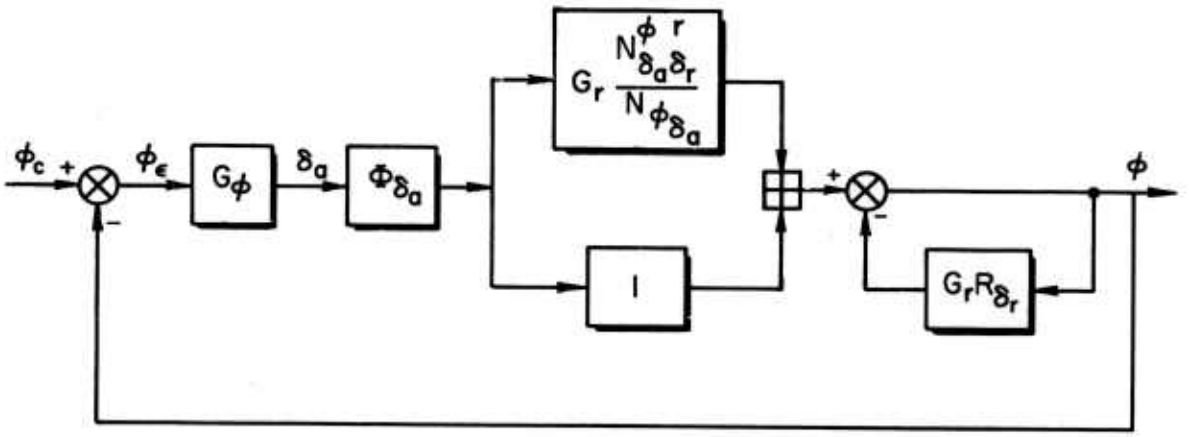

Figure 22. Equivalent Block Diagram for Bank Angle Control System

$\varphi_c \rightarrow \delta_a$, $r \rightarrow \delta_r$

$$R_{\delta_r} = \frac{(24.35)\left(\frac{s}{1.7767} + 1\right)\left[\left(\frac{s}{.293}\right)^2 + \frac{2(.00563)s}{(.293)} + 1\right]}{\left(\frac{s}{-.00135} + 1\right)\left(\frac{s}{1.777} + 1\right)\left[\left(\frac{s}{1.8775}\right)^2 + \frac{2(.0243)s}{(1.8775)} + 1\right]}$$

$$N^{\varphi\ r}_{\delta_a \delta_r} = (-1.98)\left(\frac{s}{.054} + 1\right) \qquad (103)$$

$$\Phi_{\delta_a} = \frac{(-13{,}600)\left[\left(\frac{s}{2.06}\right)^2 + \frac{2(.0043)s}{(2.06)} + 1\right]}{\left(\frac{s}{-.00135} + 1\right)\left(\frac{s}{1.777} + 1\right)\left[\left(\frac{s}{1.8775}\right)^2 + \frac{2(.0243)s}{(1.8775)} + 1\right]}$$

Besides the vehicle and servo characteristics, values are needed for the yaw loop washout time constant, T_ρ and the roll loop lead-equalization time constant, T_E. Both these time constants would ordinarily be found as part of a detailed optimization procedure in which the vehicle dynamics over the entire flight regime, and the effects of subsequent loop closures (e.g. a heading loop), are considered. Since studies of this kind are beyond the present scope, reasonable representative values are selected for the numerical example. With these values the controller transfer functions become

$$G_r = \frac{K_r s}{(\frac{s}{.20} + 1)\left[(\frac{s}{20})^2 + \frac{2(.7)s}{(20)} + 1\right]}$$

$$G_\varphi = \frac{K_\varphi(\frac{s}{.80} + 1)}{\left[(\frac{s}{20})^2 + \frac{2(.7)s}{(20)} + 1\right]} \qquad (104)$$

The principal objects of the analysis are to find values for K_r and K_φ which provide "good" closed-loop characteristics ("good" implies negligible static errors in φ, rapid and well damped responses to φ_c, adequate margins for vehicle and controller pole and zero variations, relative insensitivity to parasitic nonlinearities, etc.), and to find the poles and zeros of the closed-loop transfer function.

The first step in the analysis procedure is the simultaneous closure of the yaw rate and coupling loops to obtain $\Phi'_{\delta a}$. Bode diagrams for $G_r N^{\varphi r}_{\delta a \delta r}/N_{\varphi \delta a}$ and $G_r R_{\delta r}$ are shown in Fig. 23a and Fig. 23b respectively. The closed-loop poles resulting from closure of the first (coupling numerator) will be the zeros of $\Phi'_{\delta a}$, while the closed-loop poles from the second become the poles of $\Phi'_{\delta a}$. Only K_r is available for adjustment in either closure.

Suitable closure criteria can be expressed in several different ways, e.g. as phase margins and gain margins, closed-loop root values, integral performance measures such as ITAE or IE^2 based on dominant modes (Ref 16) etc. The actual criteria selected are somewhat a matter of taste and convenience, but, whatever

they are, the resulting system should possess good closed-loop characteristics. For the present case the closure selected will be based on design to a specified damping ratio of 0.8 for the closed-loop Dutch roll mode. The selection of a specified damping ratio as the closure criterion provides an alternative example to the use of a phase margin criterion, as in the altitude control case. The value of $\zeta_d' = 0.8$ might, at first glance, appear rather high. However, the corresponding value of ζ_φ', obtained from the simultaneous closure of the coupling loop, will be somewhat lower than 0.8, and the final $\varphi \rightarrow \delta_a$ closure will tend to force the modified Dutch roll roots to values near ζ_φ'. An alternative, of course, is to specify a damping ratio, ζ_φ', for the Φ'_{δ_a} numerator. As it will turn out, a specification of $\zeta_d' = 0.8$ is equivalent to $0.5 < \zeta_\varphi' < 0.6$.

The value of gain, K_r, consistent with a ζ_d' of 0.8 can be found in one of several ways, e.g. from a detailed root locus plot. In the present example it is expedient to use a short segment of a so-called ξ Bode plot (see Ref 9), for $\xi = -0.8$, as shown in Fig. 23b. The value of $|s|$ where $\angle G(\xi, |s|)$ is -180 degrees is then the undamped natural frequency, ω_d', of the Dutch roll as modified by the yaw rate closure, and the zero db line location is found by running it through $|G(\xi, |s|)|_{db}$ at this value of $|s|$. K_r is thus found to be -8.88 in linear units. (K_r is negative because the sign convention for δ_r results in N'_{δ_r} being negative.) The other closed-loop Φ'_{δ_a} numerator and denominator roots are found on the plots of Fig. 23 using the decomposition method. The resulting Φ'_{δ_a} transfer function is

$$\Phi'_{\delta_a} = \left.\frac{\varphi}{\delta_a}\right]_{r \rightarrow \delta_r} \doteq \frac{(-13{,}600)\left(\frac{s}{.23}+1\right)\left[\left(\frac{s}{2.12}\right)^2 + \frac{2(.58)s}{(2.12)} + 1\right]\left[\left(\frac{s}{18.2}\right)^2 + \frac{2(.7)s}{(18.2)} + 1\right]}{\left(\frac{s}{-.00105}+1\right)\left(\frac{s}{.31}+1\right)\left(\frac{s}{1.777}+1\right)\left[\left(\frac{s}{1.82}\right)^2 + \frac{2(.8)s}{(1.82)} + 1\right]\left[\left(\frac{s}{18.3}\right)^2 + \frac{2(.69)s}{(18.3)} + 1\right]} \tag{105}$$

The last quadratic in the numerator and denominator of Eq 105 derive from the servo characteristics. These are nearly identical, and can be presumed to cancel with only negligible error. This type of near cancellation invariably occurs when coupling numerators are present. It will be recalled that a similar numerator quadratic was not present in the altitude controller case because of the absence of a coupling numerator closure. Cancelling these quadratics gives the result,

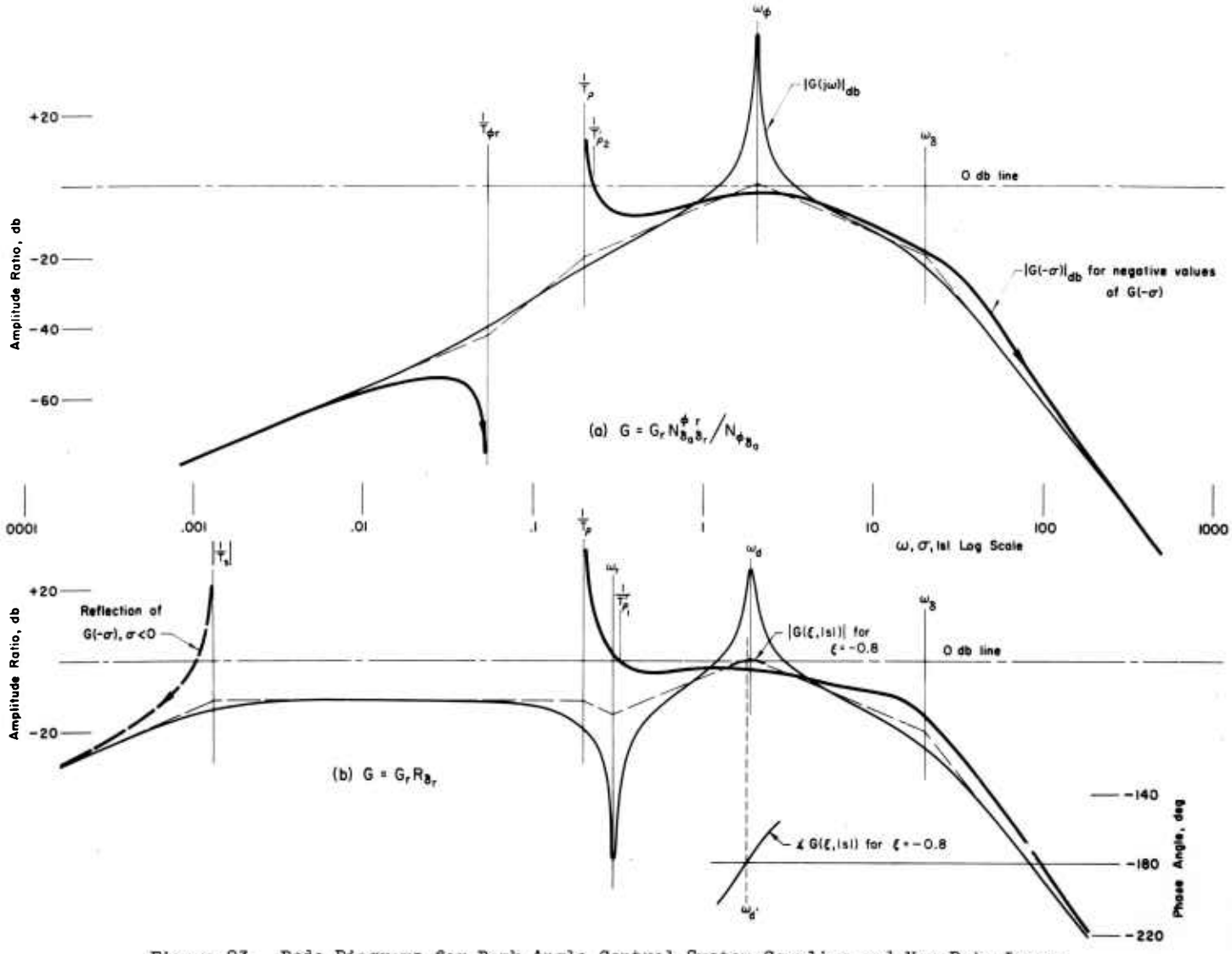

Figure 23. Bode Diagrams for Bank Angle Control System Coupling and Yaw Rate Loops; $G_r N^{\phi\ r}_{\delta_a \delta_r} / N_{\phi\delta_a}$ and $G_r R_{\delta_r}$, Respectively

$$\Phi'_{\delta_a} = \frac{\left(\frac{A_\varphi T'_s T'_{\rho_1} T'_R \omega'^2_\varphi}{T'_{\rho_2} \omega'^2_d}\right)(T'_{\rho_2}s + 1)\left[\left(\frac{s}{\omega'_\varphi}\right)^2 + \frac{2\zeta'_\varphi s}{\omega'_\varphi} + 1\right]}{(T'_s s + 1)(T'_{\rho_1} s + 1)(T'_R s + 1)\left[\left(\frac{s}{\omega'_d}\right)^2 + \frac{2\zeta'_d s}{\omega'_d} + 1\right]} \tag{106}$$

$$= \frac{(-13,600)\left(\frac{s}{.23} + 1\right)\left[\left(\frac{s}{2.12}\right)^2 + \frac{2(.58)s}{(2.12)} + 1\right]}{\left(\frac{s}{-.00105} + 1\right)\left(\frac{s}{.31} + 1\right)\left(\frac{s}{1.777} + 1\right)\left[\left(\frac{s}{1.82}\right)^2 + \frac{2(.8)s}{(1.82)} + 1\right]}$$

The Φ'_{δ_a} transfer function given by Eq 106 is now combined with G_φ (Eq 104), to form the outer, open-loop transfer function. Bode diagrams and a root locus sketch for closure about this open-loop transfer function are shown in Figs. 24 and 25. To make the closed-loop transfer function $\varphi/\varphi_c\Big]_{\substack{\varphi_c \rightarrow \delta_a \\ r \rightarrow \delta_r}}$ approximately invariant with flight condition a high gain closure shall be used and the equalization, $(T_E s + 1)$, will actually be placed in the feedback path, i.e. as shown in Fig. 26. The closed-loop transfer function will then have the form

$$\frac{\varphi}{\varphi_c}\Big]_{\substack{\varphi_c \rightarrow \delta_a \\ r \rightarrow \delta_r}} = \frac{1}{(T_E s + 1)}\left\{\frac{G_\varphi \Phi'_{\delta_a}}{1 + G_\varphi \Phi'_{\delta_a}}\right\} \tag{107}$$

To the extent that the high gain closure makes the quotient in braces approach unity, $\varphi/\varphi_c\Big]_{\substack{\varphi_c \rightarrow \delta_a \\ r \rightarrow \delta_r}}$ will approach $(T_E s + 1)^{-1}$. T_E is a function only of controller parameters, so its value can be controlled readily.

To accomplish the high gain closure, but still preserve some stability (in the closed-loop servo mode), a phase margin of 40 degrees is selected. The gain, K_φ, will then be -6.6 db or 0.467 in linear units. Using unified servo-analysis techniques, the closed-loop transfer function is

$$\frac{G_\varphi \Phi'_{\delta_a}}{1 + G_\varphi \Phi'_{\delta_a}} = \frac{(1)(T'_{\rho_2}s + 1)(T_E s + 1)\left[\left(\frac{s}{\omega'_\varphi}\right)^2 + \frac{2\zeta'_\varphi s}{\omega'_\varphi} + 1\right]}{(T''_s s + 1)(T''_{\rho_1} s + 1)(T''_R s + 1)\left[\left(\frac{s}{\omega''_d}\right)^2 + \frac{2\zeta''_d s}{\omega''_d} + 1\right]\left[\left(\frac{s}{\omega'_\delta}\right)^2 + \frac{2\zeta'_\delta s}{\omega'_\delta} + 1\right]}$$

$$= \frac{(1)\left(\frac{s}{.23} + 1\right)\left(\frac{s}{.80} + 1\right)\left[\left(\frac{s}{2.12}\right)^2 + \frac{2(.58)s}{(2.12)} + 1\right]}{\left(\frac{s}{.225} + 1\right)\left(\frac{s}{.78} + 1\right)\left(\frac{s}{21.7} + 1\right)\left[\left(\frac{s}{2.01}\right)^2 + \frac{2(.56)s}{(2.01)} + 1\right]\left[\left(\frac{s}{16.3}\right)^2 + \frac{2(.25)s}{(16.3)} + 1\right]} \qquad (108)$$

Note that the prime notation is here extended to two loop closures by the double-prime quantities. The entire numerator is approximately cancelled by corresponding denominator terms, leaving

$$\frac{G_\varphi \Phi'_{\delta_a}}{1 + G_\varphi \Phi'_{\delta_a}} \doteq \frac{1}{\left(\frac{s}{21.7} + 1\right)\left[\left(\frac{s}{16.3}\right)^2 + \frac{2(.25)s}{(16.3)} + 1\right]} \qquad (109)$$

This is nearly unity at frequencies below 12 rad/sec, or so, and hence $\varphi/\varphi_c\Big]_{\substack{\varphi_c \rightarrow \delta_a \\ r \rightarrow \delta_r}}$ is very close to just $(T_E s + 1)^{-1}$ for these same low frequencies.

The width of this frequency region, and the near cancellation indicated by Eq 108, cannot be materially improved without serious degradation of the damping ratio of the closed-loop servo mode.

While the φ response to φ_c signals will approximate that of a first order system having a time constant of $T_E = 1/0.8$, the aircraft response to external disturbances will not be of such simple form. For example, the transfer function relating yawing velocity to a side gust will not contain the numerator (ω'_φ) quadratic which essentially cancels the closed-loop Dutch roll (ω''_d) mode, as shown in Eq 108. Instead, the dominant yawing velocity mode will in fact be the modified Dutch roll; but it will be adequately damped ($\zeta''_d = .56$). Similar remarks can be made about the other augmented-airframe characteristics which, in general, have values compatible with good suppression of external disturbances of almost any type likely to be encountered.

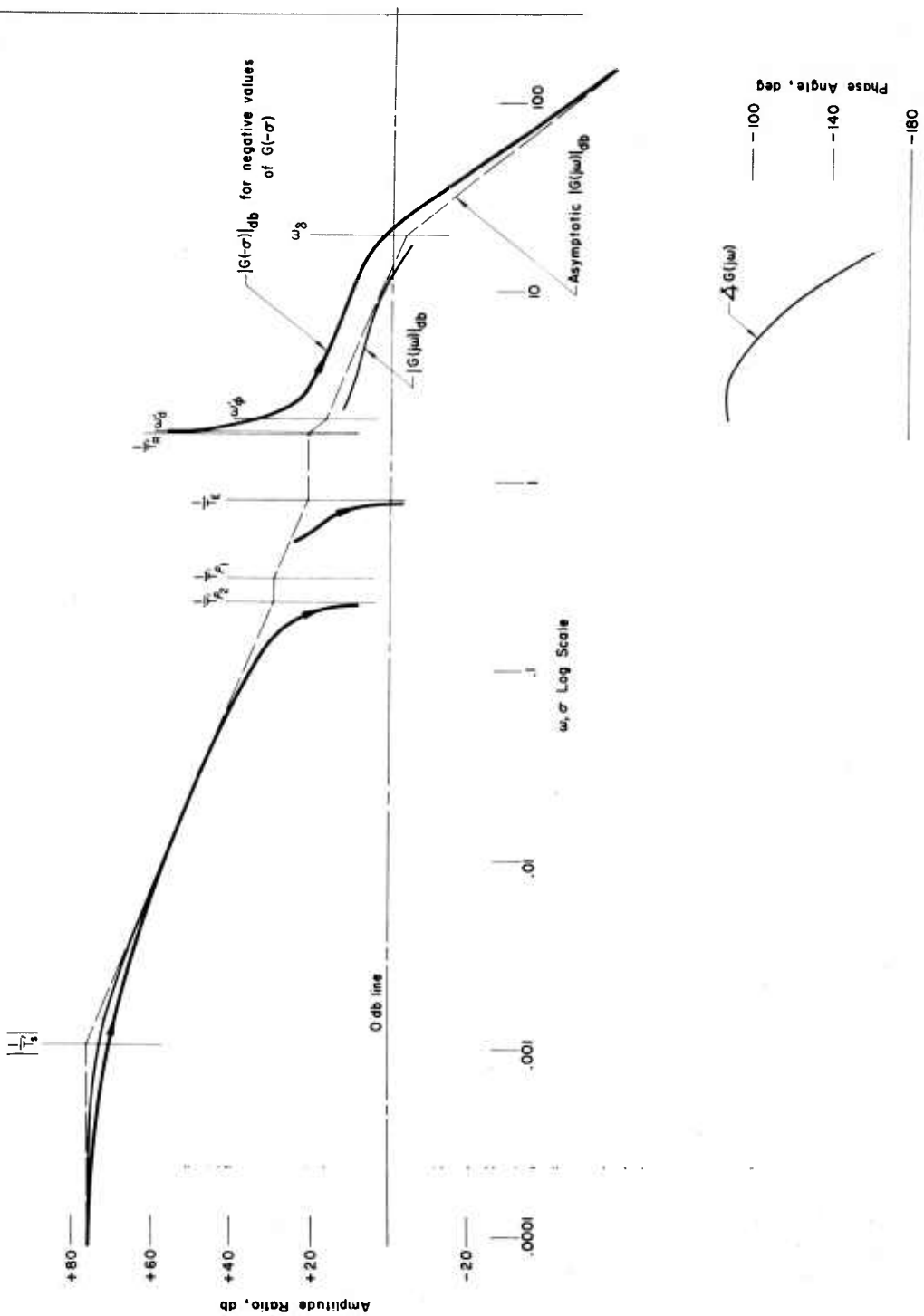

Figure 24. Bode Diagram for Example Bank Angle Control System Outer Loop, $G = G_\varphi \Phi_{\delta_a}'$

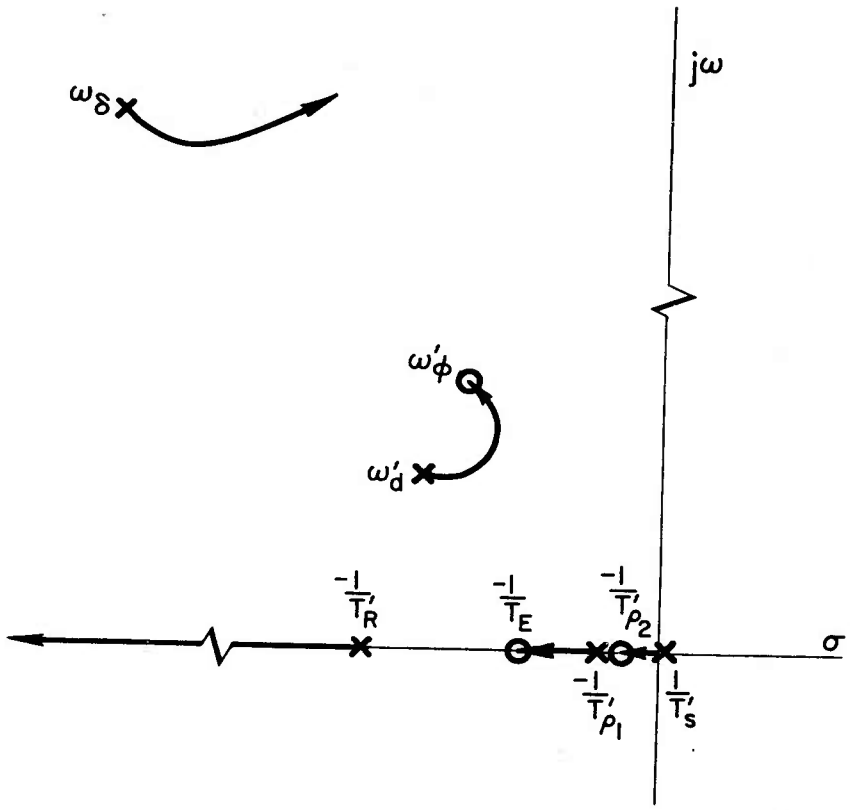

Figure 25. Root Locus Sketch of Bank Angle Control System Outer Open-Loop Transfer Function, $G_\varphi \Phi'_{\delta_a}$

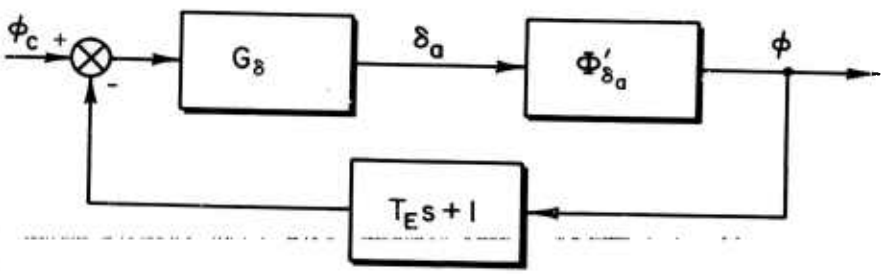

Figure 26. Block Diagram Indicating Location of Outer-Loop Equalization

REFERENCES

1. Mesarović, Mihajlo D., The Control of Multivariable Systems, John Wiley and Sons, Inc., New York, 1960.

2. Ashkenas, Irving L., and Duane T. McRuer, Approximate Airframe Transfer Functions and Application to Single Sensor Control Systems, WADC TR 58-82, June 1958.

3. Ashkenas, Irving L., and Duane T. McRuer, Optimization of the Flight-Control Airframe System, Journal of the Aero/Space Sciences, Volume 27, No. 3, March 1960.

4. Klemin, A., Pepper, P. A., and Wittner, H. A., Longitudinal Stability in Relation to the Use of an Automatic Pilot, NACA TN 666, 1938.

5. Imlay, F. H., A Theoretical Study of Lateral Stability with an Automatic Pilot, NACA Report No. 693, 1940.

6. Povejsil, D. J., and A. M. Fuchs, A Method for the Preliminary Synthesis of a Complex Multiloop Control System, AIEE Trans., Pt. II, Vol. 74, pp. 129-134, 1955.

7. Brown, A. T., et al., Model XRSSM-N-9 (Regulus II) Guided Missile Pre-flight Stability and Control Analyses, Chance Vought Aircraft Report 10118, February 1956.

8. Mataga, Suikei, A Technique for the Synthesis of n-Input, m-Output Servo Systems to Meet System Requirements, M.S. Thesis, UCLA, May 1958.

9. McRuer, Duane T., Unified Analysis of Linear Feedback Systems, ASD TR 61-118, July 1961.

10. McRuer, D. T., and R. L. Stapleford, Sensitivity and Modal Response for Single-Loop and Multiloop Systems, ASD-TDR-62-812, January 1963.

11. Dynamics of the Airframe, BuAer Report AE-61-4-II, Northrop Aircraft, Inc., September 1952.

12. Aitken, A. C., Determinants and Matrices, Interscience Publishers, Inc., New York, N. Y., 1956.

13. Ashkenas, I. L., and D. T. McRuer, The Determination of Lateral Handling Quality Requirements from Airframe-Human Pilot System Studies, WADC TR 59-135, June 1959.

14. McRuer, Duane T., Irving L. Ashkenas, and C. L. Guerre, A Systems Analysis View of Longitudinal Flying Qualities, WADD TR 60-43, January 1960.

15. Ashkenas, I. L., and D. T. McRuer, Competing Flight Control Systems for Entry Glider Lateral Control, ASD-TDR-62-699, October 1962.

16. Wolkovitch, J., R. Magdaleno, D. McRuer, D. Graham, and J. McDonnell, Performance Criteria for Linear Constant-Coefficient Systems with Deterministic Inputs, ASD TR 61-501, February 1962.

APPENDIX A

DEVELOPMENT OF EQUATION 24, Δ_{sys}

The characteristic function of the generalized multiloop system, Δ_{sys}, is given in both determinant and expanded form by Eq 24. The expansion of the determinant is considerably expedited by writing it as shown in Eq A-1, in which each of the element columns is denoted by a Roman numeral and each subcolumn by a capital letter. The complete expansion of Eq A-1 produces $3^4 = 81$ fourth-order determinants in which all elements are single (non-summed) quantities. However, as will shortly be seen, 60 of the determinants are zero, one is equal to Eq 25, and the remaining 20 are in the form of Eq 26 or 27.

$$\Delta_{sys} = \begin{array}{c} \begin{array}{cccccccccccc} & \multicolumn{3}{c}{\text{I}} & \multicolumn{3}{c}{\text{II}} & \multicolumn{3}{c}{\text{III}} & \multicolumn{3}{c}{\text{IV}} \\ & \text{A} & \text{B} & \text{C} & \text{A} & \text{B} & \text{C} & \text{A} & \text{B} & \text{C} & \text{A} & \text{B} & \text{C} \end{array} \\ \begin{vmatrix} a_{11} + F_{11}G_{11} + F_{12}G_{21} & a_{12} + F_{11}G_{12} + F_{12}G_{22} & a_{13} + F_{11}G_{13} + F_{12}G_{23} & 0 + F_{11}G_{14} + F_{12}G_{24} \\ a_{21} + F_{21}G_{11} + F_{22}G_{21} & a_{22} + F_{21}G_{12} + F_{22}G_{22} & a_{23} + F_{21}G_{13} + F_{22}G_{23} & 0 + F_{21}G_{14} + F_{22}G_{24} \\ a_{31} + F_{31}G_{11} + F_{32}G_{21} & a_{32} + F_{31}G_{12} + F_{32}G_{22} & a_{33} + F_{31}G_{13} + F_{32}G_{23} & 0 + F_{31}G_{14} + F_{32}G_{24} \\ -a_{41} + 0 + 0 & -a_{42} + 0 + 0 & -a_{43} + 0 + 0 & 1 + 0 + 0 \end{vmatrix} \end{array} \qquad \text{(A-1)}$$

Before proceeding with the systematic expansion of Eq A-1, and by way of review, six fundamental properties of determinants are stated (Ref. 12):

1. If <u>all</u> elements in a row or column are zero, the determinant is zero.

2. If all elements but one in a row or column are zero, the determinant is the product of that element and its cofactor.

3. If two columns or two rows of a determinant are identical, the determinant is zero.

4. If all elements in any column are multiplied by a factor, the determinant is multiplied by that factor.

5. If each element in any column or row is expressed as the sum of two quantities, the determinant can be expressed as the sum of two determinants of the same order.

6. If two columns or two rows of a determinant are interchanged, the determinant is not changed in absolute value but is changed in sign.

The systematic expansion of Eq A-1 is easily accomplished by covering two of the three subcolumns in each column with paper strips and evaluating the visible fourth-order determinant. By systematically shifting strips, but always keeping two subcolumns in each column covered, which is equivalent to applying property 5, Eq A-1 is completely expanded as a sum of determinants. As examples of the evaluation of each determinant:

With subcolumns IA, IIA, IIIA, and IVA exposed, the visible determinant is equal to Δ (Eq 25).

Shifting one strip in the fourth column exposes subcolumns IA, IIA, IIIA, and IVB, and the visible determinant, using property 4 and the definition of $N_{q_{i\delta_j}}$, is $G_{14}N_{q_{4\delta_1}}$; i.e.,

$$\begin{vmatrix} a_{11} & a_{12} & a_{13} & F_{11}G_{14} \\ a_{21} & a_{22} & a_{23} & F_{21}G_{14} \\ a_{31} & a_{32} & a_{33} & F_{31}G_{14} \\ -a_{41} & -a_{42} & -a_{43} & 0 \end{vmatrix} = G_{14} \begin{vmatrix} a_{11} & a_{12} & a_{13} & F_{11} \\ a_{21} & a_{22} & a_{23} & F_{21} \\ a_{31} & a_{32} & a_{33} & F_{31} \\ -a_{41} & -a_{42} & -a_{43} & 0 \end{vmatrix} = G_{14}N_{q_{4\delta_1}}$$

Shifting one strip in the first column exposes subcolumns IB, IIA, IIIA, and IVB, and the visible determinant, using property 4 and then property 3, is zero; i.e.,

$$\begin{vmatrix} F_{11}G_{11} & a_{12} & a_{13} & F_{11}G_{14} \\ F_{21}G_{11} & a_{22} & a_{23} & F_{21}G_{14} \\ F_{31}G_{11} & a_{32} & a_{33} & F_{31}G_{14} \\ 0 & -a_{42} & -a_{43} & 0 \end{vmatrix} = G_{11}G_{14} \begin{vmatrix} F_{11} & a_{12} & a_{13} & F_{11} \\ F_{21} & a_{22} & a_{23} & F_{21} \\ F_{31} & a_{32} & a_{33} & F_{31} \\ 0 & -a_{42} & -a_{43} & 0 \end{vmatrix} = 0$$

In general, whenever two or more exposed subcolumns have similar alphabetical designations other than "A", the determinant is identically zero by properties 3 and 4.

The complete set of possible combinations of subcolumns is evaluated in Table A-I. The dots in a particular row indicate the subcolumns of Columns II, III, and IV which are combined with each of the three subcolumns of I. The evaluation (nonzero or zero) of the resultant determinants is indicated in the appropriate subcolumn of I. The nonzero determinants are given in Table A-II using vehicle transfer function numerator, $N_{q_i\delta_j}$, and coupling numerator, $N^{q_i q_j}_{\delta_1\delta_2}$, notation (Eq 26 and 27, respectively).

The characteristic function, Δ_{sys}, is the sum of all determinants shown in Table A-II, and is given below.

$$
\begin{aligned}
\Delta_{sys} = \Delta &+ G_{11}N_{q_1\delta_1} + G_{12}N_{q_2\delta_1} + G_{13}N_{q_3\delta_1} + G_{14}N_{q_4\delta_1} \\
&+ G_{21}N_{q_1\delta_2} + G_{22}N_{q_2\delta_2} + G_{23}N_{q_3\delta_2} + G_{24}N_{q_4\delta_2} \\
&+ G_{11}\Big(+ G_{22}N^{q_1q_2}_{\delta_1\delta_2} + G_{23}N^{q_1q_3}_{\delta_1\delta_2} + G_{24}N^{q_1q_4}_{\delta_1\delta_2}\Big) \\
&+ G_{12}\Big(G_{21}N^{q_2q_1}_{\delta_1\delta_2} + G_{23}N^{q_2q_3}_{\delta_1\delta_2} + G_{24}N^{q_2q_4}_{\delta_1\delta_2}\Big) \\
&+ G_{13}\Big(G_{21}N^{q_3q_1}_{\delta_1\delta_2} + G_{22}N^{q_3q_2}_{\delta_1\delta_2} + G_{24}N^{q_3q_4}_{\delta_1\delta_2}\Big) \\
&+ G_{14}\Big(G_{21}N^{q_4q_1}_{\delta_1\delta_2} + G_{22}N^{q_4q_2}_{\delta_1\delta_2} + G_{23}N^{q_4q_3}_{\delta_1\delta_2}\Big)
\end{aligned}
\qquad \text{(A-2)}
$$

Noting from property 6 of determinants that $N^{q_iq_j}_{\delta_1\delta_2} = -N^{q_jq_i}_{\delta_1\delta_2}$, and recognizing that controller functions other than those chosen can be factored out, it is clear that various simplifications and modifications to Eq A-2 are possible. But the simplest of all is the shorthand form given in the text (Eq 24):

$$
\Delta_{sys} = \Delta + \sum_{i=1}^{4}\sum_{j=1}^{2} G_{ji}N_{q_i\delta_j} + \sum_{\substack{i=1 \\ i\neq k}}^{4}\sum_{k=1}^{4} G_{1i}G_{2k}N^{q_iq_k}_{\delta_1\delta_2} \qquad \text{(A-3)}
$$

TABLE A-I

EVALUATION OF ALL POSSIBLE SUBCOLUMN COMBINATIONS IN EQUATION A-1

I			II			III			IV		
A	B	C	A	B	C	A	B	C	A	B	C
✓	✓	✓	·			·			·		
✓	0	✓	·			·				·	
✓	✓	0	·			·					·
✓	0	✓	·				·		·		
0	0	0	·				·			·	
✓	0	0	·				·				·
✓	✓	0	·					·	·		
✓	0	0	·					·		·	
0	0	0	·					·			·
✓	0	✓		·		·			·		
0	0	0		·		·				·	
✓	0	0		·		·					·
0	0	0		·			·		·		
0	0	0		·			·			·	
0	0	0		·			·				·
✓	0	0		·				·	·		
0	0	0		·				·		·	
0	0	0		·				·			·
✓	✓	0			·	·			·		
✓	0	0			·	·				·	
0	0	0			·	·					·
✓	0	0			·		·		·		
0	0	0			·		·			·	
0	0	0			·		·				·
0	0	0			·			·	·		
0	0	0			·			·		·	
0	0	0			·			·			·

✓ Denotes that determinant of indicated combination of subcolumns is nonzero
0 Denotes that determinant of indicated combination of subcolumns is zero

TABLE A-II

NONZERO DETERMINANTS IN EXPANSION OF EQUATION A-1

EXPOSED SUBCOLUMNS	VISIBLE DETERMINANT
IA, IIA, IIIA, IVA	Δ
" " " IVB	$G_{14}{}^{N}q_4\delta_1$
" " " IVC	$G_{24}{}^{N}q_4\delta_2$
" " IIIB, IVA	$G_{13}{}^{N}q_3\delta_1$
" " " IVC	$G_{13}G_{24}{}^{N}{}^{q_3q_4}_{\delta_1\delta_2}$
" " IIIC, IVA	$G_{23}{}^{N}q_3\delta_2$
" " " IVB	$G_{14}G_{23}{}^{N}{}^{q_4q_3}_{\delta_1\delta_2}$
IA, IIB, IIIA, IVA	$G_{12}{}^{N}q_2\delta_1$
" " " IVC	$G_{12}G_{24}{}^{N}{}^{q_2q_4}_{\delta_1\delta_2}$
" " IIIC, IVA	$G_{12}G_{23}{}^{N}{}^{q_2q_3}_{\delta_1\delta_2}$
IA, IIC, IIIA, IVA	$G_{22}{}^{N}q_2\delta_2$
" " " IVB	$G_{14}G_{22}{}^{N}{}^{q_4q_2}_{\delta_1\delta_2}$
" " IIIB, IVA	$G_{13}G_{22}{}^{N}{}^{q_3q_2}_{\delta_1\delta_2}$
IB, IIA, IIIA, IVA	$G_{11}{}^{N}q_1\delta_1$
" " " IVC	$G_{11}G_{24}{}^{N}{}^{q_1q_4}_{\delta_1\delta_2}$
" " IIIC, IVA	$G_{11}G_{23}{}^{N}{}^{q_1q_3}_{\delta_1\delta_2}$
IB, IIC, IIIA, IVA	$G_{11}G_{22}{}^{N}{}^{q_1q_2}_{\delta_1\delta_2}$
IC, IIA, IIIA, IVA	$G_{21}{}^{N}q_1\delta_2$
" " " IVB	$G_{14}G_{21}{}^{N}{}^{q_4q_1}_{\delta_1\delta_2}$
" " IIIB, IVA	$G_{13}G_{21}{}^{N}{}^{q_3q_1}_{\delta_1\delta_2}$
IC, IIB, IIIA, IVA	$G_{12}G_{21}{}^{N}{}^{q_2q_1}_{\delta_1\delta_2}$

APPENDIX B

TYPICAL COUPLING NUMERATORS

Examples of longitudinal and lateral coupling numerators are given in Tables B-I and B-II, respectively, for the approximate equations of motion shown below:

Longitudinal

$$\begin{bmatrix} s - X_u & -X_w & g & 0 \\ -Z_u & (s - Z_w) & -U_o s & 0 \\ -M_u & -M_{\dot{w}} s - M_w & s^2 - M_q s & 0 \\ 0 & 1/s & -U_o/s & 1 \end{bmatrix} \begin{Bmatrix} u \\ w \\ \theta \\ h \end{Bmatrix} = \begin{Bmatrix} X_\delta \delta \\ Z_\delta \delta \\ M_\delta \delta \\ 0 \end{Bmatrix} \qquad \text{(B-1)}$$

Lateral

$$\begin{bmatrix} s - Y_v & -g/U_o & 1 & 0 \\ -L'_\beta & s(s - L'_p) & -L'_r & 0 \\ -N'_\beta & -N'_p s & s - N'_r & 0 \\ -U_o s & g - l_x s^2 \sin \alpha_o & -U_o - l_x s \cos \alpha_o & 1 \end{bmatrix} \begin{Bmatrix} \beta \\ \varphi \\ r \\ a_y \end{Bmatrix} = \begin{Bmatrix} Y^*_\delta \delta \\ L'_\delta \delta \\ N'_\delta \delta \\ 0 \end{Bmatrix} \qquad \text{(B-2)}$$

The characteristic determinants of both the longitudinal and lateral equations of motion are the usual quartics, Δ_{long} and Δ_{lat}, with unity coefficients of the s^4 terms. The coupling numerators are thus compatible with the conventional airframe transfer functions in Ref 2.

In the tables the A, B, C coefficients are those for terms of descending order in s (e.g., A is the coefficient of either s^2 or s; B, the coefficient of s or s^o; C, the coefficient of s^o, or nonexistent). The complete literal expressions for each coefficient are shown, as are the forms of the coupling numerators, and approximate literal values of the gains, time constants, frequencies, etc., appropriate to these forms. In most cases the approximations involved are obvious by reference to the complete expressions and stem largely from the usually negligible nature of certain control effectiveness derivatives (e.g., X_{δ_e} longitudinally and $Y^*_{\delta_a}$ laterally) and products of cross-control effectiveness derivatives (e.g., $N'_{\delta_a} L'_{\delta_r} \ll L'_{\delta_a} N'_{\delta_r}$).

One property of coupling numerators, i.e., $N^{q_i q_j}_{\delta_k \delta_l} = -N^{q_j q_i}_{\delta_k \delta_l}$, is used extensively in the tables to simplify the presentation. An additional property applicable for the determination of coupling numerators containing an auxiliary output motion quantity is also used. With q_i (i = 1,2,3) the independent degrees of freedom and q_4 an auxiliary variable,

$$q_4 = a_{41}q_1 + a_{42}q_2 + a_{43}q_3$$

then

$$N^{q_i q_4}_{\delta_1 \delta_2} = a_{41} N^{q_i q_1}_{\delta_1 \delta_2} + a_{42} N^{q_i q_2}_{\delta_1 \delta_2} + a_{43} N^{q_i q_3}_{\delta_1 \delta_2} \tag{B-3}$$

where one of the coupling numerators on the right side will be zero because $N^{q_i q_j}_{\delta_k \delta_l}$ is zero if i = j or k = l.

For example, the independent degrees of freedom for the longitudinal equations of motion are u, w, and θ, and two auxiliary motion quantities are

$$\alpha = \frac{1}{U_o} w \tag{B-4}$$

$$h = \frac{U_o}{s}\theta - \frac{1}{s} w \tag{B-5}$$

Using Eq B-3 and B-4,

$$N^{\theta\ \alpha}_{\delta_e \delta_T} = \frac{1}{U_o} N^{\theta\ w}_{\delta_e \delta_T} \tag{B-6}$$

Similarly, using Eq B-3 and B-5,

$$N^{\theta\ h}_{\delta_e \delta_T} = -\frac{1}{s} N^{\theta\ w}_{\delta_e \delta_T} \tag{B-7}$$

Thus from Eq B-6 and B-7,

$$sN^{\theta\ h}_{\delta_e \delta_T} = -U_o N^{\theta\ \alpha}_{\delta_e \delta_T} \tag{B-8}$$

The property of Eq B-3 that coupling numerators can be summed to yield new numerators applies even when an auxiliary output motion quantity is expressed in terms of other auxiliary variables. If Eq B-5 is written

$$h = \frac{U_o}{s}\theta - \frac{U_o}{s}\alpha \tag{B-9}$$

then

$$N^{\alpha\ h}_{\delta_e\delta_T} = \frac{U_o}{s} N^{\alpha\ \theta}_{\delta_e\delta_T} = -\frac{U_o}{s} N^{\theta\ \alpha}_{\delta_e\delta_T} \tag{B-10}$$

or

$$sN^{\alpha\ h}_{\delta_e\delta_T} = -U_o N^{\theta\ \alpha}_{\delta_e\delta_T} \tag{B-11}$$

Comparison of Eq B-8 and B-11 shows that

$$sN^{\alpha\ h}_{\delta_e\delta_T} = sN^{\theta\ h}_{\delta_e\delta_T} \tag{B-12}$$

TABLE B-I

LONGITUDINAL COUPLING NUMERATORS

	A	B	C
$N^{\theta\ u}_{\delta_e\delta_T}$ or $-N^{u\ \theta}_{\delta_e\delta_T}$	$M_{\delta_e}X_{\delta_T} - M_{\delta_T}X_{\delta_e} + M_w(Z_{\delta_e}X_{\delta_T} - Z_{\delta_T}X_{\delta_e})$	$M_w(Z_{\delta_e}X_{\delta_T} - Z_{\delta_T}X_{\delta_e}) + Z_w(X_{\delta_e}M_{\delta_T} - X_{\delta_T}M_{\delta_e}) + X_w(M_{\delta_e}Z_{\delta_T} - M_{\delta_T}Z_{\delta_e})$	
	$A_{\theta u}\left(s + \frac{1}{T_{\theta u}}\right)$		
	$A_{\theta u} \doteq X_{\delta_T}M_{\delta_e}$; $\frac{1}{T_{\theta u}} \doteq -Z_w + M_w\frac{Z_{\delta_e}}{M_{\delta_e}}$		
$sN^{\theta\ h}_{\delta_e\delta_T}$ or $-sN^{h\ \theta}_{\delta_e\delta_T}$ or $U_oN^{a\ \theta}_{\delta_e\delta_T}$ or $-U_oN^{\theta\ a}_{\delta_e\delta_T}$ or $sN^{a\ h}_{\delta_e\delta_T}$ or $-sN^{h\ a}_{\delta_e\delta_T}$	$Z_{\delta_e}M_{\delta_T} - Z_{\delta_T}M_{\delta_e}$	$X_u(M_{\delta_e}Z_{\delta_T} - M_{\delta_T}Z_{\delta_e}) + Z_u(X_{\delta_e}M_{\delta_T} - X_{\delta_T}M_{\delta_e}) + M_u(Z_{\delta_e}X_{\delta_T} - Z_{\delta_T}X_{\delta_e})$	
	$A_{\theta h}\ s + \frac{1}{T_{\theta h}}$		
	$A_{\theta h} \doteq -Z_{\delta_T}M_{\delta_e}$; $\frac{1}{T_{\theta h}} \doteq -X_u + \frac{X_{\delta_T}}{Z_{\delta_T}}Z_u - M_u\frac{Z_{\delta_e}}{M_{\delta_e}}$		
$sN^{h\ u}_{\delta_e\delta_T}$ or $-sN^{u\ h}_{\delta_e\delta_T}$	$X_{\delta_e}Z_{\delta_T} - X_{\delta_T}Z_{\delta_e}$	$(X_{\delta_T}Z_{\delta_e} - Z_{\delta_T}X_{\delta_e})(M_q + M_{\dot{\alpha}})$	$Z_\alpha(X_{\delta_e}M_{\delta_T} - X_{\delta_T}M_{\delta_e}) + (X_\alpha - g)(Z_{\delta_T}M_{\delta_e} - M_{\delta_T}Z_{\delta_e}) + M_u(X_{\delta_T}Z_{\delta_e} - X_{\delta_e}Z_{\delta_T})$
	$A_{hu}\left[s^2 + 2(\zeta\omega)_{hu}s + \omega^2_{hu}\right]$		
	$A_{hu} \doteq -X_{\delta_T}Z_{\delta_e}$; $2(\zeta\omega)_{hu} = -(M_q + M_{\dot{\alpha}})$; $\omega^2_{hu} \doteq -\left(M_\alpha - \frac{M_{\delta_e}}{Z_{\delta_e}}Z_\alpha\right)$		
$U_oN^{\alpha\ u}_{\delta_e\delta_T}$ or $-U_oN^{u\ \alpha}_{\delta_e\delta_T}$	$X_{\delta_T}Z_{\delta_e} - Z_{\delta_T}X_{\delta_e}$	$U_o(X_{\delta_T}M_{\delta_e} - M_{\delta_T}X_{\delta_e}) - M_q(X_{\delta_T}Z_{\delta_e} - Z_{\delta_T}X_{\delta_e})$	$g(M_{\delta_e}Z_{\delta_T} - Z_{\delta_e}M_{\delta_T})$
	$A_{\alpha u}\left(s + \frac{1}{T_{\alpha u_1}}\right)\left(s + \frac{1}{T_{\alpha u_2}}\right)$		
	$A_{\alpha u} \doteq X_{\delta_T}Z_{\delta_e}$; $\frac{1}{T_{\alpha u_1}} \doteq \frac{g}{U_o}\left(\frac{Z_{\delta_T}}{X_{\delta_T}} - \frac{Z_{\delta_e}}{M_{\delta_e}}\frac{M_{\delta_T}}{X_{\delta_T}}\right)$; $\frac{1}{T_{\alpha u_2}} \doteq \frac{U_oM_{\delta_e}}{Z_{\delta_e}}$		

TABLE B-II

LATERAL COUPLING NUMERATORS

	A	B	C
$N^{\varphi\ r}_{\delta_a\delta_r}$ or $-N^{r\ \varphi}_{\delta_a\delta_r}$	$L'_{\delta_a}N'_{\delta_r} - N'_{\delta_a}L'_{\delta_r}$	$-Y_v(L'_{\delta_a}N'_{\delta_r} - N'_{\delta_a}L'_{\delta_r}) + L'_\beta(Y^*_{\delta_a}N'_{\delta_r} - N'_{\delta_a}Y^*_{\delta_r}) - N'_\beta(Y^*_{\delta_a}L'_{\delta_r} - L'_{\delta_a}Y^*_{\delta_r})$	
	$A_{\varphi r}\left(s + \frac{1}{T_{\varphi r}}\right)$		
	$A_{\varphi r} \doteq L'_{\delta_a}N'_{\delta_r}\ ;\ \frac{1}{T_{\varphi r}} \doteq -Y_v + \frac{Y^*_{\delta_r}}{N'_{\delta_r}}\left(N'_\beta - L'_\beta\frac{N'_{\delta_a}}{L'_{\delta_a}}\right)$		
$N^{\varphi\ \beta}_{\delta_a\delta_r}$ or $-N^{\beta\ \varphi}_{\delta_a\delta_r}$	$L'_{\delta_a}Y^*_{\delta_r} - Y^*_{\delta_a}L'_{\delta_r}$	$-N'_r(L'_{\delta_a}Y^*_{\delta_r} - Y^*_{\delta_a}L'_{\delta_r}) + L'_r(N'_{\delta_a}Y^*_{\delta_r} - Y^*_{\delta_a}N'_{\delta_r}) + (N'_{\delta_a}L'_{\delta_r} - L'_{\delta_a}N'_{\delta_r})$	
	$A_{\varphi\beta}\left(s + \frac{1}{T_{\varphi\beta}}\right)$		
	$A_{\varphi\beta} \doteq L'_{\delta_a}Y^*_{\delta_r}\ ;\ \frac{1}{T_{\varphi\beta}} \doteq -N'_r - \frac{N'_{\delta_r}}{Y^*_{\delta_r}}$		
$N^{\varphi\ a_y}_{\delta_a\delta_r}$ or $-N^{a_y\varphi}_{\delta_a\delta_r}$	$U_o(L'_{\delta_a}Y^*_{\delta_r} - Y^*_{\delta_a}L'_{\delta_r}) + l_x\cos\alpha_o(L'_{\delta_a}N'_{\delta_r} - N'_{\delta_a}L'_{\delta_r})$	$-U_oN'_r(L'_{\delta_a}Y^*_{\delta_r} - Y^*_{\delta_a}L'_{\delta_r}) + U_oL'_r(N'_{\delta_a}Y^*_{\delta_r} - Y^*_{\delta_a}N'_{\delta_r}) + l_x\cos\alpha_o\left[-Y_v(L'_{\delta_a}N'_{\delta_r} - N'_{\delta_a}L'_{\delta_r}) + L'_\beta(Y^*_{\delta_a}N'_{\delta_r} - N'_{\delta_a}Y^*_{\delta_r}) - N'_\beta(Y^*_{\delta_a}L'_{\delta_r} - L'_{\delta_a}Y^*_{\delta_r})\right]$	$U_o\left[-Y_v(L'_{\delta_a}N'_{\delta_r} - N'_{\delta_a}L'_{\delta_r}) + L'_\beta(Y^*_{\delta_a}N'_{\delta_r} - N'_{\delta_a}Y^*_{\delta_r}) - N'_\beta(Y^*_{\delta_a}L'_{\delta_r} - L'_{\delta_a}Y^*_{\delta_r})\right]$
	$A_{\varphi a_y}\left[s^2 + 2(\zeta\omega)_{\varphi a_y}s + (\omega_{\varphi a_y})^2\right]$		
	For $\cos\alpha_o \doteq 1$; $l_{x_o} \equiv -\frac{U_oY^*_{\delta_r}}{N'_{\delta_r}} \sim$ Center of percussion		
	$l_x \equiv l_{x_o} + \Delta l_x$		
	$A_{\varphi a_y} \doteq L'_{\delta_a}(U_oY^*_{\delta_r} + l_xN'_{\delta_r}) \doteq -L'_{\delta_a}U_oY^*_{\delta_r}\frac{\Delta l_x}{l_{x_o}}$		
	$(\omega_{\varphi a_y})^2 \doteq \frac{U_o}{\Delta l_xN'_{\delta_r}}\left[Y^*_{\delta_r}\left(N'_\beta - \frac{N'_{\delta_a}}{L'_{\delta_a}}L'_\beta\right) - Y_vN'_{\delta_r}\right] \doteq -\frac{U_oY_v}{\Delta l_x}$		
	$2(\zeta\omega)_{\varphi a_y} \doteq \frac{l_x}{\Delta l_xN'_{\delta_r}}\left[Y^*_{\delta_r}\left(N'_\beta - \frac{N'_{\delta_a}}{L'_{\delta_a}}L'_\beta\right) - Y_vN'_{\delta_r}\right] - \frac{U_oY^*_{\delta_r}}{\Delta l_xN'_{\delta_r}}\left(N'_r - \frac{N'_{\delta_a}}{L'_{\delta_a}}L'_r\right) \doteq -\frac{l_x}{\Delta l_x}Y_v$		

APPENDIX C

AN ALTERNATE FORMULATION OF NUMERATOR AND DENOMINATOR EXPANSIONS*

Although the mathematical equations for the effective (closed-loop) system transfer function numerators and denominator may appear quite complex, they are simple straightforward expansions. These expansions can be defined by a few rules similar to the ones used in signal flow diagrams. The sensing, actuation, and equalization components of the system are treated as feedbacks, all acting to modify the vehicle open-loop transfer functions. The resultant closed-loop system is analogous to an effective vehicle which may have command control deflection or disturbance inputs.

The rules are:

1. The effective numerator is equal to:
   a. The open-loop numerator
   b. Plus the sum of all the feedback transfer functions, each one multiplied by the appropriate coupling numerator
2. The effective denominator is equal to:
   a. The open-loop denominator
   b. Plus the sum of all the feedback transfer functions, each one multiplied by the appropriate numerator
   c. Plus the sum of all the feedback transfer functions taken two at a time, each pair multiplied by the appropriate coupling numerator

Rule 1 simply states that each feedback modifies a numerator by adding to that numerator the product of the feedback transfer function and the appropriate coupling numerator. The appropriate coupling numerator is the one for the output/input pair of the original numerator plus the feedback output/input pair. For example, the feedback $q_2 \rightarrow \delta_1$ modifies the q_i/δ_j numerator by adding to it the term $G_{12}N^{q_i q_2}_{\delta_j \delta_1}$ and modifies the q_i/η_j numerator by adding to it the term $G_{12}N^{q_i q_2}_{\eta_j \delta_1}$.

---

*Developed by Robert L. Stapleford.

The effective denominator has been shown in Appendix A to be given by

$$\Delta_{sys} = \Delta + \sum_{i=1}^{4}\sum_{j=1}^{2} G_{ji}N_{q_i\delta_j} + \sum_{i=1}^{4}\sum_{k=1}^{4} G_{1i}G_{2k}N_{\delta_1\delta_2}^{q_i q_k} \qquad \text{(C-1)}$$

The equivalence of Eq C-1 and Rule 2 should be obvious. The appropriate numerator, Rule 2-b, is the one with the same output/input pair as the feedback and the appropriate coupling numerator, Rule 2-c, is the one with the same two output/input pairs as the feedbacks.

For example, consider the system shown in Fig. C-1, which is the same as in Fig. 4, redrawn to form the command control deflection input, δ_{2_c} (the product of the command input, q_{1_c}, and the command controller feedback transfer function, G_{21}).

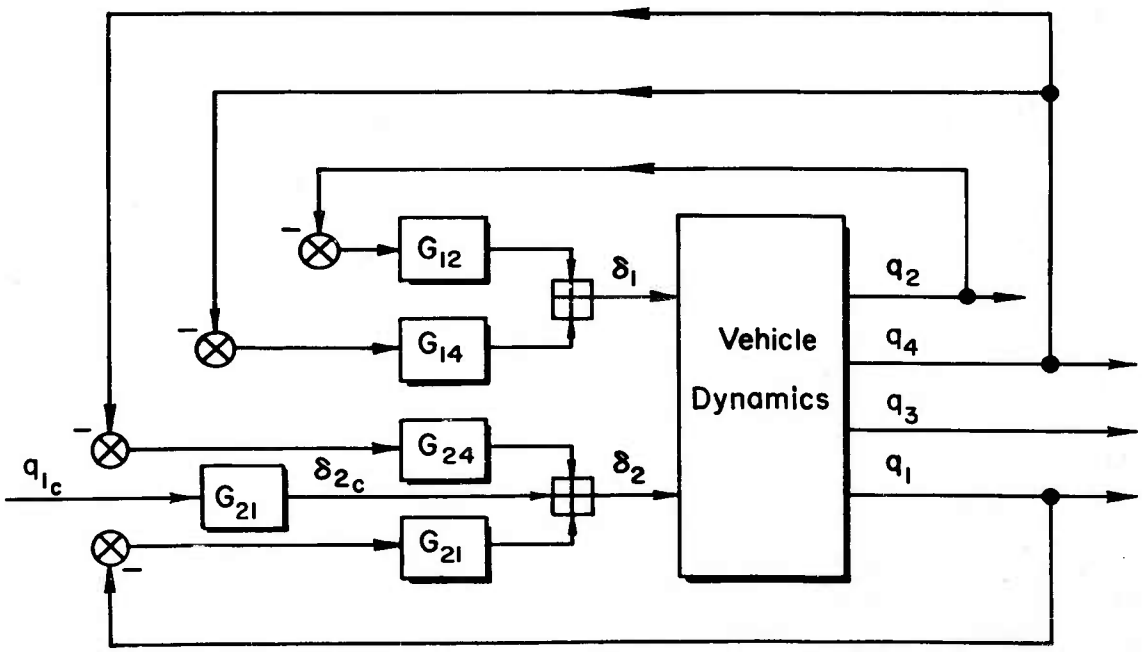

Figure C-1. Block Diagram of Multiloop System
q_{1_c}, $q_4 \rightarrow \delta_2$; q_2, $q_4 \rightarrow \delta_1$

The closed-loop system transfer function q_1/q_{1_c} can be written

$$\frac{q_1}{q_{1_c}} = G_{21}\frac{q_1}{\delta 2_c} = G_{21}\frac{N''''_{q_1\delta_2}}{\Delta''''} \tag{C-2}$$

The effective numerator for the system with four loops closed is determined by applying Rule 1.

$$N''''_{q_1\delta_2} = N_{q_1\delta_2} + G_{12}N^{q_1q_2}_{\delta_2\delta_1} + G_{14}N^{q_1q_4}_{\delta_2\delta_1} + \left[G_{24}N^{q_1q_4}_{\delta_2\delta_2}\right] + \left[G_{21}N^{q_1q_1}_{\delta_2\delta_2}\right] \tag{C-3}$$

where the two bracketed terms are zero because $N^{q_iq_j}_{\delta_k\delta_l}$ is zero if $i=j$ or $k=l$. Using Rule 2,

$$\begin{aligned}\Delta'''' = \Delta_{sys} = \Delta &+ G_{12}N_{q_2\delta_1} + G_{14}N_{q_4\delta_1} + G_{24}N_{q_4\delta_2} + G_{21}N_{q_1\delta_2} \\ &+ \left[G_{12}G_{14}N^{q_2q_4}_{\delta_1\delta_1}\right] + G_{12}G_{24}N^{q_2q_4}_{\delta_1\delta_2} \\ &+ G_{12}G_{21}N^{q_2q_1}_{\delta_1\delta_2} + \left[G_{14}G_{24}N^{q_4q_4}_{\delta_1\delta_2}\right] \\ &+ G_{14}G_{21}N^{q_4q_1}_{\delta_1\delta_2} + \left[G_{24}G_{21}N^{q_4q_1}_{\delta_2\delta_2}\right]\end{aligned} \tag{C-4}$$

where the three terms in brackets are zero because of the coupling numerator property stated previously.

While the above discussion and example and the derivations in the body of the report have considered only the cases of the command response with feedbacks to two independent controls or the disturbance response with feedbacks to one control, a complete generalization (for a three degrees of freedom system) is quite straightforward with the introduction of the coupling–coupling

numerator. The coupling–coupling numerator has three columns of the open-loop characteristic determinant replaced by the appropriate control or disturbance coefficients.

Rule 1 is generalized by adding "c. Plus the sum of all the feedback transfer functions taken two at a time, each pair multiplied by the appropriate coupling–coupling numerator."

Rule 2 is generalized by adding "d. Plus the sum of all feedback transfer functions taken three at a time, each combination multiplied by the appropriate coupling–coupling numerator."

For example, with feedbacks $q_1 \rightarrow \delta_1$, $q_2 \rightarrow \delta_2$, and $q_3 \rightarrow \delta_3$ the disturbance response, q_1/η, is given by:

$$\frac{q_1}{\eta} = \frac{N'''_{q_1\eta}}{\Delta'''} \tag{C-5}$$

$$N'''_{q_1\eta} = N_{q_1\eta} + \left[G_{11}N_{\eta}^{q_1 q_1}{}_{\delta_1}\right] + G_{22}N_{\eta}^{q_1 q_2}{}_{\delta_2} + G_{33}N_{\eta}^{q_1 q_3}{}_{\delta_3}$$
$$+ \left[G_{11}G_{22}N_{\eta}^{q_1 q_1 q_2}{}_{\delta_1\delta_2}\right] + \left[G_{11}G_{33}N_{\eta}^{q_1 q_1 q_3}{}_{\delta_1\delta_3}\right]$$
$$+ G_{22}G_{33}N_{\eta}^{q_1 q_2 q_3}{}_{\delta_2\delta_3} \tag{C-6}$$

$$\Delta''' = \Delta + G_{11}N_{q_1\delta_1} + G_{22}N_{q_2\delta_2} + G_{33}N_{q_3\delta_3}$$
$$+ G_{11}G_{22}N_{\delta_1\delta_2}^{q_1 q_2} + G_{11}G_{33}N_{\delta_1\delta_3}^{q_1 q_3} + G_{22}G_{33}N_{\delta_2\delta_3}^{q_2 q_3}$$
$$+ G_{11}G_{22}G_{33}N_{\delta_1\delta_2\delta_3}^{q_1 q_2 q_3} \tag{C-7}$$

where the bracketed terms of Eq (C-6) are zero. Note that a coupling–coupling numerator is zero if any two of the outputs or any two of the inputs are identical.